The mechanical and volumetric behaviour of sisal fibre reinforced concrete blocks

by
Gerrit Coetzee

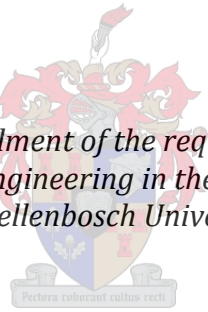

Thesis presented in fulfilment of the requirements for the degree of Masters of Science in Engineering in the Faculty of Engineering at Stellenbosch University

Supervisor: Prof William Peter Boshoff

March 2013

Declaration

By submitting this dissertation electronically, I declare that the entirety of the work contained therein is my own, original work, that I am the owner of the copyright thereof (unless to the extent explicitly otherwise stated) and that I have not previously in its entirety or in part submitted it for obtaining any qualification.

March 2013

Signature:_____

Summary

Natural fibre reinforced concrete (NFRC) is a type of concrete that has become of particular interest in recent years, due to its potential for being used as a sustainable and economically viable building material. Natural fibres are often cheap and widely available in developing nations. Sisal is one such fibre predominantly grown in Brazil and has been identified as having the potential to be commercially cultivated in Southern Africa.

The durability of sisal fibres in a cementitious environment tends to be adversely affected due to the high alkalinity of pore water and the presence of calcium hydroxide.

This research dealt with the use of sisal fibre reinforced concrete (SFRC) blocks. It focused on the mechanical and volumetric properties of blocks with varying fibre and condensed silica fume content (CSF).

Two different SFRC blocks were produced (solid and hollow) using an average fibre length of 10 mm. Two matrix types were used: one using a 70:30 cement:fly-ash ratio and another using a 60:30:10 cement:fly-ash:CSF ratio by weight. Samples of each matrix type were prepared with 0, 0.5 and 1% fibre content by volume.

Hollow blocks were tested for compressive strength and capillary water absorption, while solid blocks were tested for compressive strength, flexural strength, capillary water absorption, dimensional stability, drying shrinkage, density, total water absorption and void content. All tests were performed on samples with an age of 28 days. Solid block compressive tests were also performed on samples with an age of 7 days.

The hollow blocks had significantly lower average compression strength than the solids, but an increase in fibre content caused a slight increase in strength.

For solid blocks, it was found that the addition of natural fibres decreases the strength, although a partial substitution of cement with CSF, in conjunction with fibres, did increase the strength relative to blocks without CSF. The flexure strength was also lowered somewhat by the addition of fibres, but an increase in ductility was noted, although not quantified.

The addition of CSF to fibre-containing blocks led to an increase in capillary water absorption, but a decrease in absorption through immersion. This shows that the addition of CSF does significantly alter the pore system of a cementitious matrix reinforced with natural fibres.

Also, the dimensional stability increased with the addition of CSF and fibres. The same can be said for drying shrinkage. Even though an increase in fibre and CSF caused samples to shrink more under drying, they were more stable under cycles of wetting and drying.

It was concluded that the addition of fibres to a matrix had a detrimental effect on strength, although ductility did increase. The volumetric properties of concrete were also adversely affected by the addition of fibres, although dimensional stability was improved. The partial substitution of cement with CSF did improve many of the mechanical and volumetric properties of samples containing sisal fibre.

Opsomming

Natuurlike vesel bewapende beton (NVBB) is ’n tipe beton wat onlangs heelwat belangstelling ontlok het weens die potensiaal om gebruik te word as ‘n volhoubare en ekonomiese haalbare boumateriaal. Natuurlike vesels is dikwels baie goedkoop en wyd beskikbaar in ontwikkelende lande. Sisal is een so ‘n vesel wat verkry word vanaf die blare van ’n garingboom. Die plant word hoofsaaklik in Brasilië verbou en is al uitgewys weens sy potensiaal om op kommersiële skaal in Suidelike Afrika verbou te word.

Die duursaamheid van sisal vesels is geneig om nadelig geaffekteer te word in die teenwoordigheid van kalsium hidroksied en ’n hoë-alkali omgewing, soos gevind in die porie-water van beton.

Hierdie navorsing handel oor die gebruik van sisal vesel bewapende beton (SVBB) boublokke. Dit fokus op die meganiese- en duursaamheids eienskappe van blokke met verkillende inhoude van vesel en gekondenseerde silika dampe (GSD).

Twee verskillende SVBB blokke is geproduseer (solied en hol) deur gebruik te maak van 10 mm vesels. Twee matriks tipes is gebruik: een met ’n 70:30 sement:vliegas verhouding en een met ’n 60:30:10 sement:vliegas:GSD verhouding, volgens gewig. Blokke van elke matriks tipe is geproduseer met 0, 0.5 en 1% vesel inhoud, volgens volume.

Hol blokke is getoets vir druksterkte en kapillêre water absorpsie, terwyl soliede blokke getoets is vir druksterkte, buigsterkte, kapillêre water absorpsie, dimensionele stabiliteit, krimp onder uitdroging, digtheid, totale water absorpsie en luginhoud. Alle toetse is gedoen op blokke met ’n ouderdom van 28 dae. Druktoetse is ook gedoen op soliede blokke met ’n ouderdom van 7 dae.

Die hol blokke het ’n aansienlike laer gemiddelde druksterkte as die soliede blokke gehad, maar ’n toename in veselinhoud het gelei tot ’n effense verhoging in druksterkte.

’n Toename in veselinhoud van soliede blokke het gelei tot ’n afname in druksterkte, alhoewel ’n gedeeltelike vervanging van sement met GSD gelei het tot ’n hoër druksterkte vir blokke met vesels. Die buigsterkte van soliede blokke het ook afgeneem met ’n verhoging in veselinhoud. ’n Verhoging in duktiliteit is waargeneem met ’n toename in veselinhoud, alhoewel dit nie gekwantifiseer is nie.

Die toevoeging van GSD tot blokke bevattende vesels het gelei tot ’n verhoging in kapillêre water absorpsie, maar ’n verlaging in totale water absorpsie. Dit kan daarop wys dat die toevoeging van GSD die poriestelsel van NVBB noemenswaardig verander.

Beide die dimensionele stabiliteit en krimp onder uitdroging het toegeneem met die toevoeging van GSD en vesels tot die blokke. Dus, die toevoeging het gelei tot ’n hoër krimpvervorming tydens uitdroging en ’n hoër stabiliteit tydens nat/droog siklusse.

Daar is tot die gevolgtrekking gekom dat die toevoeging van sisal vesels tot ’n beton blok oor die algemeen ’n negatiewe effek het op sterkte, alhoewel duktiliteit toeneem. Die volumetriese eienskappe van beton word ook negatief geaffekteer met die toevoeging van sisal vesels, alhoewel dimensionele stabiliteit verbeter. Die gedeeltelike vervanging van sement met GSD lei tot die verbetering van beide meganiese en volumetriese eienskappe van beton blokke wat sisal vesels bevat.

Acknowledgements

I would like to thank the following people for the assistance and support:

- My study leader, Prof W.P. Boshoff, for his guidance during this study, for allowing me space to develop my own ideas and for his expert opinion.

- Prof R.D. Tolêdo Filho, for his guidance during my stay in Brazil as well as his hospitality and willingness to allow me in his laboratory to do experiments.

- Clodoaldo, Ivan, Rodrigo and all the other COPPE/LabEST laboratory technicians for their time and assistance during experimental work.

- Saulo, Fabrício and Emilien for providing much needed friendship and translation in a foreign country.

- My parents and friends, for their unconditional love and support.

- The National Research Foundation for their funding.

- Sepere, Alex and Daniël for providing a fun atmosphere in the office.

- My Creator, for giving me the opportunity and inspiration to complete this study.

"Try not to become a man of success. Rather become a man of value." – Albert Einstein

Table of Contents

List of figures

List of tables

List of abbreviations

ABNT	Associação Brasileira de Normas Técnicas (Brazilian Association of Technical Standards)
ABT	Alternative building technology
ARC	Agricultural Research Council
ASTM	American Society for Testing and Materials
C&CI	Cement & Concrete Institute
CH	Calcium hydroxide
CoV	Coefficient of variation
CSF	Condensed silica fumes
CWCCB	Crushed waste calcined clay bricks
DAFF	Department of Agriculture, Forestry and Fisheries
DHS	Department of Human Settlements
DP	Degree of polymerization
DTG	Derivative thermogravimetry
FAO	Food and Agriculture Organization
GGBS	Ground granulated blastfurnace slag
GHG	Greenhouse gas
hp	Horse power
LCH	Low cost housing
LVDT	Linear variable differential transformer
MK	Metakaolin
MOR	Modulus of rupture
OPC	Ordinary Portland cement
NFRC	Natural fibre reinforced concrete
NFRCC	Natural fibre reinforced cement composites

RH	Relative humidity
SANS	South African National Standards
SFRC	Sisal fibre reinforced concrete
TG	Thermogravimetry
TGA	Thermogravimetric analysis
THC	Tetracannabinol

Nomenclature

Dicotyledonous	Group of plants whose seed typically have two embryonic leaves
Ettringite	A hydrous calcium aluminium sulphate mineral found in hydrated Portland cement
Fibril	Very fine fibre-like strand consisting of glycoproteins and cellulose
Herbaceous plant	Plant that has stems and leaves that die at the end of the growing season
Hygroscopic	Ability to attract and hold water molecules from the surrounding environment, usually through absorption and adsorption
Industrial crop	Crops grown commercially for products of economic value that have limited value for food or feed
Mineralisation	The process of conversion to a mineral substance
Perennial plant	A plant that lives for more than two years
Polymerization	A process where monomer molecules react together in a chemical reaction to form polymer chains
Polysaccharide	Long carbohydrate units of repeated monomer units
Porosity	Property of concrete that relates the volume of the pores to the total volume
Tobermorite	A calcium silicate hydrate material found in hydrated cement paste

1. Introduction

1.1 Background

A lack of adequate housing is not a problem restricted to Africa, nor to developing countries. According to the United Nations (2007) the percentage slum-dwellers in developing countries has decreased over the past two decades, but due to substantial population growth, the number of slum-dwellers has increased, with a reported one billion people living in slums worldwide.

It is well known that the adverse effects of global warming are becoming more problematic, especially in developing nations. According to the World Business Council for Sustainable Development (2005) up to 27% of greenhouse gases (GHG's) are emitted during the construction and operation of buildings and about 5% of man-made GHG's emitted worldwide are caused directly by the production of cement.

In South Africa, where 12 million people are in need of proper housing (Statistics South Africa, 2012), there have been numerous attempts at developing alternative building technologies that address both the financial and environmental issues typically associated with low cost housing (LCH). The success of these technologies has, however, been very limited, primarily due to inadequate structural performance, poor policies and management and a lack of acceptance by beneficiaries. The need has since arisen for a sustainable, economically viable building material that uses the existing construction methods and political structures already in place.

Natural fibres have been used as reinforcing material, in some way or another, since man started building shelters. In more recent years, since the popularization of plastics and other synthetic materials, natural fibres have come to be considered a traditional building material. With mounting pressure worldwide to develop economically viable, sustainable construction materials, there has been growing interest in the development of new materials that enhance the optimal usage of natural resources, particularly renewable resources.

Fibres such as sisal, jute, hemp and coir present exciting opportunities for use in the construction industry. These fibres are relatively cheap compared to similar-use synthetic fibres, due to the low degree of industrialization required for their processing. In most developing nations these fibres are readily available.

Due to their low cost and availability, these fibres have been used extensively in non-structural composites. Hemp fibre in particular has been used widely for its thermal insulating properties.

As our understanding of the behaviour of these fibres has improved, the potential for use in structural applications has been realized. Hemp, sisal and flax fibres have tensile strengths in excess of 650 MPa. Much research has been done in Brazil, India, Israel and Portugal in recent years to investigate the tensile and ductility behaviour of structural natural fibre reinforced cement composites (NFRCC) with varying results.

Although the mechanical behaviour of these composites was found to be favourable, there have been numerous issues with durability. It is especially fibre degradation due to the high alkaline environment of NFRCC and weathering that is of concern. The detrimental effect of calcium hydroxide (CH) on the durability of NFRCC, found as a by-product of cement hydration, has been noted by various authors.

Various methods of improving fibre durability have been developed, of which cement substitution with pozzolanic materials, such as silica fume and metakaolin, has been the most successful. These pozzolans react with calcium hydroxide, lowering the calcium ion content and alkalinity of the matrix pore water.

Sisal is a fibre that is widely available in Brazil and has been identified as having potential for being cultivated on a commercial scale in Southern Africa. The fibre has been shown to possess favourable mechanical properties. Due to the need in South Africa to develop a building technology aimed at the LCH sector that uses existing building techniques and government policies, there has arisen an interest in the use of natural fibre reinforced concrete building blocks.

Very little is known about the behaviour of sisal fibre in a high-porosity cementitious environment (as is typical of concrete blocks) and it is especially the durability and dimensional stability aspects that are of interest. Also, the addition of condensed silica fume (CSF), as a means of lowering the alkalinity and therefore potentially improving the durability, is of interest.

1.2 Objectives

The reason for the research was to assess the use of sisal fibre as a material that can be used to produce cheaper and more environmentally sustainable masonry units. This includes the ability of sisal fibre to reduce the cement content in blocks and provide additional volume to blocks.

The primary objectives were to investigate the mechanical and volumetric properties of sisal fibre reinforced concrete blocks (SFRC). The research focussed specifically on the influence of fibre and CSF content on the mentioned concrete properties. The blocks used were based on what is currently used in the South African LCH sector.

1.3 Scope and methodology

This research project involved the testing of solid and hollow sisal fibre reinforced concrete blocks. Two similar cement matrices were used: one containing CSF and one without. A 30% substitution of cement with fly-ash (by weight) was made for both matrices. Furthermore, three groups of specimens of each matrix type were prepared containing 0%, 0.5% and 1% sisal fibres by volume, respectively. In total six different mix types were prepared for each block type (solid and hollow).

Compression, flexure, capillary water absorption, dimensional stability, density, total water absorption and void content tests were performed on all mix types of solid blocks. Shrinkage beams were prepared using the same mixes for use in drying shrinkage tests. Compression and capillary water absorption tests were performed on all six mix types of hollow blocks.

All specimens were tested at the age of 28 days. Seven day compression tests were also performed on solid blocks.

1.4 Outline of thesis

This thesis consists of seven chapters. The present chapter presents an introduction to the thesis. Chapter 2 presents a background study reviewing the current LCH situation in South Africa and the fundamentals of natural fibres and cement matrices used with natural fibres. It includes an extensive study on the cultivation of fibre-giving plants. Chapter 3 discusses the materials used and the experimental framework, while Chapter 4 details the results and analysis of results of each test performed. A discussion of results follows in Chapter 5. Chapter 6 presents conclusions and recommendation for future work. Chapter 7 contains the references.

2. Background study

This Chapter presents a study on the current situation of LCH in South Africa. A brief overview is also given of the natural fibres available worldwide with possible structural uses. Possible cement matrices for use with natural fibres are discussed.

2.1 Low cost housing in South Africa

LCH and the problems associated with it is not unique to South Africa, or to developing countries. It is also not the largest sector in terms of energy consumption in residential buildings. However, the environmental impact of the LCH industry in South Africa has largely been neglected, mainly due to a lack of incentives (Brits et al., 2011). As a result there is a large potential to reduce the environmental impact of this industry.

2.1.1 Population living in LCH

According to the 2011 South African Census conducted by Statistics South Africa (2012), the percentage of South Africans living in informal and traditional settlements have reduced from 34.5% in 1996 to 21.5% in 2011. When considering the population growth of 14.2% from 1996 to 2011 the actual amount of people living in informal or traditional settlements has decreased from about 14 million to 11 million.

In 2010, Human Settlements minister Tokyo Sexwale (2010) was quoted as saying that the state subsidized housing backlog was 2.1 million houses (or 12 million people) and that the State plans on building 220 000 houses per annum between 2010 and 2014. A budget of R22 billion had been allocated to the construction of LCH for the fiscal year 2011-2012, while Sexwale has mentioned that the government needs to spend close to R50 billion to rectify sub-standard houses (SAPA, 2012).

2.1.2 Alternative building technologies used in LCH

Between 1994 and 2010 various initiatives were put in place by the Government to research and implement alternative building technologies (ABT's) in South Africa. During the abovementioned time span 2.9 million houses were built for low income earners, of which only 17 000 made use of ABT's. Therefore, only 0.6% of the total government housing delivery made use of ABT's (Chief Directorate: Research, 2010).

The Department of Human Settlements (DHS) conducted studies in 2004 and 2010 to investigate the use of ABT's in the LCH sector. The 2004 study (DHS, 2004) found that compressed earth blocks, interlocking blocks, shutters and concrete, ecoframe building materials and Everite fibre cement

were the most popular ABT's in use, while concrete panels, the hydraform building system and the polystyrene system based on Imison technology were found to be the most popular in the 2010 study (Van Wyk, 2010).

There have been many problems associated with the ABT's used for LCH in South Africa. According to the DHS (2004) many technologies exhibited limited material strength and stability (houses showed different cracking patterns). It was also found that some technologies had problems with roof leakages, seepage and the inability to withstand extreme weather conditions. Extensions also proved difficult with some ABT's. The DHS (2004) found that 70% of beneficiaries indicated that they intended on extending their houses. Many of the abovementioned problems, however, are caused by inferior workmanship and not necessarily inferior building technologies (Chief Directorate: Research, 2010).

Another problem with the current ABTs in use is a strong belief amongst beneficiaries that they are being devalued by the state and therefore given inferior technologies (Chief Directorate: Research, 2010).

One of the problems with the government's current subsidy scheme is that the same subsidy is paid per house, regardless of the technology used for construction (Chief Directorate: Research, 2010). This means that in cases where ABT's are less expensive than conventional building methods, the savings go to the developers and not the government or the beneficiaries.

The Chief Directorate: Research (2010) has also stated that most houses using ABT's can be constructed in four to seven days, whereas conventional houses take on average thirty days. In practice, however, ABT projects tend to take longer to complete due to training of the labour force at the start of the project. If the use of ABT's become more common, this trend should minimise.

It can be concluded that the problems associated with ABT's are not necessarily a direct result of the technology, but rather the inability of Government and contractors to properly implement them. This naturally leads to the need to research an ABT based on the commonly used and preferred brick and mortar method that has possible economic and environmental benefits.

An ABT that is based on the typical brick and mortar house could possibly solve many of the problems associated with ABT's. Firstly, it would not require retraining of labourers, because the construction methods will not change. Secondly, extensions to the house could be done more easily and the problems with acceptability by beneficiaries might diminish.

2.1.3 Bricks and blocks in use

This section discusses the bricks and blocks used in construction of typical LCH in South Africa.

There are many different bricks being used in South Africa, with burnt clay and cement units being the most popular brick materials. Bricks and blocks come in many different sizes, shapes, colours and profiles.

According to SANS 10400 (1990) a block is any masonry unit which has a length of more than 300 mm or a width of more than 120 mm. A brick is any masonry unit that is not a block.

De Beer (2012) has stated that most bricks used in South Africa come in either 7 or 14 MPa nominal compressive strengths, while blocks are typically 3.5 or 7 MPa. When building with bricks 7 MPa is suitable for single storey structures and 14 MPa for the lower storey of double storey structures. The same is true for 3.5 and 7 MPa blocks, respectively. The nominal strength refers to the maximum stress calculated using the total surface area (including cavities). Table 2.1 shows the compressive strength requirements for cement masonry units.

Table 2.1: *Compressive strength for cement masonry units (SANS 1215, 2008)*

Nominal compressive strength [MPa]	**Minimum compressive strength [MPa]**	
	Average (for 5* units)	**Individual units**
3.5	4.0	3.0
7	8.0	5.5
10.5	11.5	8.5
14	15.5	11.0
21	23.5	17.0

*In the case of units having an overall length of 290 mm or less, an average for 12 units is taken.

Lane (2007) states that, when building single storey units or the upper storey of double storey units, the average compressive strength for hollow and solid masonry units should be no less than 3.5 and 4 MPa, respectively.

As stated by Laing (2011) the most commonly used masonry units for low-cost housing in the inland provinces in South Africa are “Maxi” bricks, which are 290 mm long, 140 mm wide and 90 mm high (Figure 2.1 (a)). They are also known as “Daimond Maxi” bricks. In coastal provinces the favoured masonry unit is the 390mm long, 140mm wide and 190mm high hollow concrete block (Figure 2.1 (b)). The hollow block is the preferred block due to its better thermal properties and action against the wet climate in coastal provinces. A 7 MPa “Maxi” brick and a 3.5 MPa hollow block is deemed sufficient for single storey buildings.

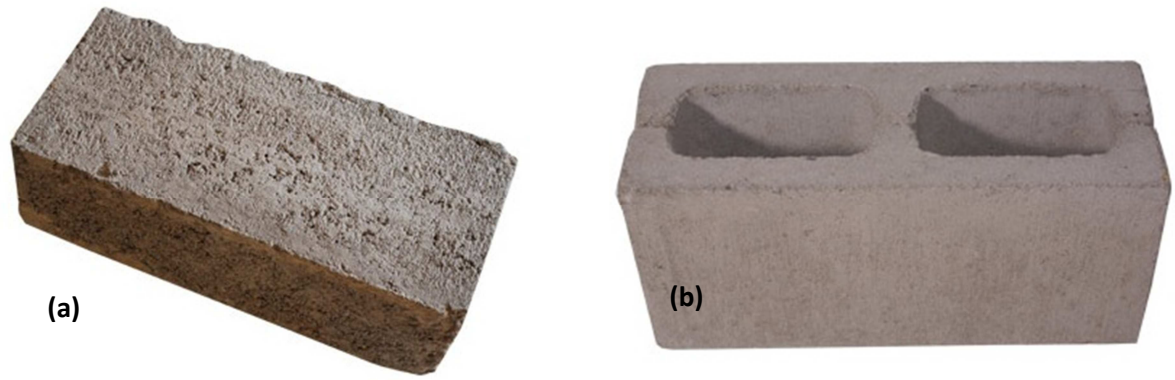

Figure 2.1: *Blocks commonly used in South African LCH sector (a) "Maxi" brick (Savanna Bricks, 2012); (b) hollow block (Cape Cement Products, 2012)*

Even though the "Maxi" brick should be classified as a brick, for the sake of simplicity both "Maxi" bricks and hollow blocks will, henceforth, be referred to as blocks.

This study will focus on concrete samples produced in the shapes of the two blocks.

2.2 Natural fibres

The recent rise in the amount of research being done on the structural uses of natural fibres can be attributed to two factors. Firstly, there is a world-wide need for sustainable materials (construction, packaging, etc.). Secondly, there are large amounts of naturally occurring fibres that are unused after harvesting of vegetation. These two factors led to a mounting need for knowledge on how these fibres behave under various circumstances. For engineering purposes the durability properties of fibres and its behaviour under tensile loading are of great interest.

The following vegetable fibres have been identified over the years as being most suitable for use in structural applications: abaca, coir, cotton, flax, hemp, jute, kenaf, ramie and sisal. These fibres were identified as being economically viable and as having the most suitable mechanical properties. This background study will focus on these fibres.

This section deals with how natural fibres are classified, the structure of natural fibres and how it contributes to its mechanical properties as well as how various fibres are cultivated and extracted.

2.2.1 Classification

Fibres suitable for use in industrial applications can be classified as either natural or synthetic (Kirby, 1963). Synthetic fibres generally have superior mechanical properties in comparison to natural fibres,

but have the environmental drawbacks of not being bio-degradable or renewable. Synthetic fibres are also often more expensive than natural fibres. These environmental and economic factors have recently led to an increase in research on the possible uses of natural fibres in industrial applications (Mohanty, Misra and Drzal, 2005).

In nature, fibres in plants act as the basis of a strength-providing skeleton. Fibres are bound together by natural gums and resins. These fibres run through the roots, stems and leaves of plants (Cook, 1984).

As mentioned by Kirby (1963) natural fibres can be subdivided into three classes (vegetable, animal and mineral), according to their morphology. Vegetable fibres can further be subdivided into bast, leaf, seed and fruit (or nut) fibres. These classes, as well as examples of each are shown in Figure 2.2. This study will only investigate vegetable fibres and will henceforth refer to vegetable fibres with the collective name of natural fibres.

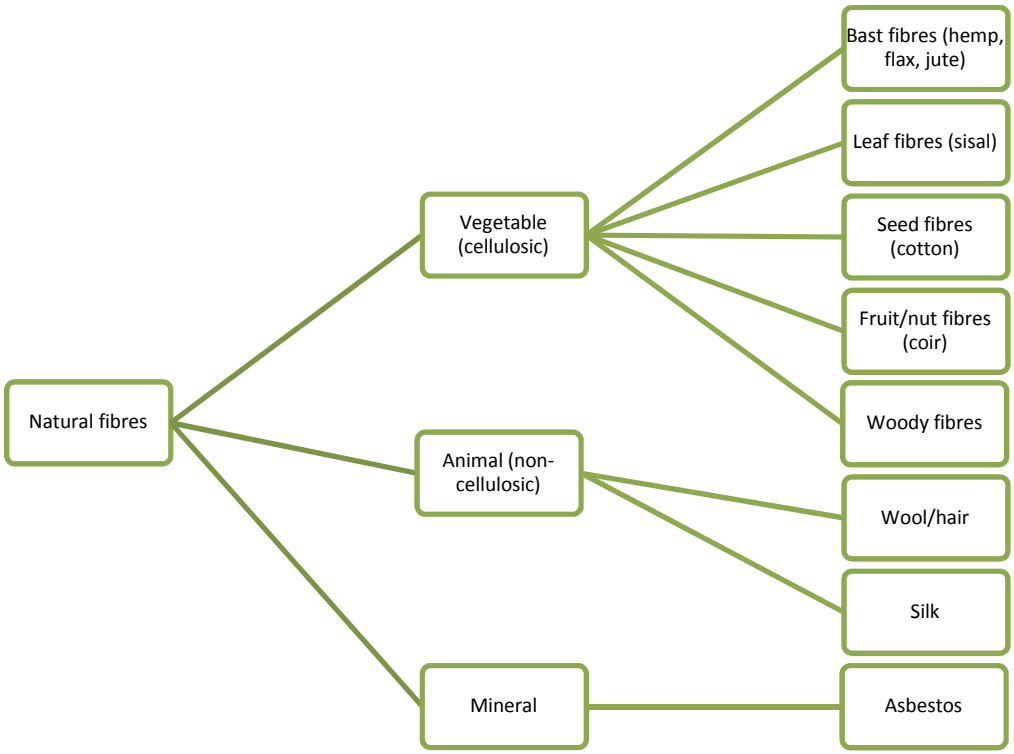

Figure 2.2: *Types and examples of natural fibres (Kirby, 1963)*

Bast fibres are obtained from the stem of dicotyledonous plants. A typical biological structure of a fibre plant stem consists of a bark layer, a bast layer and a stem core (Figure 2.3). The bark layer is a thin skin that protects the whole stem (Singh, 2010). The bast layer consists of a primary fibre layer (where fibres are extracted) and a secondary layer, called the phloem. The stem has two parts: the

xylem (woody part used for transport of water) and the pith (spongy core used for storage and transport of nutrients). Fibres are held together by the cellular tissue of the phloem and other gummy substances (Cook, 1980). Jute, hemp and flax are the most commonly used bast fibres.

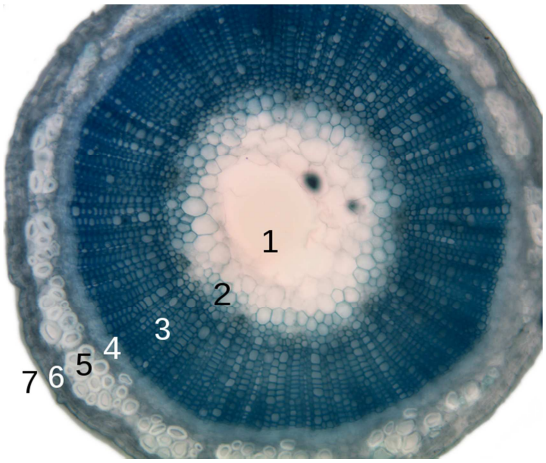

Figure 2.3: *Cross section of flax stem (McKenzie, 2006)*

Leaf fibres are obtained from the leaves of certain plants. They tend to be harder, stiffer and coarser in texture than bast fibres, since they provide the strength and rigidity in the leaf (Bentur and Mindess, 2007). These fibres are surrounded by cellular tissue and gummy substances that are removed during the processing of the leaves.

Seed and fruit fibres can collectively be called surface fibres. These fibres are single cell fibres found on the surface of seeds, stems and fruit.

2.2.2 Chemical composition

All vegetable fibres covered in this report are cellulosic fibres, i.e. their major chemical component is cellulose. Apart from cellulose, hemicellulose, lignin and pectin are the basic chemical components in vegetable fibres (Singh, 2010). This molecular structure is often called a lignocellulosic structure.

Rong et al. (2001) and Singh (2010) describe a single vegetable fibre as essentially being a composite in which rigid cellulose fibrils are embedded in a matrix of soft lignin, hemicellulose, pectin and other substances. Cellulose, a simple sugar, has been shown to be a long-chain natural polymer.

Lignin keeps water in fibres, acts as a stiffener and protects the fibre from biological attack. It is non-crystalline and can be broken down in an alkaline environment (Bentur and Mindess, 2007). Higher lignin content typically leads to a lower quality fibre in terms of mechanical performance (Singh, 2010).

Hemicellulose is believed to ensure compatability between cellulose and lignin (Kalia et al., 2011). In natural fibres, hemicellulose is rarely ever crystalline and is easily broken down in an alkaline environment. Bentur and Mindess (2007) state that both lignin and hemicellulose have a much lower degree of polymerization (DP) than cellulose. Pectin, a polysaccharide common in the cell walls of all terrestrial plants, has a higher DP than hemicellulose, but a considerably lower DP than cellulose (Hardwick, 1992).

Cross-linking of the cellulose bonds relies on hydrogen-bonds. More cellulose chains and hydrogen bonds produce more crystalline regions, which produce longer and stronger fibres (Singh, 2010).

Table 2.2 shows the chemical composition of various vegetable fibres.

Table 2.2: *Chemical composition of vegetable fibres (as % of dry mass)*

Fibre	Cellulose	Hemicellulose	Lignin	Pectin	Fat, wax and extractives	Reference
Abaca	70.2	21.7	5.6	0.6	0.4	*1
Coir	35.6-36.7	15.2-15.4	32.5-32.7	4.7-5.1	3.0-3.1	*1
Cotton	91.8-95	5.7-6.3	-	0-1.2	1.8-2.3	*1, *2
Flax	62-71.2	16-18.5	2-2.5	1.8-2	3.1-3.2	*1, *2
Jute	59-71.5	12-13.3	11.8-13.1	0.2-4.4	1.2	*1, *2
Hemp	67-78.3	5.4-18	2.9-3.3	0.8-2.5	0.0-0.7	*1, *2
Kenaf	65.0	13.0	21.6	-	-	*2
Ramie	68-76	13.0-14.0	0.6-0.7	1.9-2.1	0.3	*2
Sisal	73.1	13.3	11.0	0.9	1.6	*1, *3

**1 – (Van Dam, 2002); *2 – (Singh, 2010); *3 – (Müssig, 2010)*

Sources vary somewhat with regard to the chemical composition of vegetable fibres. The chemical composition of a fibre can vary due to cultivation conditions, retting conditions (see Section 2.2.7) and plant variety.

There are also confusing naming methods that are sometimes used. For example, a fibre such as sisal is recovered from the variety of *agave* plants called *sisalana*. The term “sisal”, however, is often used in literature to describe fibres from all three varieties of *agave* and can have different physical and mechanical properties. This can lead to large variability in information obtained from literature. To avoid confusion, these fibres are sometimes classified according to country or district of origin (Hardwick, 1992).

2.2.3 Morphological structure

The morphological structure of different vegetable fibres can vary somewhat. In this section, the basic structure of most fibres is explained.

Figure 2.4 illustrates the structure of a natural fibre cell. The cell wall is not a homogenous membrane, but rather has a layered structure (Kalia et al., 2011). The primary wall is the first layer deposited during cell growth and encircles the secondary wall. The cellulose fibres in the primary wall are disorderly arranged. The fibre is hollow in the centre (the lumen).

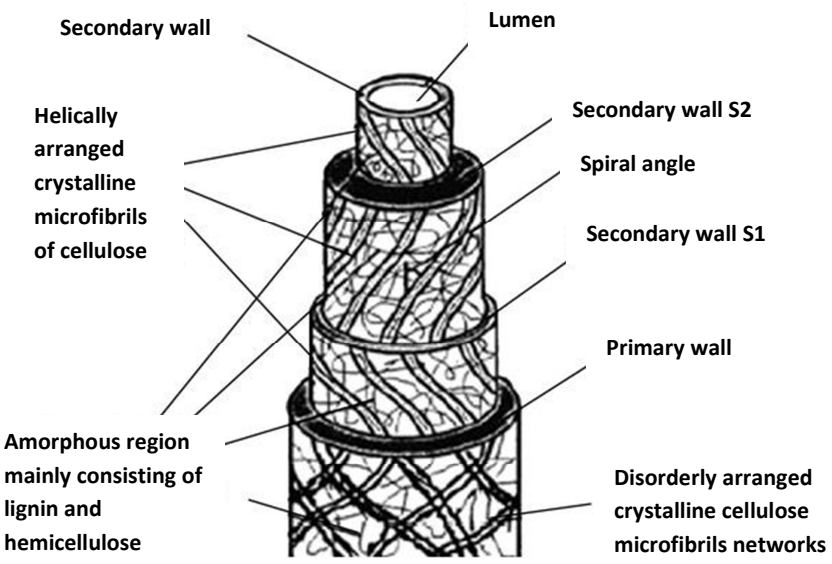

Figure 2.4: Structure of a natural fibre cell (Rong, 2011)

The secondary wall consists of three layers, with the middle layer (S2) making up around 80% of the total wall thickness and contributing most towards the mechanical properties of the fibre (Rong 2011). Kalia et al. (2011) have reported that the secondary wall consists of helically wound microfibrils with the angle between the fibre axis and the microfibrils called the microfibular angle. This angle varies from fibre to fibre. Uncoiling the spirals consumes large amounts of energy and is one of the predominant failure modes. The fibre tensile strength and modulus of elasticity is highly dependent on this angle, with a zero angle leading to the highest values. Microfibrils are composed of cellulose molecular chains and are linked together with hemicellulose (Tolêdo Filho et al., 2009).

Figure 2.5 shows that a single fibre can consist of many cells that are linked together through the middle lamella, which consists of hemicellulose and lignin (Bentur and Mindess, 2007). The cross-section shape and number of cells per cross-section can vary widely by fibre type.

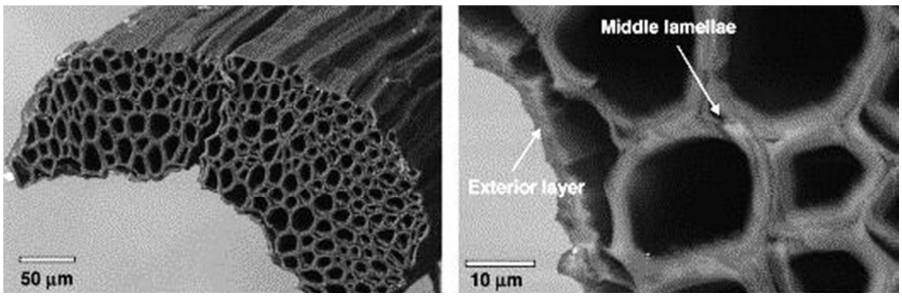

Figure 2.5: *Sisal fibre morphology showing: (a) fibre consisting of fibre-cells joined by the middle lamella and (b) the middle lamella and exterior layer (Silva et al., 2010)*

2.2.4 Physical properties

This section discusses the physical properties of various natural fibres. These properties are listed in Table 2.3. As with the chemical composition, the physical properties tend to have a high variability. This can also be attributed to varying cultivation and retting conditions as well as different cultivars. As a result Table 2.3 should be interpreted with care.

Table 2.3: *Physical properties of various natural fibres*

Fibre	Fibre bundle length [mm]	Single Fibre length [mm]	Fibre bundle width [µm]	Single fibre width [µm]	Reference
Abaca	2500-3500	6	500-750	10-46	*1
Coir	330	2.5	20-500	20	*1, *2, *3
Cotton	n/a	15-56	n/a	14-21	*4
Flax	250-1200	3-55	n/a	32	*1, *2, *4
Jute	175-3600	1-6	n/a	15-20	*1, *2, *4
Hemp	1000-3000	20-28	n/a	22-34	*1, *3, *4
Kenaf	900-1800	2-4	n/a	14-33	*4, *5
Ramie	1500	40-250	n/a	16-64	*4
Sisal	600-900	3	50-400	20	*1

**1 – (Müssig, 2010); *2 – (Owens, 2009); *3 – (Brouwer, 2000); *4 - (Singh, 2010) ; *5 – (Sen and Jagannatha Reddy, 2011)*

Fibre bundle length is the most important physical property listed in Table 2.3. These bundles are what are left over after extraction and this is the actual fibre length that is worked with. The single fibres are bonded by various gummy substances to form bundles.

2.2.5 Mechanical properties

The mechanical properties of various natural fibres are discussed in this section. These properties are listed in Table 2.4. The mechanical properties of polyester, polyethylene and polypropylene fibres typically used for concrete reinforcement are listed for comparative purposes.

When comparing the tensile strength of the fibres it is clear that cotton, flax, hemp, kenaf, ramie and sisal all fall in the range of that of the synthetic fibres (polyester, polyethylene and polypropylene).

The modulus of elasticity of all the natural fibres is considerably higher (up to 28 times higher) than that of the synthetic fibres, with the exception of cotton and sisal. Flax and hemp fibres are the stiffest fibres by a wide margin (70-100GPa). The comparatively high tensile strength and stiffness of natural fibres can be attributed to the orientation and bond strength of their main components (Yarenko, 2012).

Coir is the only natural fibre with a maximum elongation that is comparable to that of the synthetic fibres, although several others have moderate deformability which may benefit structural applications.

Table 2.4: *Mechanical properties of various natural fibres*

Fibre	Tensile strength [MPa]	Density [g/cm^3]	Modulus of elasticity [GPa]	Elongation at break [%]	Moisture absorption [% by mass]	Reference
Coir	120-200	1.12-1.15	19-26	10-25	93-180	*1,*2
Cotton	287-800	1.27-1.6	5.5-12.6	7-8	-	*3,*4
Flax	840	1.4-1.5	100	2.7-3.2	180	*2
Jute	250-350	1.02-1.4	26-32	1.5-1.9	150-190	*1,*2
Hemp	690	1.4-1.47	70	3-7	85-105	*4
Kenaf	930	1.4	53	1.6	-	*4
Ramie	400-900	1.4	61.4-128	1.2-3.8	60-70	*4
Sisal	280-750	0.8-1.45	9.4-26	2.5-5.0	60-110	*1,*2,*5,*6
Polyester	230-1100	1.34-1.39	17	12-150	0.4	*2
Polyethylene	75-590	0.92-0.96	5	3-80	Nil	*2
Polypropylene	140-700	0.9-0.91	3.5-4.8	15	nil	*2

**1 – (Bentur and Mindess, 2007); *2 – (Yarenko, 2012); *3 – (Singh, 2010); *4 – (Anandjiwala, 2006); *5 – (Müssig, 2010); *6 – (Kuruvilla et al.)*

The moisture absorption of natural fibres compare very poorly to that of synthetic fibres. Large moisture absorption can lead to a dimensionally unstable fibre that can have great deformations as water is absorbed and lost. Sisal and Ramie fibres compare most favourably to synthetic fibres with respect to water absorption.

In the light of all the mechanical properties, of which tensile strength is most important, it seems as though hemp, kenaf, ramie and sisal fibres are most suited for use in structural applications.

2.2.6 Cultivation

This section discusses how and where different natural fibres are typically cultivated.

Abaca

Abaca leaf fibre, otherwise known as Manila hemp, comes from the perennial *Musa textilis* plant. It belongs to the Musaceae family, which includes the banana plant. The plant closely resembles the banana plant in appearance and they can easily be mistaken for each other (Kirby, 1963).

The plant is indigenous to the Philippines (Cook, 1984), which is where the majority of abaca fibre comes from. The plant is also cultivated for its fibres in Ecuador, although to a much lesser extent (Müssig, 2010).

The *M. textilis* plant can grow in a wide range of conditions, but for the best fibre properties and yields it requires annual rainfall of 2000 – 4000 mm (Kirby, 1963) evenly spread out over the year. It also requires proper drainage, a mean annual temperature of 27 to 29°C and humidity in the range of 78 – 88% (Brosens, 1982). It grows best in sloped mid-mountain regions at heights up to 500 m above sea level, where it requires little input and does not compete with food crops (Müssig, 2010).

The first cutting is taken within two to three years of planting and a good yield is obtained for five to six years before starting to decline (Catling and Grayson, 1982).

The fibre is extracted from the leaf sheath around the trunk of the plant. Depending on variety, climate, soil type and planting density, dry fibre yields can vary between 600 and 1200 kg per hectare (Müssig, 2010).

The abaca plant can be cultivated in Southern Africa, but due to poorly suited climatic conditions sufficient fibre quality and yield cannot be obtained (Jacobz, 2012).

Coir

Coir fibre comes from the husk of the coconut palm (*Cocos nucifera* L.). The coconut palm is economically the most important of all the cultivated palms, occupying an estimated 12.17 million hectares globally and producing around 57 billion nuts annually (Müssig, 2010).

The coconut palm grows best in the tropics in regions with average temperatures between 20 and 32°C, altitudes ranging from sea level to 600 m above and with rainfalls between 1500 and 2500 mm annually. The Philippines, Indonesia, India and Sri Lanka are the top coconut producers in the World (Müssig, 2010). Although the coconut palm grows well in many African countries, it is only in Tanzania that the plant is cultivated for its fibre.

As can be seen in Figure 2.6 the coconut fruit has a large seed in the middle, surrounded by an exocarp and a fibrous mesocarp. The exocarp end mesocarp combined is called the husk and can vary in thickness from 2 to 5 cm (Müssig, 2010).

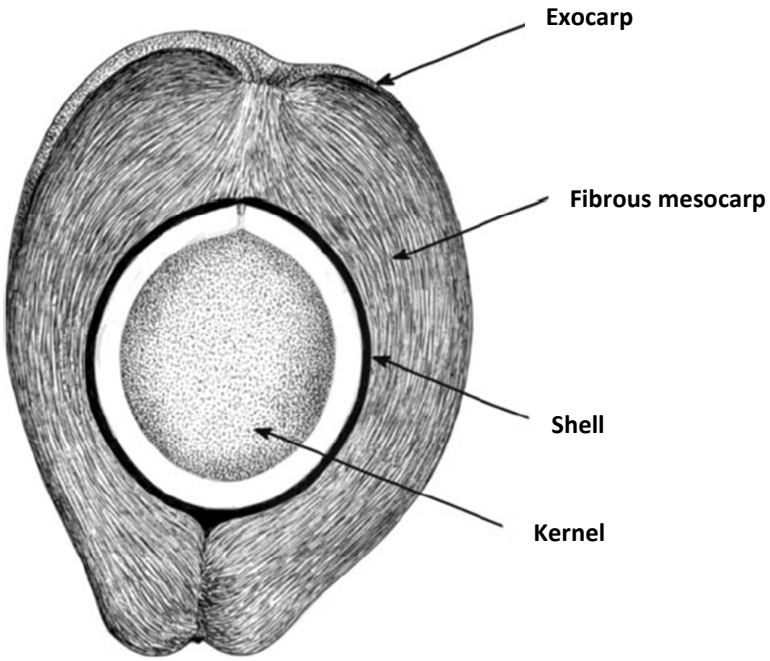

Figure 2.6: *Cross-section of a coconut (Müssig, 2010)*

For the best fibre yield and mechanical properties, coconuts are harvested just before they are ripe. When the fruit is split, the fibres can be found in the mesocarp. Coir fibres can be classified according to length – short (30 - 69 mm), medium (70 – 135 mm) and long (> 135 mm). Müssig (2010) states that the ratio of yield of long to medium to short fibres is more or less 60:30:10. Coconut sizes vary considerably due to different climatic and soil conditions, but on average 30% of a coconut consists of fibre on a dry mass basis.

According to Kirby (1963) the coconut palm takes seven to ten years to reach maturity and delivers between 70 and 100 nuts per year.

Jacobsz (2012) mentions that coconut palms for coir fibre cannot be cultivated in South Africa due to the unsuited climatic conditions, although there is potential for cultivation in the coastal areas of Mozambique.

Cotton

Cotton is the most important fibre in the world, used mainly in the textiles industry. Unlike most bast and leaf fibres, cotton is not produced by the plant as part of its skeleton structure. Cotton comes from the seeds of plants of the Malvaceae family (Cook, 1984). Many species have been identified, although only four are cultivated commercially. The *Gossypium hirsutum* variety accounts for 97% of world production (Müssig, 2010). It's difficult to say where it originated, although evidence has been found of cotton use in Egypt in 12000 B.C. (Cook, 1984).

In 1960, cotton represented 60% of all fibres consumed in the world. By 2009, due to advances in non-cotton fibre production techniques, the share had dropped down to 38% (Müssig, 2010).

More than fifty countries plant 10 000 hectares or more of cotton every year. Cotton is a true developing country crop, with only 13% of cotton cultivation area situated in developed countries. Since 1950/51 worldwide production has increased from 6.5 million tons fibre to 26.3 million tons in 2007/08. Since the production area has remained more or less constant, this increase can be attributed to higher yields due to better cultivation techniques and higher yielding plant strains (Müssig, 2010).

Cotton is mostly cultivated in the warmer regions of the world. It requires six to seven months of warm weather, lots of sunshine and appreciable amounts of rainfall. The plants can be annuals or perennials (Brosens, 1982).

In South Africa, cotton is usually planted in October and is harvested 200 days later. Cotton can be handpicked (giving better quality) or machine harvested. This usually depends on labour costs (Müssig, 2010).

The majority of cotton produced worldwide in 2011 came from China, USA, Brazil, Pakistan and India, with the bulk of processing being done in China. Egypt, Burkina Faso, Cameroon and Zimbabwe were the largest producers in Africa (National Cotton Council of America, 2012).

In South Africa, there are about 450 commercial farms and 2000 to 3000 small-scale farmers using more or less 20 000 hectares for cotton cultivation. Competition from other African countries has increased over the last few years and many farmers are leaving the cotton industry to focus on other, more lucrative crops (MyFundi, 2010).

Estimating fibre yield is difficult in that it varies widely by region and whether it is irrigated or rain fed (Müssig, 2010).

Flax

Flax fibre comes from the *Linum usitatissum* L. plant, a member of the Linacceae family. It is an annual plant and the fibre is used mainly to produce linen. Kvavadze et al. (2009) has identified tools containing 30 000 year old flax fibres, indicating that these fibres have been used for at least as long.

Two types of flax is grown worldwide – seed flax and fibre flax. Seed flax gives coarser fibres, since the stem does not grow straight, but divides towards various flower heads (Bos, 2004). Fibre flax gives thin, strong fibres.

According to Kirby (1963) flax is widely cultivated in temperate and sub-tropical areas. The majority of fibre flax is grown in Europe and Asia, with China, Russia, France and Belarus being the top producers in recent years (Kaith, Kalia and Kaur, 2011).

When cultivating flax, good climatic conditions are more important to fibre quality than favourable soils (Kirby, 1963). Proper flax cultivation requires a temperate and equable climate, free from heavy rains and frost. A hot, dry summer produces a shorter, stronger fibre, while a moderate, moist summer would produce a finer, more silky fibre. Flax grows best in similar soil conditions as wheat requires (Jacobsz and Van der Merwe, 2010). Flax have been shown to be an excellent alternative rotational crop to wheat in winter rainfall regions

Unlike most other fibre crops, flax is pulled from the ground rather than cut down. This saves the flax from deteriorating at the point of cut. Also, on average 150 mm of the stem goes to waste when cut. Machines have been developed for pulling flax, which greatly reduces the amount of labour needed for harvesting (Kirby, 1963).

Under South African conditions, fibre yields average about 25% by mass, which equates to about 2 ton fibres per hectare (Jacobsz and Van der Merwe, 2010). The yield can be up to 7 tons fibres per hectare in favourable conditions (Agricultural Research Council, n.d.(b)).

Hunter (2012) has stated that flax is currently at agricultural research stage in South Africa. Only about 500 ha is cultivated in the Overberg area (Jacobsz and Van der Merwe, 2010). According to Cawdry (2012) flax has been grown commercially in the North-West province, but the venture has proved to be commercially unsustainable. Large parts of the Western- and Eastern Cape provinces have been identified as suitable for the cultivation of flax (Jacobsz and Van der Merwe, 2010).

Hemp

Industrial hemp (or just hemp) fibre comes from the bast of the *Cannabis sativa* L. plant, a member of the Moraceae family. It originated in Central Asia and has been grown in China for at least 4500 years (Kirby, 1963). Hemp is the cousin of marijuana (or dagga as it is known in South Africa) and, although they are from the same species, hemp is grown for its fibre, while marijuana is grown for its psychoactive tetracannabinol (TCH) content. Most industrial hemp has a THC content of less than 0.3%, while marijuana has a THC content of 5 - 10% (Müssig, 2010).

The *C. sativa* plant is grown for its psychoactive properties in tropical regions and for its fibre in temperate regions. When cultivated for its fibre it also requires a humid atmosphere and a rainfall of at least 675 mm per annum (Kirby, 1963).

Many types of hemp strains have been produced over the years and some of these are able to adapt well to changes in terrains and climates. They can endure considerable changes in temperature and frost only negatively influences very young plants (Kirby, 1963).

During its growing season, hemp seems to exhaust the soil, although most of what's taken out is replaced after the plants are cut down (Kirby, 1963). The crop requires little or no biocides and fertilizers, suppresses weeds efficiently and has limited demand for crop rotation (Struik et al., 2000). Rotation of hemp crops is, however, beneficial to many other crops (Müssig, 2010).

Plant density greatly impacts the yield and quality of fibre. When cultivated for fibre, a very high plant density is required (50 – 75 plants/m^2). When cultivated for the drug, the optimum density is closer to 10 plants/m^2 (Müssig, 2010). Fibre strains tend to have long, straight stalks and very little branching. This, together with a high planting density, can lead to very large yields (Kirby, 1963).

In 1998 average yield in Ontario, USA, was 6.1 ton dry, retted stalks per hectare. In the same year the average yield in Kent County, USA was 8.5 ton/ha (Baxter and Scheifele, 2009). In 2002 the average yield in the European Union was 6 ton/ha (Karus, 2004). Approximately 2 – 3 tons of fibre can be extracted from 3 – 4 tons of dry, retted stalks (Baxter and Scheifele, 2009).

Cultivating hemp is currently illegal in South Africa, although the fibre itself is not. The Department of Agriculture, Forestry and Fisheries (DAFF) and the private sector is working on new legislation that might legalise the cultivation of fibre hemp in the future (DAFF, 2010). It is already legal in over 30 other countries (Müssig, 2010).

According to Budden (2007) one of the main obstacles towards hemp legalisation in South Africa is the legislation that will allow DAFF to manage industrial hemp as an agricultural crop. Thereby, it will

be separated from the psychoactive/medicinal strains that will remain under the control of the Department of Health. Struik et al. (2000) has, however, stated that it is impossible to distinguish between psychoactive and fibre strains before seed set without costly detailed analysis. This complicates the policing of the crop.

According to Jacobsz (2012) there are some experimental farms scattered across South Africa where the Agricultural Research Council (ARC) are doing tests on adapting strains for local conditions. These farms are situated in the Western Cape, Eastern Cape and the North West Province. The ARC has stated that a hybrid strain has been developed for local conditions with yields on par with the best strains being cultivated in Europe (ARC, 2010)

Jute

Jute is an annually grown bast fibre coming from the plants of the genus *Corchorus.* Two species of *Corchorus*, namely *C. capsularis* L. and *C. olitorius* L., are cultivated for their fibres (Kirby, 1963). The fibres have been used since prehistoric times and probably originated in the Mediterranean. It was subsequently taken to India and was found to flourish in the hot, damp regions of Asia (Cook, 1984). Bangladesh and India are the largest jute fibre producers in the world, together accounting for over 90% of total world production (Müssig, 2010).

The jute plant requires rainfall of more than 1000 mm annually, a relative humidity of 65 - 95% and temperatures ranging between 21 and 38°C. It is grown in the rainy season. Müssig (2010) states that the crop is very labour intensive to cultivate, but requires few pesticides and fertilisers. The roots of the jute plant can extend more than 30 cm into the ground, and consequently requires deep ploughing to remove the stubble from the previous year's crop (Cook, 1984). Jute is typically harvested after 100 to 135 days (Müssig, 2010).

According to Kirby (1963) the jute plant yields, on average, 8% of its green weight in dry fibre (around 1400 kg dry fibre per hectare).

Studies have found that one hectare of jute uses about 15 tons of carbon dioxide (CO_2) while releasing about 11 tons of oxygen (O_2). Its CO_2 assimilation rate is several times higher than that of trees and during the agricultural stage it is carbon negative (Müssig, 2010).

Jacobsz (2012) states that jute cannot be cultivated anywhere in Southern Africa, due to unsuited climatic conditions (mainly due to insufficient and uneven rainfall).

Kenaf

Kenaf fibre is extracted from the *Hibiscus cannabinus* L. plant, a member of the Malvaceae family, the same as cotton. From a fibre point of view, it is the second most important member of the Malvaceae family. The plant is an herbaceous annual that can grow up to 3.6 m (Kirby, 1963).

H. cannabinus is a warm season annual crop. It originated in ancient Africa and is now cultivated almost exclusively in Asia and some parts of Latin America. In the textile industry, kenaf fibres have often been used to substitute jute, as it has very similar fibre properties and cultivation conditions. The plant matures in 120 – 130 days, after which it is harvested and the fibres are extracted (Raji, 2007). The Food and Agriculture Organization (FAO, 2009) has stated that, under favourable conditions, kenaf fibre yields can be up to 2.3 tons per hectare.

Currently, Sustainable Fibre Solutions (SFS) is the only company cultivating kenaf in South Africa, albeit on a limited scale (Jacobsz, 2012). Kirby (1963) has stated that kenaf was cultivated in South-Rhodesia (now Zimbabwe) and Mozambique in the 1950's.

Ramie

Ramie fibres come from the stem of the plants of genus *Boehmeria*. There are many species of *Boehmeria* cultivated around the world, although the *B. nivea* seems to be the most important (Singh, 1998). The plant is of perennial nature and is also widely known as "China grass".

China is the top ramie producer in the world. It is also cultivated in Japan, Taiwan, The Philippines and Brazil (Singh, 1998).

The ramie plant prefers warm, moist climates and sandy, loamy soils. It is negatively affected by frost and strong winds (Kirby, 1963). The plant usually lasts about five years and can be cut four times a year. The fibre yield varies from year to year, with the largest yield usually occurring in the third year and the smallest yields in years one and five. The fibre yields can be anything between 500 and 1200 kg/ha, with an average of 4500 kg/ha over a lifetime of five years (Singh, 1998).

Kirby (1963) reports that ramie grows in a wide range of conditions, but in slightly unfavourable conditions the fibre yield goes down considerably. The plant requires a large amount of relatively skilled labourers and fertilizers to ensure a high fibre yield.

Ramie fibres have a high pectin concentration. Because of this, ramie stems are not retted like other bast fibres, but rather decorticated (see Section 2.2.7). After decortation, the resultant fibres still contain 25 - 30% gummy substances and proper degumming is crucial to obtaining fibres with good mechanical properties (Singh, 1998).

Jacobsz (2012) states that ramie cannot be cultivated anywhere in Southern Africa, due to unsuited climatic conditions (mainly insufficient and uneven rainfall).

Sisal

Sisal fibre is a leaf fibre that comes from the *Agave sisalana* plant (Figure 2.7). In South Africa the plant is widely known by its Afrikaans name of "garingboom", although this name is often used to refer to all *Agave* varieties due to their similar appearance. It is a member of the *Agavacae* family of which three genera (sisal, fourcroydes and cantala) are commercially grown for its fibres (Hardwick, 1992). However, only sisal has been identified as a viable candidate for use in composites. Sisal is a very labour intensive crop to cultivate.

Bith Cook (1984) and Catling and Grayson (1982) mention that the plant originated in Mexico, but has successfully been cultivated commercially in Brazil, India, Indonesia, Haiti, East Africa and China. Brazil and China have been the largest producers in recent years, with Brazil having a 43% and China a 24% share of world production (FAO, 2009). Kenya, Tanzania, Madagascar and Mozambique all produce sisal fibres and together accounted for about 26% of world production in 2008. Sisal fibres are found in the leaves, meaning a plant can be harvested many times over, instead of only once as with bast fibre plants.

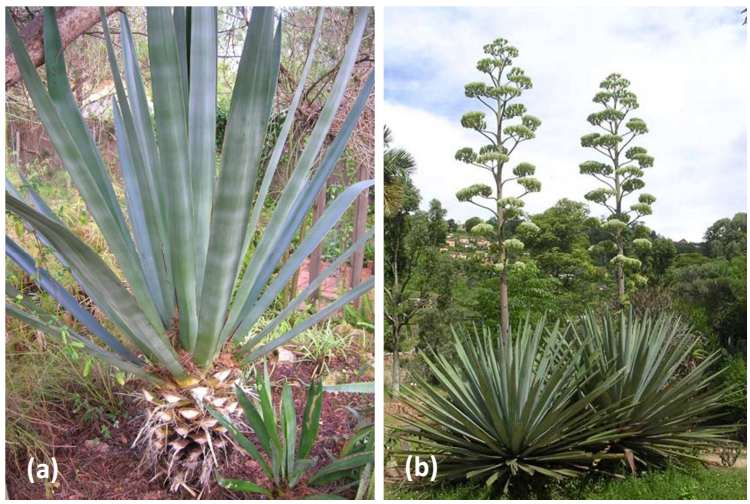

Figure 2.7: *Sisal plant (a) after having its leaves cut (Recregarden, n.d.) and (b) with its distinctive flowering spike*

In the 1970's and 1980's, sisal was successfully cultivated at small scale in certain parts of South Africa (Brosens, 1982). In 1974 South Africa produced 9000 tons of sisal fibre. More recently, however, the industry has shrunk considerably. Between 2002 and 2008 the production was closer to 1600 ton fibre, or about 0.6% of world production) (FAO, 2009). DAFF (2004) has stated that this is

predominantly as a result of high labour costs. According to Jacobsz (2012) there are two new projects in the Limpopo and North West Provinces of South Africa that have recently been initiated to kick-start the sisal industry once again.

Kirby (1963) has stated that the life expectancy and yield of sisal plants is mostly dependant on the soil conditions and climate in which it is grown. The sisal plant can be cultivated in many different soil conditions, but prefers dry, permeable, sandy-loam soils. It will grow at altitudes ranging from sea level to 2000 m. In East Africa sisal grows best in rainfall regions that range between 1000 and 1300 mm per annum, although the ARC (2010) has found that 500 mm per annum is suitable in South African conditions. Sisal plants are not frost tolerant.

Sisal leaves have an average fibre content of 3% by weight. In South Africa sisal plants can be harvested from year five to year twelve, with an average yield of 4 tons fibre per hectare (or 250 leaves) over its lifetime (ARC, 2010). In East Africa, harvesting has been reported to begin as early as year three (Kirby, 1963). Each leaf contains about 1000 fibres.

Sisal fibres are used mainly to produce rope, carpets, paper and geotextiles. In recent years it has been used increasingly as an asbestos and fibreglass replacement in the automotive industry (Müssig, 2010).

2.2.7 Extraction of fibres

Natural fibres can be extracted in various ways. Bast fibres are typically extracted by a bacterial process called retting. Leaf fibres are extracted by a scraping process, while seed and fruit fibres are often removed by a soaking process.

Retting

Retting is an extraction process which uses the combined actions of bacteria and moisture to dissolve the cellular tissue surrounding bast fibres (Bentur and Mindess, 2007). This is done to facilitate the separation of the fibre from the stem.

According to Kholiya et al. (2011) water retting is the most commonly used retting process. Bundles of stalks are submerged in water. The water penetrates to the central stalk and swells the inner cells, causing the outermost cellular layers to burst. The result is an increase in absorption of moisture and decay-producing bacteria.

The retting time is crucial to obtaining good fibre properties. Under-retting can result in difficult fibre separation, while over-retting can reduce the strength of fibres significantly. Double retting is a

process yielding favourable fibre properties, whereby the stalks are under-retted, dried for several months and then retted again.

In developing countries bast fibres are commonly naturally water retted, whereby fibre bundles are weighted down in stagnant or slow-moving waters, such as ponds and streams. Kholiya et al. (2011) state that water retting can take between 8 and 14 days, depending on water temperature and mineral content.

Dew retting is a process popular in areas with limited water resources. It is most effective in climates with ample night-time dew and warm day-time temperatures. The combined action of the sun, air, bacteria and dew causes a fermentation process that dissolves the cellular material surrounding the bast fibres. Dew retting typically takes between two and three weeks and the fibres are generally of poorer quality than those attained through water retting (Kholiya et al., 2011).

Tank retting is a process whereby retting is done in tanks and water quality and temperature can be controlled (Kholiya et al. , 2011). It takes four to six days to complete and usually produces fibres of more uniform quality. This method is feasible in any season and waste retting water is often used as liquid fertilizer.

The retted stalks are dried in open air or by mechanical means and stored for a short period to facilitate fibre removal. The brittle, woody stalks are then broken by hand or machine. Finally, fibres are separated from the stalks by hand.

Scraping

Scraping is mostly performed on the harder leaf fibres, such as sisal. Leaves are crushed and scraped using a decorticator machine (Figure 2.8). This is followed by either a machine or sun drying process. The cellular tissue surrounding the fibres is removed during decortication. Decorticators vary widely in size, function and quality of end product. Therefore, it will not be discussed in detail.

Figure 2.8: *Mechanical sisal decorticator in Kenya (TED Blog, 2012)*

Soaking

Surface fibres such as coir and cotton are usually extracted by soaking the husks in water to soften them, crushing the material and tearing it with spikes to separate out the long fibres (Cook, 1980). Many fibres tend to break as a result of the tearing process.

2.2.8 Durability of fibres

NFRCC undergo an ageing process in which they tend to lose strength and toughness, especially in humid environments. According to Davis (2011) the coastal regions of South Africa have a mean annual relative humidity (RH) of 60-80%, while the mean RH of the inland regions varies between 40 and 60%. Thus, fibre degradation would be a larger problem in the coastal areas of South Africa.

Tolêdo Filho el al. (2002) has stated that these durability problems are associated with an increase in fibre fracture and decrease in fibre pull-out, mainly due to the weakening of fibres by alkali attack, fibre mineralisation due to migration of hydration products to voids and volume variations due to the high moisture absorption. All these actions tend to lead to fibre embrittlement.

Fibre sealing and impregnation

Several approaches have been studied over the past two decades to enhance the durability of these fibres. Gram (1988) tried impregnating various fibres with blocking agents (like sodium silicate, sodium sulphate and magnesium sulphate), but none offered a significant improvement to fibre durability in a cement matrix.

Gram also tried impregnating fibres with water repelling agents (such as formine and stearic acid). This slowed down the embrittlement process, but could not prevent mineralisation.

Berhane (1994) found that sealing the matrix pores, adding small beads of wax or zink stearate powder to fresh concrete or impregnating the hardened concrete with sulphur led to favourable results. Sealing the pores reduced the porosity and water absorption of the matrix, slowing down, but not preventing, the embrittlement process.

Alkaline attack

As stated earlier, natural fibres can also suffer a loss of durability due to attack from an alkaline environment. The pH of concrete pore water is typically about 12.5 (Owens, 2009). Bentur and Mindess (2007) have stated that much research has been devoted to this topic and it has been concluded that the effect of alkalines on natural fibres can vary somewhat by fibre and alkaline type. It was found that the tensile strength of coir fibre was affected only slightly, while there was a sharp drop in the strength of sisal, hemp and jute fibre. Singh (1985) established that the degree of alkaline attack was greater in calcium hydroxide (CH) solution than in sodium hydroxide solution, even though the pH of the latter is higher. It has been speculated that the presence of Ca^{2+} ions could cause crystallisation of lime in the pores and lumens of fibres, leading to further degradation.

Gram (1988) has proposed two mechanisms of alkaline degradation in natural fibres:

1) A peeling off effect, whereby the ends of molecular chains are unhooked and end groups are freed from chains. This effect, however, is very small at temperatures under 75°C (Bentur and Mindess, 2007).
2) Alkaline hydrolysis, which causes the degree of polymerization to reduce drastically and molecular chains to divide. Hemicellulose and lignin is most influenced by this effect.

Moisture absorption

As stated in Chapter 2.2.2, a natural fibre can essentially be described as a cellulose fibril composite embedded in a matrix of soft lignin, hemicellulose and other substances. Hemicellulose and lignin are hygroscopic thermoplastic substances and are, therefore, highly influenced by changes in temperature and humidity.

Nevell and Zeronian (1984) found that, with increasing moisture content, the torsional stiffness of various natural fibres decreased by about 50% (with an increase in RH of 25% to 90%). It was concluded that this effect was due to the softening of the hemicellulose wall. This reduction in stiffness was only 11% in the longitudinal direction.

The tensile strength of natural fibres is often lower when relatively dry (Ni, 1995). This is due to a poor stress distribution in dry fibres. The failure mechanisms for natural fibre reinforced concrete

(NFRC) under different fibre moisture conditions was found to be fibre fracture (when dry) and fibre pull-out (when saturated).

Pacheco-Torgal & Jalali (2011) have stated that water absorption in fibres can lead to volume changes that can cause cracking in concrete. Contrary to this, Ramaswamy, Ahuja and Krishnamoorthy (1983) found that jute, coir and bamboo fibres did not show any volume changes after absorbing between 120 and 180% water by mass.

Biological attack

The possibility exists of bacterial and fungal attack in moist and humid environments. Bentur and Mendess (2007) notes that researchers have studied natural fibre behaviour under these conditions and found considerable differences between the performance of various fibres.

In tests of cementitious composites under conditions that were thought to promote biological attack, the fibres indicated immunity to degradation from biological attack. It is thought that the alkaline nature of the matrix provides resistance to this kind of degradation (Bentur and Mindess, 2007).

2.3 Matrices used for natural fibre reinforced concrete

The problem of fibre durability can primarily be addressed in two ways: fibre treatment (to prevent alkaline attack and mineralisation) or reduction of the matrix alkalinity (and CH content). For this research the method of reducing matrix alkalinity was chosen. This section discusses the method.

Several authors have discussed reducing the alkalinity of the matrix through the addition of pozzolanic materials. Tolêdo Filho et al. (2002) have stated that the addition of high alumina cement, silica fume, slag, fly-ash and natural pozzolans such as pumice rice husk ash, have been studied in order to find its effect on the alkalinity of concrete. Replacing 45% of cement with silica fume led to a significant reduction in loss of toughness. According to Mohr, Nanko and Kurtis (2005) silica fume replacement of 17% and 33% of cement by weight led to a reduction of pore water pH from 13.2 to 12.9 and 12.0, respectively.

Matrices containing high alumina cement and natural pozzolans showed a vast improvement as well. Replacement of cement with slag showed no significant improvement, even with large quantities as much as 40% (Tolêdo Filho et al., 2002). Replacement with fly-ash showed a slight improvement. Gram (1988) came to similar conclusions by substituting 70% of cement with slag by weight. This led to a reduction of pore water pH from 13.2 to 13. Also, no noteworthy improvement to durability was found after 120 cycles of wetting and drying.

It is apparent that some sort of cement substitution needs to be made to improve fibre durability. In South Africa fly-ash, ground granulated blastfurnace slag (GGBS) and CSF are the most commonly available pozzolans (although CSF to much lesser extent due to its cost). Prices of cementitious materials vary somewhat by region in South Africa. For the sake of simplicity Table 2.5 only shows the average cost in the Western Cape Province. The equivalent carbon dioxide (CO_2) emissions of cement and pozzolans in South Africa is also shown. The price of GGBS in South Africa is based almost entirely on the distance it needs to travel from the source. It varies from similar a price to fly-ash at the coast to almost free closer to the sources inland).

Table 2.5: *Cost and average CO_2e of cementitious materials*

Pozzolan	Cost [R/ton)	Average emission value [kg CO_2e]	Reference
Cement	1500	450-985	*1,*2
CSF	8000**	14	*3,*4
Fly-ash	950	2	*2,*5
GGBS	n/a	130	*2

1* - (PPC, 2012); 2* - (C&CI, 2011); 3* - (Sika, 2012); 4* - (Norchem, n.d.); *5 – (Ash Resources, 2012)
**Based on 30kg bags (not bulk price)

From an economical perspective, replacing cement with GGBS or fly-ash seems preferable for low-cost housing purposes. However, as stated above, GGBS makes no significant contribution to fibre durability. Adding GGBS to a matrix containing natural fibres would be done solely to decrease the amount of cement used, as it would not contribute to lowering the pH or CH content significantly. The reason GGBS was not used in this research as a cement substitute is based entirely on its the abovementioned property. Looking at emission values, CSF and fly-ash are superior. CSF does improve fibre durability substantially, but is expensive.

2.4 Concluding summary

The South African LCH sector presents many opportunities for sustainable development. Problems with currently used alternative building technologies include it being too expensive, poor management by government and municipalities, poor building quality and a general feeling of undervaluation by beneficiaries.

The LCH industry currently uses 290x140x90 mm “Maxi”- and 390x140x190 mm hollow concrete blocks as standard in the inland and coastal regions of South Africa, respectively. A proposal has been made to investigate a building technology that embraces and builds on practices currently in use by standard building methods, rather than to develop a whole new approach.

One such an approach is to reinforce concrete blocks using natural fibres. Natural fibres are obtained from the stalks, leaves, nuts and seeds of various plants and consist of cellulose, hemicellulose, lignin and various other substances in different proportions. Due to varying cultivars, cultivation conditions and extraction conditions, natural fibres tend to exhibit a large variability in physical and mechanical properties.

Some natural fibres have mechanical properties comparable to that of synthetic fibres typically used for concrete reinforcement, namely hemp, kenaf, ramie and sisal. Of these fibres sisal, hemp and kenaf are the only fibres that are cultivated in Southern Africa, albeit on a very limited scale. This is due to mostly unfavourable cultivation conditions. Hemp has been identified by the South African Government as a plant with potential for large scale cultivation, although it is currently still illegal to cultivate.

Natural fibres in a cementitious matrix tend to be susceptible to durability issues such as alkali attack and fibre mineralisation. It is especially the influence of Ca^{2+} ions in concrete pore water that seems to have a large effect on fibre durability. One way to combat these durability issues is to lower the pore water alkalinity of a matrix through the substitution of cement with highly reactive pozzolans such as condensed silica fume.

3. Materials and experimental framework

3.1 Introduction

The practical lab work performed for this research was done using the facilities of LabEST, the material testing laboratory of COPPE/UFRJ in Rio de Janeiro, Brazil. It was proposed to produce both 390x140x190 hollow and 290x140x90 mm “Maxi” blocks using three different fibre contents and an average fibre length of 10 mm. It was decided that hemp fibre would be the most promising fibre to investigate for use in South Africa, but due to a shortage at LabEST sisal fibre had to be used instead.

Two different matrix types were to be used, one with and one without condensed silica fume. Both matrix types would also contain fly-ash as partial cement substitute. The matrices would contain sand and larger aggregate.

To test the mechanical properties of the blocks it was proposed that both compression and three-point bending tests be performed. The durability tests to to be performed included testing for capillary absorption, dimensional stability, drying shrinkage, density, total water absorption and void content.

This chapter gives an overview of the materials used in testing and, where applicable, how they compare with what is typically used in South Africa. An explanation is given on how blocks were produced, including how the mixes were designed. Lastly, the experimental setup and test program that was followed, is discussed.

3.2 Material properties

The cementitious materials and aggregates used in this research are commonly found in the state of Rio de Janeiro, Brazil. In this section the physical and chemical properties of these materials are discussed and, where applicable, compared to similar materials found in South Africa.

The fibres used in this research were obtained from sisal plants cultivated in the state of Bahia, Brazil. These fibres are traditionally used for making twine, carpets and other handicrafts. This section also discusses the preparation of the fibre used.

A gas pycnometer was used to obtain the bulk densities of all aggregates and cementitious materials. Also, a Shimudzo EDX 720 Energy Dispersive X-ray fluorescence spectrometer was used to find the chemical compositions of all the cementitious materials.

The water used for the mixing of concrete was obtained from the network of the city of Rio de Janeiro. It is considered suitable for human consumption.

3.2.1 Aggregate

Different aggregates were used in the concrete mixes for the solid and hollow blocks. A 9.5 mm nominal stone size (called *brita zero* in Brazil) was used for the solid blocks. A smaller 4.8 mm nominal stone size, along with crusher dust (called *po de pedra* in Brazil) was used for the hollow blocks. The same sand was used for both block types.

The bulk densities and fineness moduli of the aggregates used are shown in Table 3.1.

Table 3.1: *Bulk densities and fineness moduli of aggregates*

Aggregate	Bulk density [g/cm^3]	Fineness modulus
Sand	2.64	2.68
Stone (9.5 mm)	2.68	5.70
Stone (4.8 mm)	2.68	4.80
Crusher dust	2.69	2.42

Figure 3.1 depicts the particle size distributions of the various aggregates. The grading was done in accordance with SANS 1083 (2002).

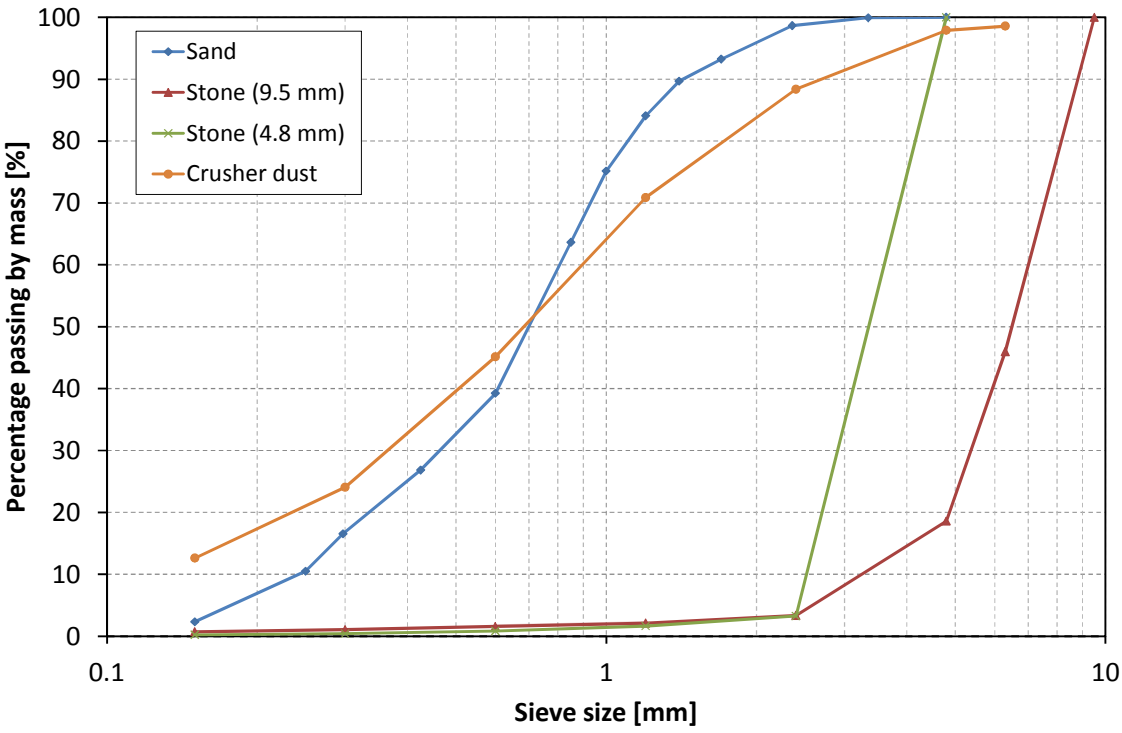

Figure 3.1: *Grading of aggregates*

3.2.2 Cement

Mauá CPV-ARI cement, manufactured by Lafarge Brazil was used for this research. It is fast reacting cement that reaches a relatively high strength in the first days of application. The clinker used is more or less the same as that used for conventional cement, although it stays in the mill for longer. CPV-ARI typically contains very little or no pozzolanic additives (Cimento.org, n.d.). It is comparable to the CEM I type found in South Africa. The ARI designation refers to a minimum 7 day compression strength of 34 MPa.

The density of the ARI cement was found to be 3.21 g/cm^3 compared to 3.14 g/cm^3 that is typical of South African CEM I. Table 3.2 shows the chemical compositions of the CPV-ARI used as well as that of typical South African ordinary Portland cement (OPC). The calcium oxide (CaO) content compares fairly well, but a typical South African OPC contains between 5 and 10% more silica dioxide (SiO_2).

Table 3.2: *Chemical composition of Brazilian CPV- ARI cement and South African OPC*

Oxide	CPV-ARI	South African OPC
	[% by mass]	
CaO	70.9	63-69
SiO_2	14.0	19-24
SO_3	5.8	-
Al_2O_3	4.3	4-7
Fe_2O_3	4.3	1-6
MgO	-	0.5-3.6
$Na_2O + 0.658K_2O$	-	0.2-0.8
K_2O	0.9	-
SrO	0.3	-
TiO_2	0.2	-
MnO	0.2	-
ZnO	0.1	-
Reference	(Grabois, 2012)	(Owens, 2009)

Figure 3.2 shows the particle size distribution of the CPV-ARI cement.

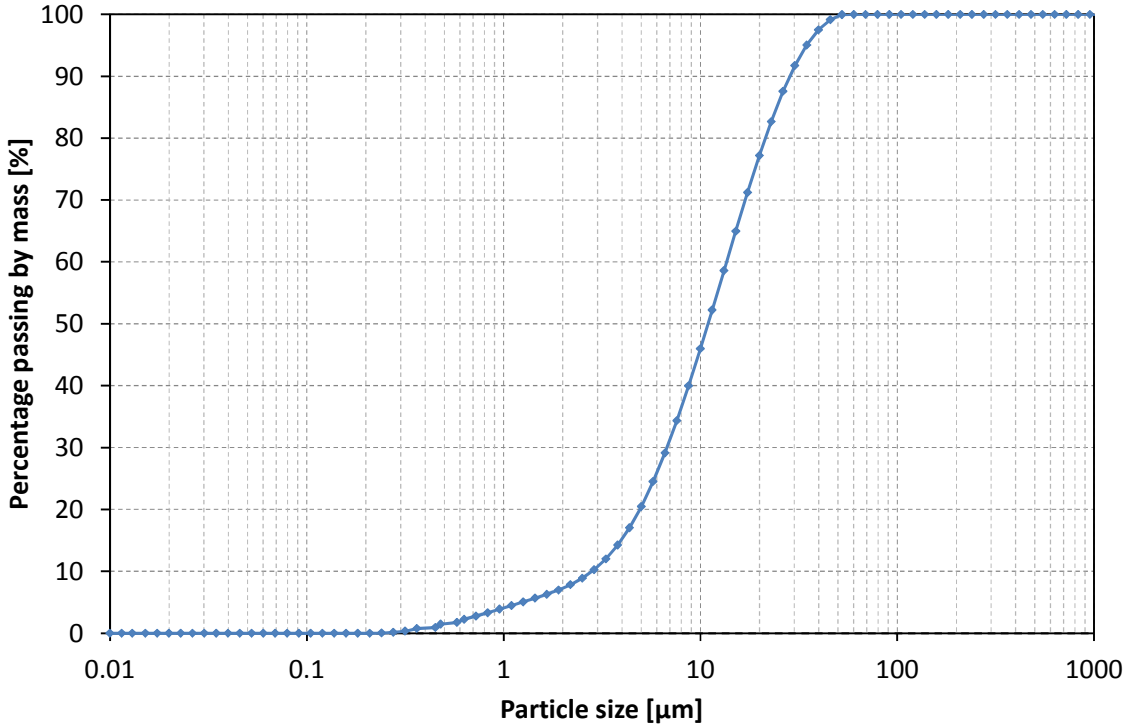

Figure 3.2: *Particle size distribution of CPV-ARI cement*

3.2.3 Fly-ash

The fly-ash used for this research was Pozofly, provided by Comércia de Conzas Lima Ltda. This is a pozzolan commonly used in the state of Rio de Janeiro in Brazil. In Table 3.3 the chemical composition of Pozofly is compared with that of DuraPozz and PozzFill fly-ash typically used in South Africa as a cement substitute. Both DuraPozz and Pozz-fill are classified as Class F (containing less than 20% CaO) and are provided by Ash Resources in Randburg. The density of Pozofly was found to be 2.28 g/cm^3 compared to 2.12-2.2 g/cm^3 of DuraPozz and Pozz-fill (Ash Resources, 2009 and n.d.). The chemical composition of Pozofly compares best with that of Pozz-fill. The CaO content of DuraPozz is considerably higher than that of Pozofly.

Table 3.3: *Chemical composition of Brazilian Pozofly and South African DuraPozz and Pozz-fill*

Oxide	Pozofly	DuraPozz	Pozz-fill
		(% by mass)	
SiO_2	52.3	51-55	51-65
Al_2O_3	33.2	32-34	25-35
Fe_2O_3	4.8	3-4	3-5
CaO	1.8	5-7	1-6
K_2O	3.5	-	0.5-2
TiO_2	1.1	-	1.6-2
MgO	-	1.5-2	0.5-2
P_2O_5	0.8	-	0.3-0.7
SO_3	1.9	-	0.1-0.3
Reference	(Martins, 2012)	(Ash Resources, 2009)	(Ash Resources, n.d.)

Figure 3.3 shows the particle size distribution of the Pozofly fly-ash.

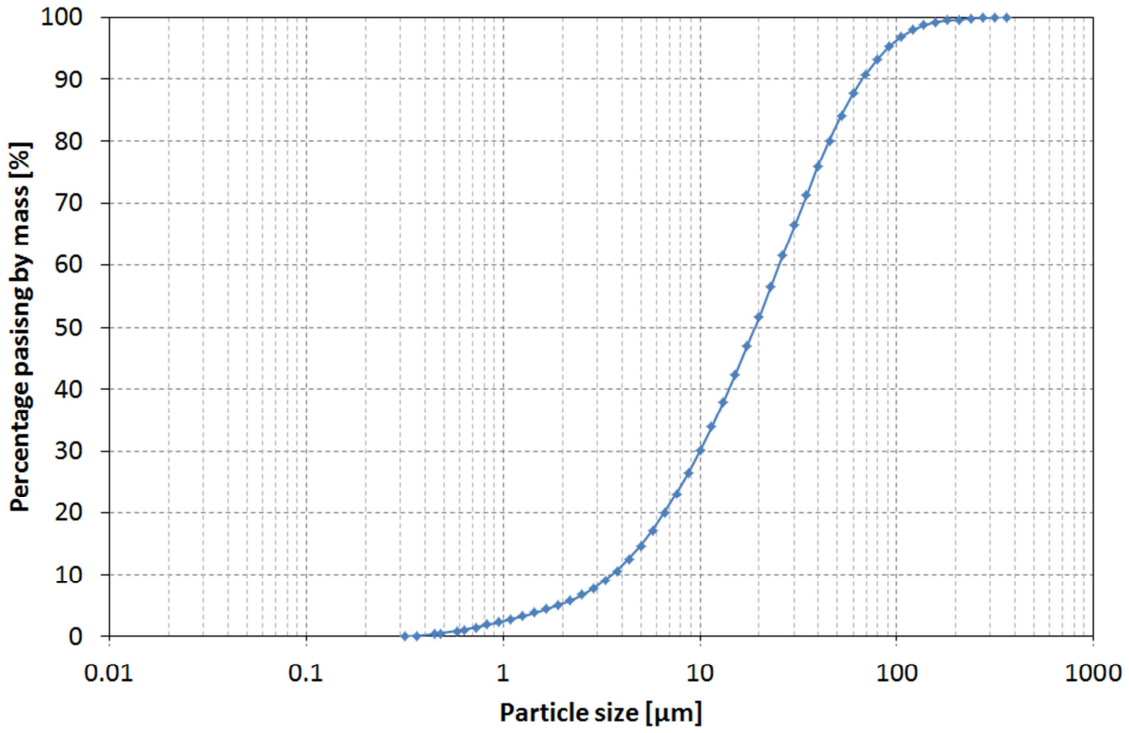

Figure 3.3: *Particle size distribution of Pozofly fly-ash*

3.2.4 Condensed silica fumes

Silmix Sílica Ativa condensed silica fumes (CSF), provided by Indústria Brasileira, was used for this research. Table 3.4 shows the chemical composition of Silmix and CSF typically found in South Africa. The bulk density of Silmix was found to be 2.33 g/cm^3, compared to 2.1 g/cm^3 for South African CSF (Owens, 2009). The particle size distribution is shown in Figure 3.4.

Table 3.4: *Chemical composition of Brazilian Silmix and South African CSF*

Oxide	Silmix	South African CSF
	(% by mass)	
SiO_2	94.5	92-96
Al_2O_3	1.2	1.0-1.5
Fe_2O_3	0.1	1.0-1.6
P_2O_5	0.9	-
CaO	0.6	0.3-0.6
ZnO	0.1	-
K_2O	0.8	1.2-2.0
MgO	-	0.6-0.8
H_2O	-	0.4-0.6
Reference	(Vitorino, 2012)	(Owens, 2009)

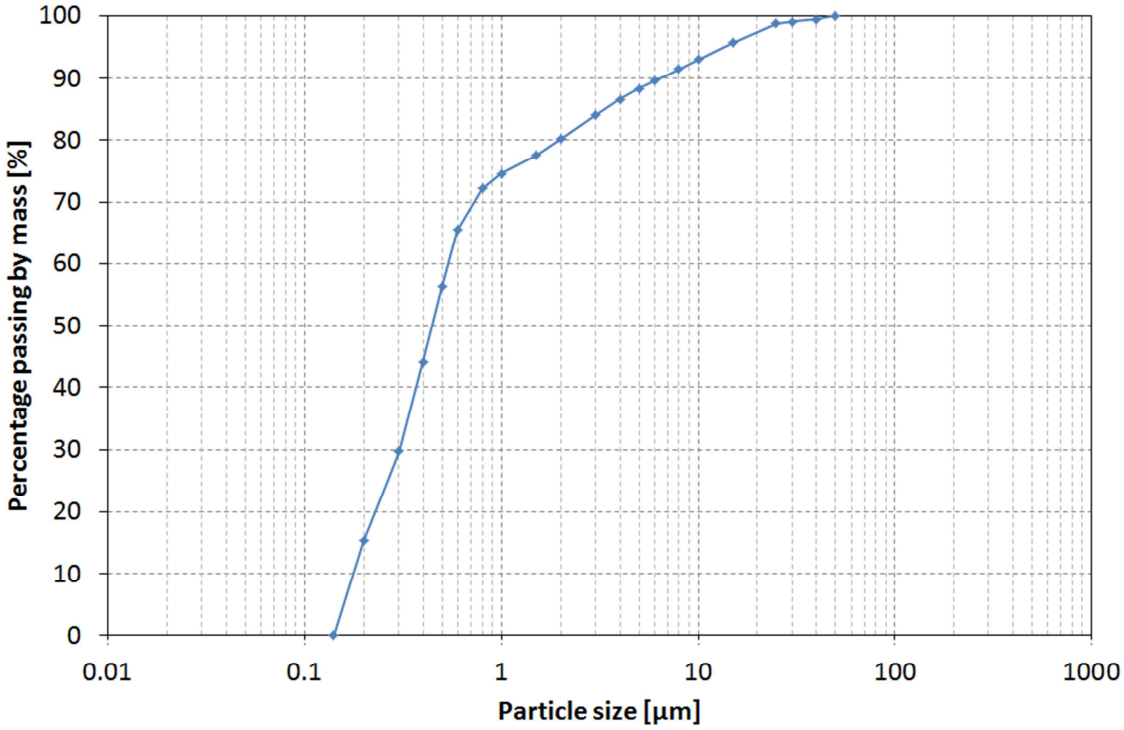

Figure 3.4: *Particle size distribution of Silmix CSF*

3.2.5 Sisal fibres

This section discusses the origin and fibre preparation of the sisal fibres used in the research. The physical and chemical properties of sisal fibre are discussed in Chapter 2. The average density of the fibres used was 1.1 g/cm^3.

Fibre origin

The sisal fibres used in the research were obtained from the Municipality of Valente situated in the state of Bahia in the north-west of Brazil. The fibres were provided by the *Associação de Desenvolvimento Sustentável e Solidário da Região Sisaleira* (Association for Sustainable Development and Solidarity of the Sisal Region).

The leaves of the sisal plant are smooth with a length and width of about 150 and 10 cm, respectively. To obtain fibres, the leaves are cut and decorticated, after which they are beaten to remove excess decortication waste and left to dry. Lastly the fibres are made into bales. Figure 3.5 shows this process.

Figure 3.5: *(a) Cut down sisal leafs; (b) leafs being decorticated; (c) fibres drying in the sun; (d) bales of fibres (Ferreira, 2012)*

Fibre preparation

The fibres had a length between 90 and 100 cm. The surface of the fibres showed signs of waste from the extraction process, such as sugar and mucilage. To clean the fibres, they were put in hot water (80-100°C) for two hours. They were then dried for two and a half days in a drying room at a constant temperature of 40°C (Figure 3.6).

Figure 3.6: *Washing process for fibres.(a) Fibre bundle as received from producers; (b) washing in warm water; (c) rinsing of fibres; (d) drying at 40°C*

After drying, the fibres were “combed” with a nail comb to align the fibres, after which they were cut to length of 10 mm with a paper guillotine (Figure 3.7). It should be noted that the “combing” process results in a fibre loss of around 30%. At LabEST the waste is cut at random lengths and used for other research.

Figure 3.7: *(a) combing of fibres on nail comb; (b) guillotine used for cutting of fibres**;** (c) combed fibres (right) and fibre waste (on comb); (d) cutting of fibres to length of 10 mm*

3.3 Block production procedure

This section discusses how mixes were designed and how blocks were produced. Different production procedures were followed for solid and hollow blocks and standard shrinkage moulds were used for producing the drying shrinkage samples.

3.3.1 Development of low calcium hydroxide matrix

As discussed in Section 2.3, natural fibres are very susceptible to alkaline attack, causing a decrease in durability. The detrimental effect of $Ca(OH)_2$ (henceforth referred to as CH) on the durability of fibres is particularly severe. Since pore water of concrete contains CH, it is important to develop a matrix free of this.

Tolêdo Filho et al. (2002) found that substituting cement with 25% metakaolin (MK) and 25% crushed waste calcined clay brick (CWCCB), by weight, a CH free matrix was developed at an age of 28 days. Similar results were obtained with a 30% MK and 20% CWCCB substitution.

No literature could be found on the amount of CSF replacement needed to obtain a CH free matrix, but since metakaolin is believed to react more aggressively than silica fumes (Justice et al., 2005), the assumption could be made that a silica content higher than 25% would be needed to achieve a CH free matrix.

Since this research is aimed at LCH and silica fume is relatively expensive in South Africa, it was decided to rather develop a matrix containing silica fumes and fly-ash, that might be more economical, but still offer some of the benefits of a lower-CH matrix.

A thermogravimetric analysis (TGA) was performed on cement pastes containing various cement:CSF:fly-ash proportions in order to establish a reasonable CSF content to be used for the blocks. A water cement ratio of 0.4 was used for all pastes and Table 3.5 shows the proportions used.

Table 3.5: *Cement paste content (% by weight)**

Mix name	Cement [%]	Fly-ash [%]	CSF [%]
HCP1(60-40-0)	60	40	0
HCP2(60-35-5)	60	35	5
HCP3(60-30-10)	60	30	10
HCP4(60-25-15)	60	25	15
HCP5(50-30-20)	50	30	20
HCP6(70-30-0)	70	30	0

*cementitious materials, as described in Section 3.2, were used

TGA is a type of testing that determines changes in weight of a material with a change in temperature. In the case of hardened cement paste, as the temperature is increased (up to around 1000°C), various chemical components decompose into gases. Using mass loss, rate of mass loss and stoichiometry, it is possible to calculate the CH content of the paste. The analysis was performed using an SDT Q600 thermogravimetric analyser, provided by TA Instruments. All paste samples were sealed in small plastic bags shortly after mixing and cured at a constant temperature of 30°C.

The results from the analysis at 28 day age are plotted as a percentage of initial mass (called thermogravimetry or TG) and rate of change of mass (derivative thermogravimetry or DTG) against temperature (Figure 3.8). The top group of curves are TG curves (belonging to the left vertical axis) and the bottom group of curves are DTG curves (belonging to the right vertical axis). The TG curves were transformed so that the mass % results align at 1000°C, as prescribed by the analysis method proposed by Neves Jr. et al. (2012). See Appendix A for the 7 and 14 day TGA results.

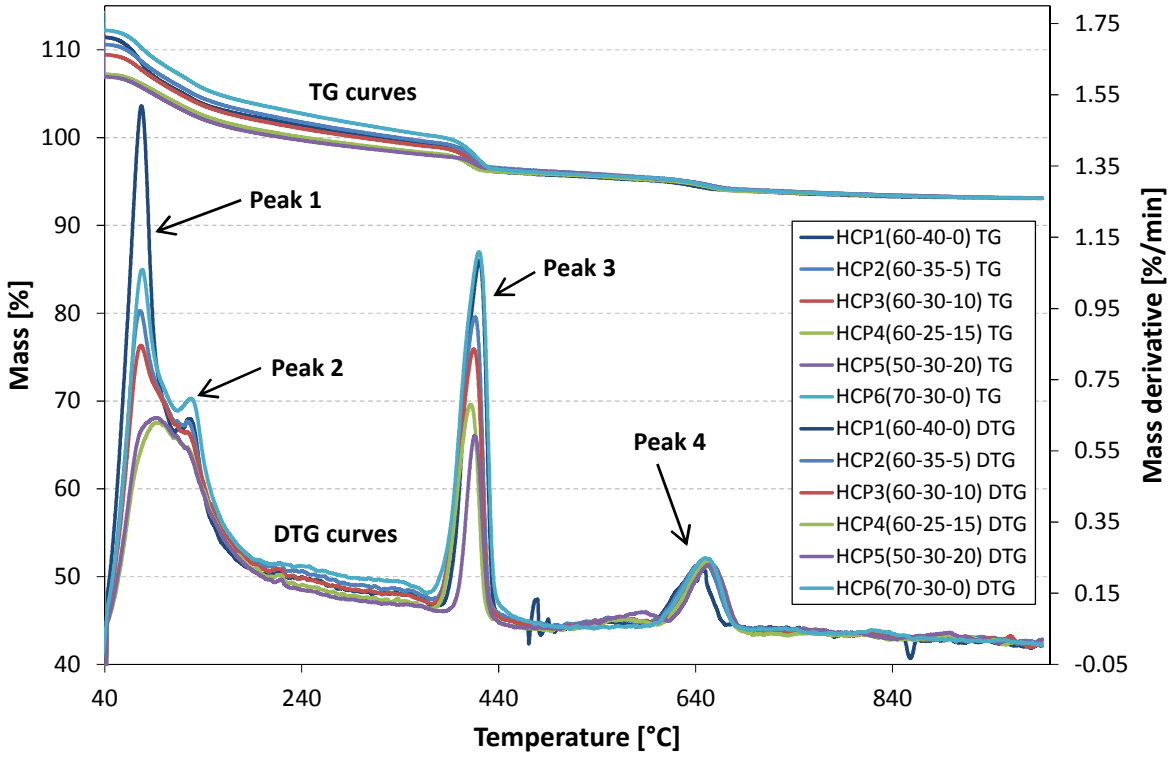

Figure 3.8: *TG and DTG curves of pastes at 28 days*

Never Jr. et al. (2012) states that when a thermal analysis is performed after an initial drying period between temperature ranges of 28 and 35°C, there are four main decomposition steps. These refer to the four sharp peaks in the DTG curves. Peak 1 shows the dehydration of tobermorite and ettringite between temperatures of 50 and 200°C. The dehydration of calcium sulphate occurs between 110 and 145°C (peak 2). Calcium hydroxide decomposes between 380 and 460°C (peak 3) while calcium carbonate does the same between 520 and 730°C (peak 4).

Careful study of the curves shows that HCP4 and HCP5 (containing 15 and 20% CSF, respectively) had the smallest mass loss between 380 and 460°C, indicating that it had the smallest CH content. This is in line with what was expected. HCP3 (10% CSF and 30 %fly-ash) seems to lie somewhere close to the middle. Quantifying these results lies outside the scope of this study. The CH content of HCP3 was seen as a good average combining a fair reduction in CH content with a more economic mix.

3.3.2 Concrete mix design and proportions

Two matrix types were developed for the solid and hollow blocks: one standard mix and one low-CH mix. Each matrix type was produced using three different fibre contents (0%, 0.5% and 1% by volume), leading to six different mix types.

For the standard mix, 30% of the cementitious content by weight was replaced by fly-ash, due to its low cost and slight ability to reduce pore water porosity (see Section 2.3). As stated in Section 3.3.1, it was decided to replace a further 10% of cementitious content by weight with CSF for the low-CH matrix.

The mix proportions that were finally used, were based on various literature sources and trial mixes. All sources specified a low cement content leading to a very dry mix, which is acceptable for producing reasonable strength blocks cheaply. Also, the machine used for producing the hollow blocks required a very dry mix for good results (Figure 3.9).

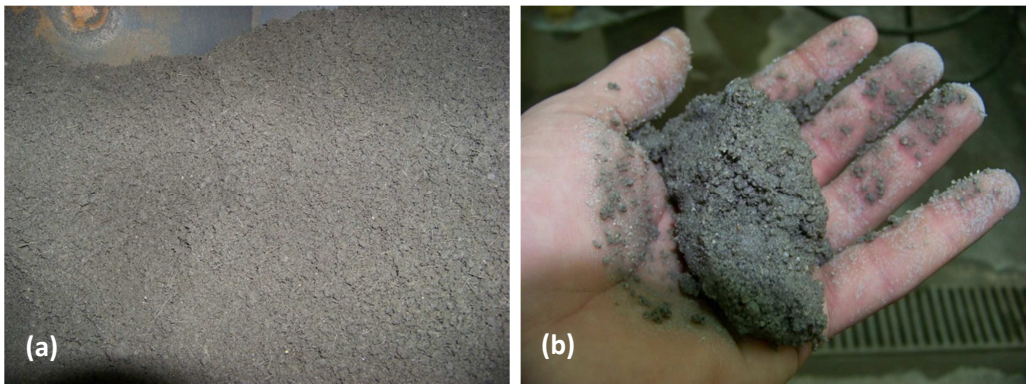

Figure 3.9: *Dry mix without fibres prepared for (a) hollow blocks and (b) solid blocks*

Holcim (2004), the Government of India (Development Institute, 2011) and Hydraform (2006) recommended water:cement (w:c) ratios of between 0.56 and 0.62 for use in concrete blocks. For this research a w:c ratio of 0.62 was used.

These sources also recommended a sand:stone ratio of about 4:6 by weight, but various trial mixes showed poor cohesiveness with this ratio and it was changed to 6:4, which yielded acceptable results.

The abovementioned sources also recommend using cement:aggregate ratios of between 1:8 and 1:10 for concrete blocks. It was expected that increased fibre content would lead to lower compressive strength. Due to the time constraints the trial mixes could not be tested for compressive strength and a cement:aggregate ratio of 1:7 was chosen for all mixes to ensure the compressive strengths of all blocks would fall within the boundaries stipulated in SANS 1215 (2008) (see Table 2.1).

Table 3.6 shows the mix proportions used. For both block types mixes M1, M3 and M5 were all essentially the same, with the only difference being the fibre content. They all had a cementious material content ratio by weight of 7:3 (cement:fly-ash). Similarly, M2, M4 and M6 had the same mix, with the fibre content being the varying factor. They had a cementitious content ratio of 6:3:1 (cement:fly-ash:CSF).

Table 3.6: *Mix proportions*

Brick type	Content	Proportions of various mixes [kg/m^3]					
		M1S	**M2S**	**M3S**	**M4S**	**M5S**	**M6S**
Solid	Cement (CPV-ARI)	192	164	192	164	192	164
	Fly-ash (Pozofly)	82	82	82	82	82	82
	CSF (Silmix)	-	27	-	27	-	27
	Sand	1153	1150	1153	1150	1153	1150
	Stone (9.5 mm)	769	766	769	766	769	766
	Water	170	170	170	170	170	170
	Sisal fibre	-	-	5	5	10	10
	Total	2366	2359	2371	2364	2376	2369
Hollow	Cement (CPV-ARI)	192	164	192	164	192	164
	Fly-ash (Pozofly)	82	82	82	82	82	82
	CSF (Silmix)	-	27	-	27	-	27
	Sand	1153	1150	1153	1150	1153	1150
	Stone (4.8 mm)	538	536	538	536	538	536
	Crusher dust	231	230	231	230	231	230
	Water	170	170	170	170	170	170
	Sisal Fibre	-	-	5	5	10	10
	Total	2366	2359	2371	2364	2376	2369

Note: The designations 'S' and 'H' in the mix naming refer to the block types. The number in the name refers to the silica and fibre content. Mix numbers 1 and 2 contain no fibre, mix numbers 3 and 4 contain 0.5% fibre and mix numbers 5 and 6 contain 1% fibre. Also, mix numbers 1, 3 and 5 contain 0% CSF, while mix numbers 2, 4 and 6 contain 10% CSF.

As previously mentioned, the sand:stone ratio used for all the solid block mixes was 6:4 by weight. This resulted in mixes with good cohesiveness and workability, given the low cement content. However, due to the thin walls of the hollow blocks and the vibrating action of the block making machine, this sand:stone ratio did not deliver a high enough cohesiveness to properly produce the hollow blocks. As a result, it was decided to substitute 30% of the stone content with crusher dust. The nominal stone size was also reduced from 9.5 mm to 4.8 mm. This came after recommendations by the manufacturer of the bock making machine. The final sand:stone:crusher dust ratio for all hollow block mixes was 6:2.8:1.2 by weight. Figure 3.10 and Figure 3.11 show the surface and shape of the hollow blocks with and without the added crusher dust and reduced nominal stone size.

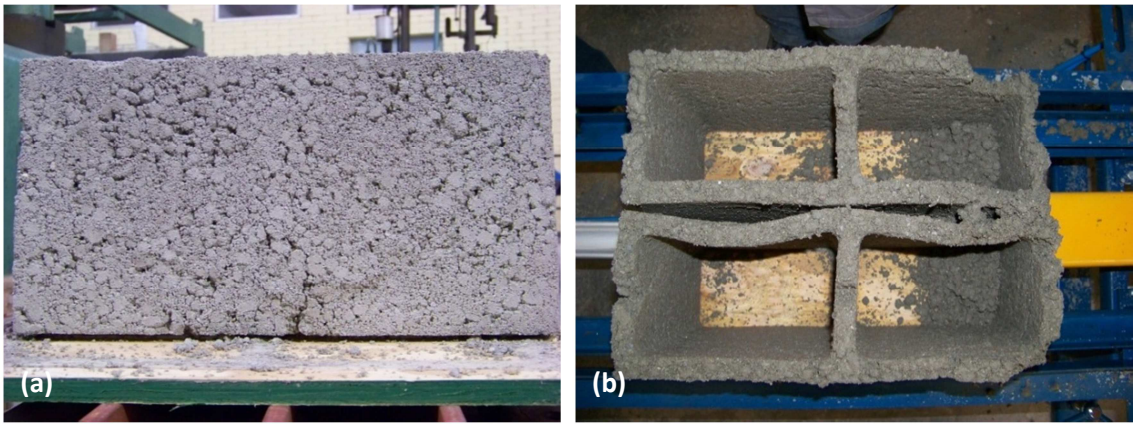

Figure 3.10: *(a) Surface and (b) shape of blocks with 9.5 mm stone and without crusher dust*

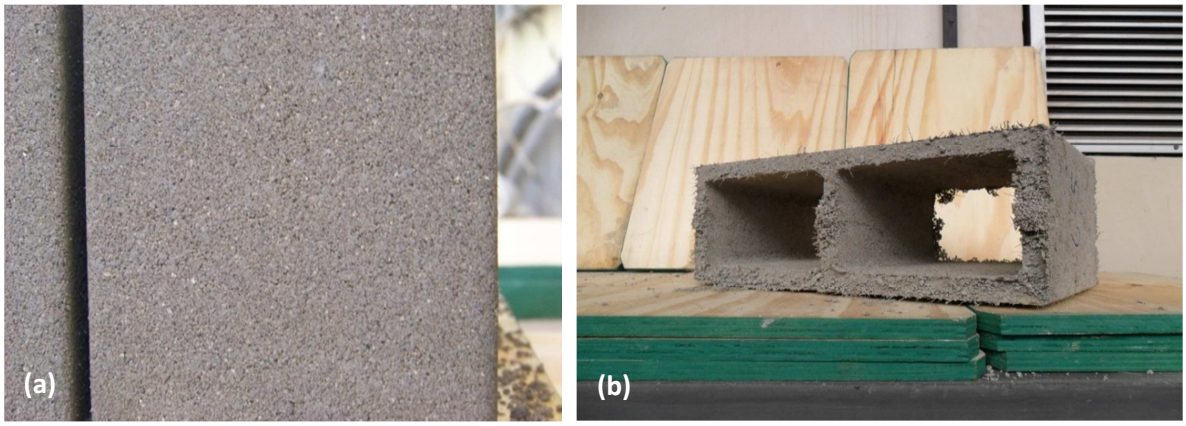

Figure 3.11: *(a) Surface and (b) shape of blocks with 4.8 mm stone and crusher dust*

The addition of fibres affected the cohesiveness and workability of the mixes somewhat. The addition of 0.5% fibre by volume tended to positively affect the cohesiveness and workability for both block types, while the addition of 1% fibre by volume tended to increase cohesiveness, but decrease workability. Furthermore, the substitution of cement with 10% CSF by weight led to a very slight increase in cohesiveness. In order to objectively measure the influence of fibre content on the mechanical and volumetric properties of the blocks, it was decided to keep all the mixes the same, apart from varying fibre content. However, it should be noted that, to obtain the best performing blocks, mixes should be tailor-made according to fibre and CSF content.

3.3.3 Concrete mixing procedure

The layout of the LabEST laboratory and the construction taking place there made it impractical to use the same concrete mixer for both solid and hollow blocks. A pan mixer was used for the solid block concrete, while a drum mixer was used for the hollow block concrete (Figure 3.12). The mixing process was the same for both block types.

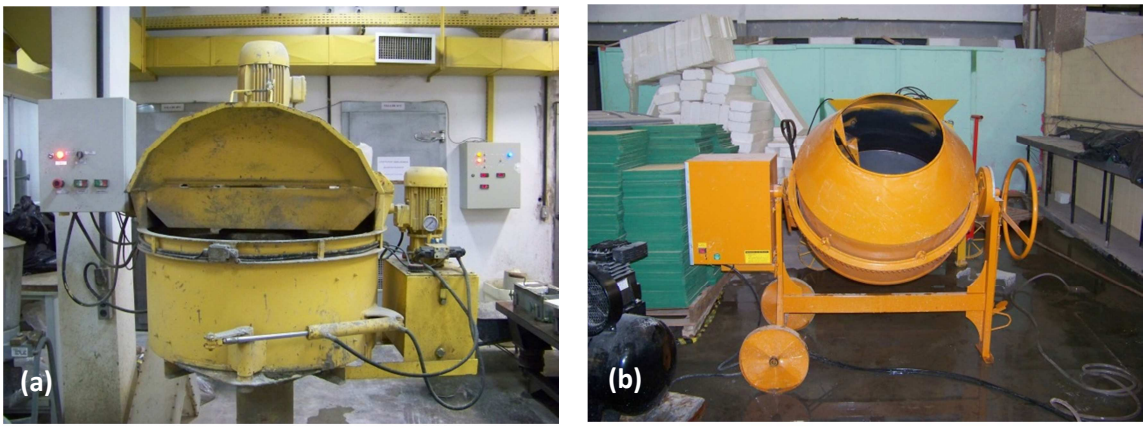

Figure 3.12: *Concrete mixers used: (a) pan mixer; (b) drum mixer*

A mixing procedure, as prescribed by Owens (2009) was followed. Between 5 and 8 solid blocks were moulded at a time, the reason being the limited moulds available and to prevent too many samples from reaching a 28-day age at the same time. Mix volumes ranged between 19l and 35l.

All constituents were weighed and held in separate containers. Firstly, the aggregate was added to a clean, dry, rotating drum and mixed for one minute. Next, all cementitious material was added and allowed to mix for another 30 seconds. After stopping the mixer and using a small trowel, the area around the mixing blades was mixed by hand since the material added first tended to accumulate there. The mixture was allowed to mix for a further 30 seconds.

Next, the fibres were added to the relevant mixes. In order to prevent balling of fibres, it had to be added slowly to a static drum, one handful at a time. The fibres had to be loosened with the fingers, as shown in Figure 3.13. In between handfuls, the drum was allowed to mix for 30 seconds to prevent all the added fibres from remaining at the surface.

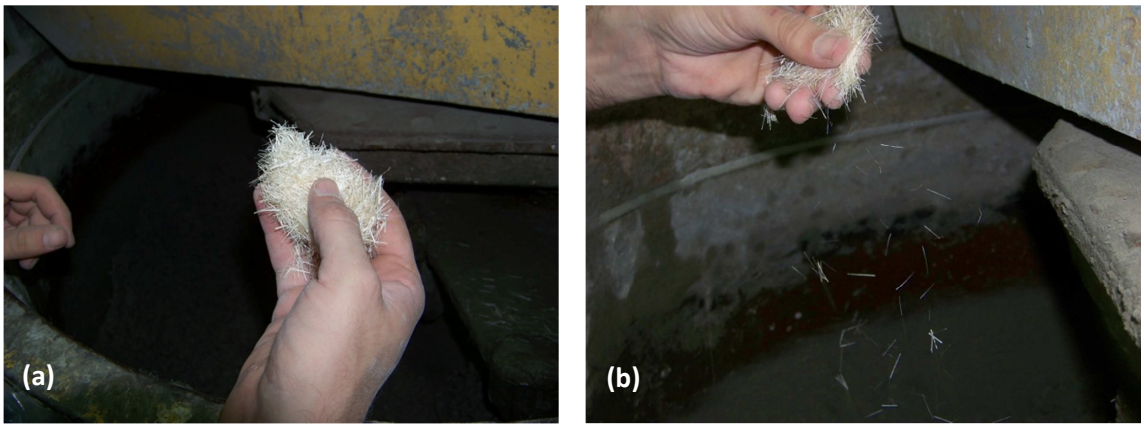

Figure 3.13: *Adding fibres to mix: (a) a handful between rotations; (b) loosening fibres with fingers*

Adding the fibres took between 20 and 30 minutes, depending on the fibre content of the mix and mix volume. Consequently, it was decided to add the water in last to ensure the minimum time between the start of the hydration reaction and the moulding process. The water was slowly added to a rotating drum in a time span of one minute. Lastly, the mixer was rotated a further one minute to ensure an even mix.

3.3.4 Block moulding

The process for moulding of the blocks is discussed in this section. The processes were very different for both block types. A smaller mould was used to prepare samples for drying shrinkage testing, but the process was similar to that of the solid blocks

Solid block moulding

Two different mould types were used. The first type was a 500x150x150 mould that was fitted with a 210x50x50 mm strong polystyrene block in order to reduce the dimensions of the mould to 290x150x150 mm. Another mould type was later provided, made from 20 mm thick presswood and with internal dimensions of 290x140x95 mm. These moulds are shown in Figure 3.14.

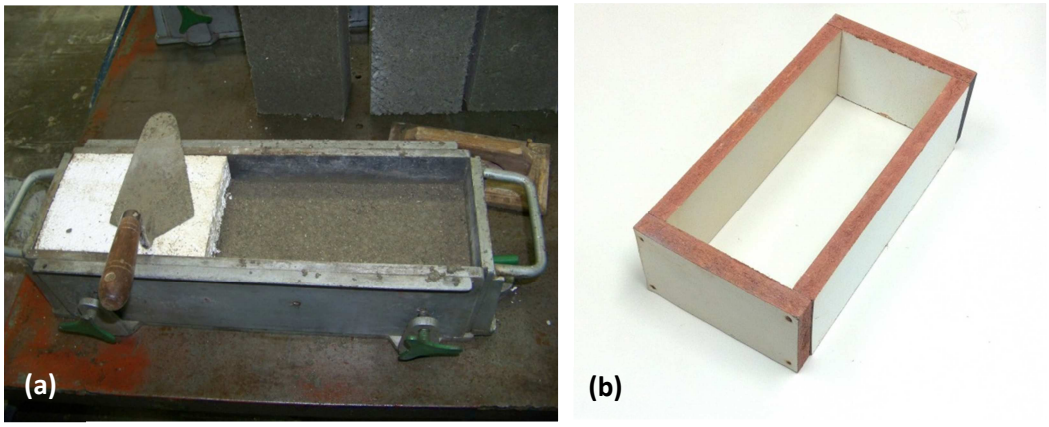

Figure 3.14: *Solid block moulds (a) steel and polystyrene mould; (b) presswood mould*

Before moulding, the moulds were painted with a thin layer of oil to aid in block removal after curing. Immediately after concrete mixing, the moulds were filled in three layers. Each layer was hand compacted using a small trowel (Figure 3.14 and Figure 3.15). The moulds were filled up to a height of 95 mm, to provide sufficient space for compaction in order to reach a 90 mm height as required for the blocks. The moulding process took between 20 and 30 minutes. The process for the plywood moulds was the same. After moulding, the bricks were compressed to 500 kPa (or 21 kN force) using an old Amsler compression testing machine. A 290x150x20 mm steel plate was used to ensure the pressure was applied uniformly. This process is shown in Figure 3.16.

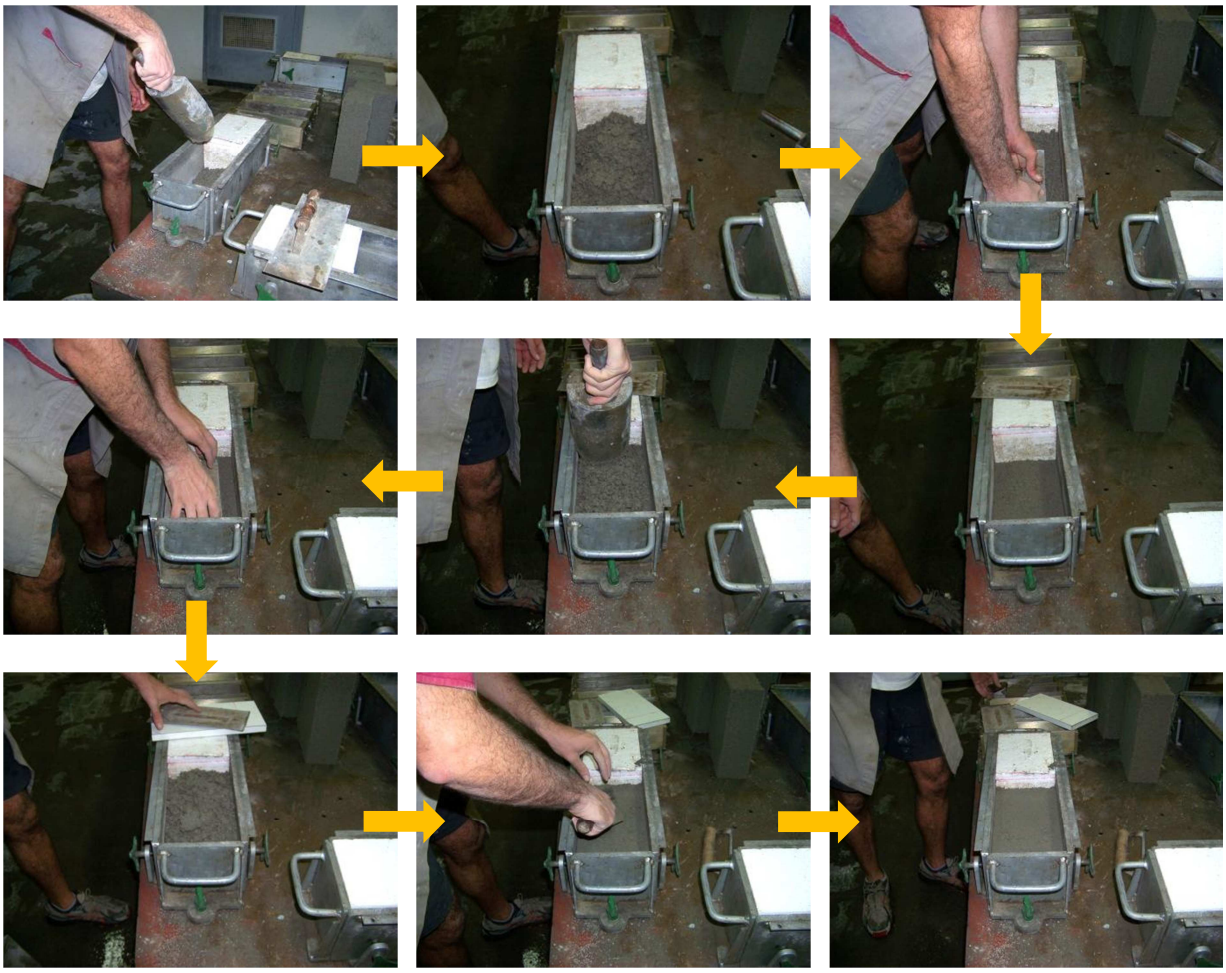

Figure 3.15: *Solid block moulding*

Figure 3.16: *Solid block compression (a) before compression; (b) during compression; (c) final product*

The steel/polystyrene moulds were not ideal, since under pressure, the block tended to expand slightly in the direction of the polystyrene. The plywood moulds tended to fare better in this regard.

Another problem with the steel/polystyrene moulds was that they produced a 150 mm wide block, 10 mm wider than the required width. Therefore, blocks produced in the steel moulds had to be cut to a narrower width after curing.

After compression, the blocks were allowed to cure for 8-9 hours in a high humidity environment. This short curing time was not ideal, but due to time constraints two batches had to be produced per day.

Shortly after demoulding, the blocks were marked appropriately and stored in a curing chamber at 100% relative humidity and 23±1°C until an age of 7 or 28 days was reached.

Shrinkage bar moulding

The shrinkage bar samples were prepared for all six solid block mixes. The production process was the same as for the solid blocks, but 280x70x70 mm shrinkage moulds were used instead of solid block moulds(Figure 3.17 (a)).

Two small steel pins were embedded in the blocks in the middle of the 70x70 mm faces (Figure 3.17 (b)). The edges of the pins were about 295 mm apart, meaning the pins protruded the surfaces by roughly 7.5 mm. The shrinkage blocks were compressed to 500 kPa as well, using a force of 10 kN, due to the smaller exposed surface. A 280x70x15 mm steel plate was used to distribute the force uniformly. Demoulding and curing was similar to that of the solid blocks.

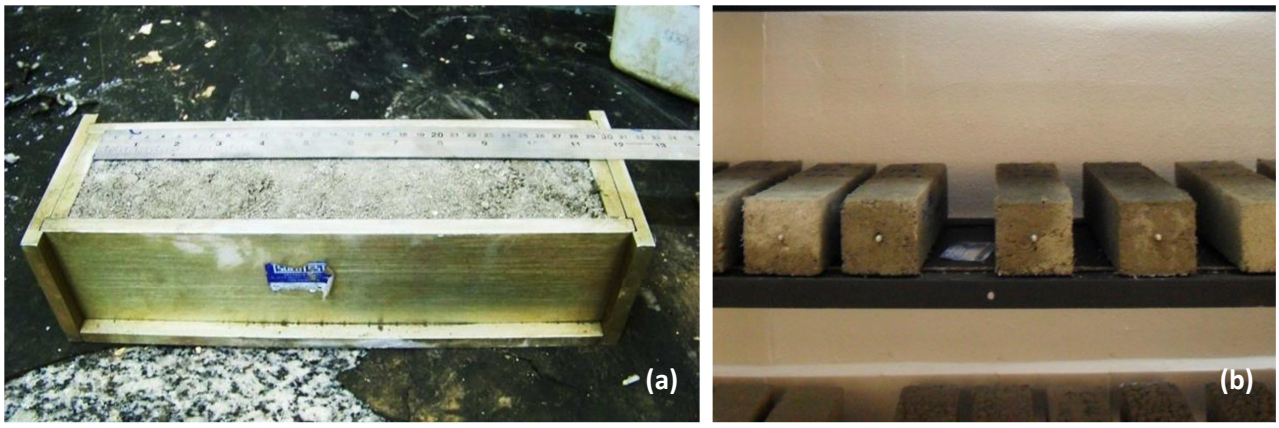

Figure 3.17: *(a) Shrinkage sample mould; (b) pins sticking out of face*

Hollow block production

A pneumatic block making machine was used to produce the hollow blocks. The machine was manufactured by Sahara, a subsidiary of Grupo Aguilar, stationed in São Paulo, Brazil. The machine was connected to a 2 hp Schulz Bravo air compressor. Figure 3.18 shows the machine and compressor. The machine had a built-in high frequency vibrating motor.

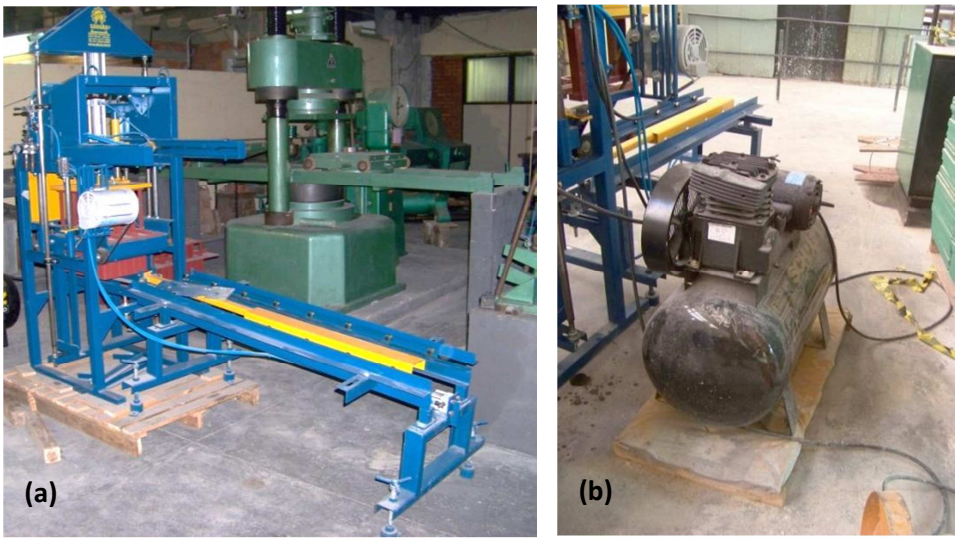

Figure 3.18: *Hollow block production equipment (a) Sahara block making machine; (b) Schultz 2hp air compressor*

The machine had the capacity to make two 390x140x190 mm hollow blocks at a time. During block production wet concrete mix was added to the mould and vibrated until the mould was full. The blocks were then compressed to 110 psi (750 kPa) by a mould-shaped steel plate connected to a pneumatic cylinder. Compression happened while the vibrator was running. Thereafter, the moulds were removed and the blocks were covered by plastic sheets for 8-10 hours until sufficiently hard to be moved to the curing chamber. Figure 3.19 shows the moulds used as well as the finished blocks.

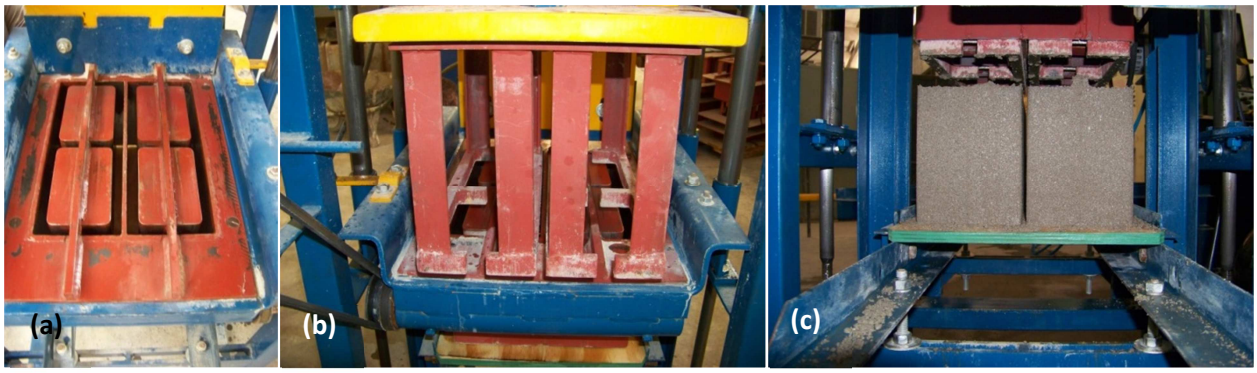

Figure 3.19: *Hollow block moulds (a) 390x190x140 mm mould; (b) mould-shaped compression plate; (c) demoulded, wet blocks*

The dimensions of the produced hollow blocks were as follows: 390 mm long, 140 mm wide and 190 mm high. Length and width dimensions varied by less than 2 mm, while height dimensions varied by less than 4 mm.

Technically, the hollow blocks produced were cellular blocks, since the top and bottom wall and web thicknesses were not equal. The walls and webs tapered towards a greater thickness at the bottom of the block. The wall and web thickness were 20 mm at the top of the blocks and 23 mm at the bottom, with a variation of less than 1 mm.

3.4 Experimental setup and test program

This section discusses the tests performed, the equipment used as well as a brief description of the methodology followed during the tests. The amount of samples used and sample preparation, where applicable, are discussed as well. The following tests were performed on the solid blocks: compression, flexure, capillary water absorption, dimensional stability, total water absorption, density and void content. Only compression and capillary water absorption tests were performed on the hollow blocks.

As stated in Section 3.3.2, six different mixes were prepared for each block type. All the tests were performed on all the mixes. Where samples were immersed or boiled in water, normal tap water sourced from the network of the city of Rio de Janiero was used. It is considered suitable for human consumption.

Where samples were oven dried, a temperature of 60°C was used instead of the more standard 100-105°C. This was chosen due to the decomposition of ettringite and other products at temperatures of 70°C and higher. Mohr et al. (2004) have mentioned that ettringite might influence the behaviour of natural fibres in cementitious matrices, although the extent of influence is unknown.

3.4.1 Compression test

The compression tests were largely performed in accordance with SANS 1215 (2008).

Age and types of mixes

Table 3.7 shows the number of blocks prepared with each mix type and testing age.

Table 3.7: *Number of blocks prepared for compression testing*

	Number of blocks	
Mix	**7 Day**	**28 Day**
M1	5S	5S, 5H
M2	5S	5S, 5H
M3	5S	5S, 5H
M4	5S	5S, 5H
M5	5S	5S, 5H
M6	5S	5S, 5H

Note: The designation 'S' and 'H' in the mix name refer to 'Solid' and 'Hollow'

Sample preparation

Compression tests were performed and samples prepared according to the method described in section 5.5 of SANS 1215 (2008). When the solid blocks were tested, no capping table was available and the blocks were capped using capping mortar, a thick steel plate and a spirit level. The capping mortar consisted of one part (by mass) CPV-ARI cement and one part calcined gypsum. Capping was done two days before testing and the blocks were returned to the curing chamber within 12 hours.

When the hollow blocks were tested, a capping table was available, but due to a shortage of calcined gypsum a sulphur-fly-ash capping mixture was used. Five parts (by volume) melted sulphur was mixed with one part fly-ash and, using the capping table, applied to bed-faces of the hollow blocks. Where the cap covered cavities, holes were made in the cap (Figure 3.20). For the hollow blocks, capping was also done two days before testing and returned to the curing chamber as soon as the caps were sufficiently hard.

Figure 3.20: *Hollow block capping (a) melting of sulphur-fly-ash mix; (b) capped block; (c) capping over cavities removed*

Test procedure

The solid blocks were tested at 7 day and 28 day ages, while the hollow blocks were only tested at an age of 28 days. All testing was done within 5 minutes of removal from the curing chamber. A Shimadzu UH-F1000kNI universal testing machine (Figure 3.21) was used to perform all the tests. SANS 1215 (2008) prescribes a stress-based testing rate of 15 MPa/min, but due to constraints of the

machine the testing rate was changed to displacement-based. The solid blocks were tested at a rate of 3 mm/min. The hollow blocks tended to fail much quicker, thus they were tested at 0.5 mm/min.

Figure 3.21: *Shimadzu UH-F1000kNI machine used for compression testing*

A small aluminium plate was glued to all the blocks shortly after removal from the curing chamber. A Linear variable differential transformer (LVDT) was attached to the plate, as shown in Figure 3.22. This was done to measure the actual displacement of the block under compression.

Packing plate thicknesses of 70 and 120 mm would be required to get a perfect force distribution along the length of the solid and hollow blocks, respectively (assuming force distribution at 45°). Due to the unavailability of such thick plates during testing, thinner plates were used. The plates used can be seen in Figure 3.22. Different plates were used for testing of solid and hollow blocks, but they were all at least 25 mm thick.

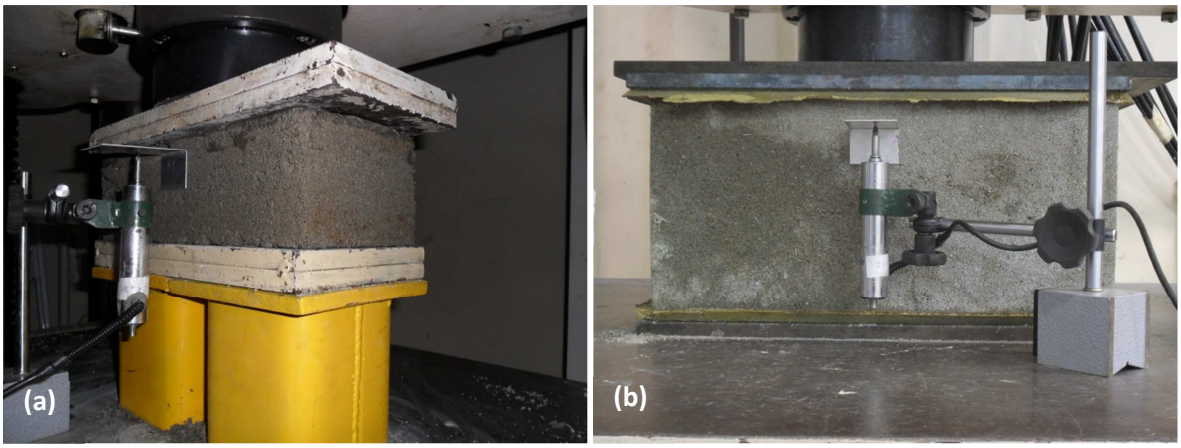

Figure 3.22: *Packing plates, LVDT and glued aluminium plate on (a) solid block and (b) hollow block*

While testing, the force exerted and machine cross head displacement was recorded in time intervals of 0.5 seconds (2 Hz), along with the LVDT displacement. The measuring was done well past the failure force of the block to capture the effect the fibre had on failure.

The use of a single LVDT assumes uniform deformation along the front, back and length of a block. This, however, was later observed to be untrue and it was decided to rather use the cross-head displacement of the machine as an indicator of deformation.

Laing (2011) states that "Maxi" bricks orientated so that the 140 mm edge is horizontal and the 90 mm edge vertical (Figure 3.23), provides enough structural integrity in a wall according to SANS 10400-K (1990). This also works out to be more economical than a traditional 230 mm double skin wall. Therefore, compression and flexure tests were performed according to this orientation.

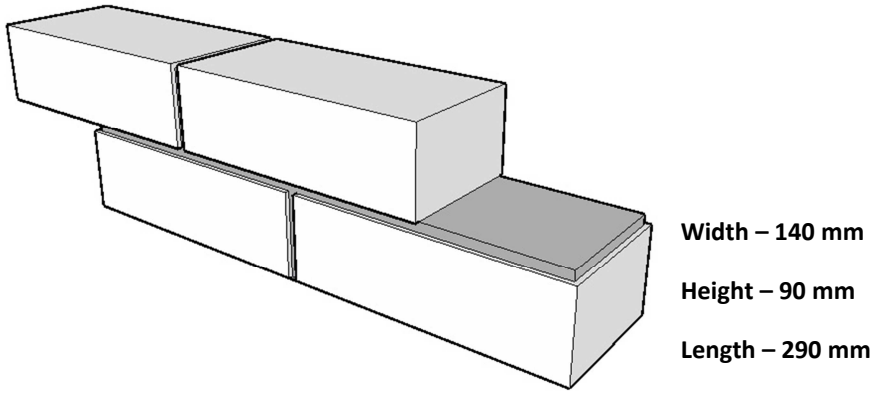

Figure 3.23: *Orientation of "Maxi" bricks (solid blocks) in a wall*

3.4.2 Flexure test

The three-point flexure tests were largely performed in accordance with SANS 1575 (2007). This standard was written for burnt clay bricks, but since no South African standard describes a flexure test for non-paving concrete blocks, this method was followed.

Age and types of mixes

Five samples of each solid block mix types were tested at an age of 28 days.

Sample preparation

Each sample was removed from the curing chamber five minutes before testing. It was wiped with a damp cloth to remove any excess surface water. All samples had a length of 290±3 mm and a width of 90±2 mm. Samples were tested in bending about the strong axis (i.e. as a beam as opposed to a

plate – see Figure 3.23 for the orientation of a block in a wall). A small rigid aluminium beam was attached to the bottom of each block at mid span. Each sample was fitted with a brace holding an LVDT at mid height. The LVDT was fitted in such a way that it measured the vertical displacement relative to the connecting points (Figure 3.24). This is not the overall deflection of the beam between the supports. Nevertheless, it did give a fair impression of relative deformation.

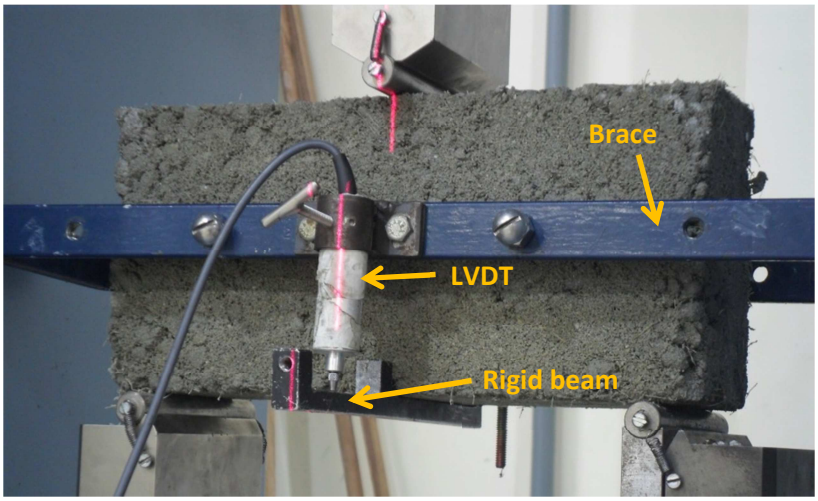

Figure 3.24: *LVDT setup for flexure test*

Test procedure

SANS 1575 (2007) recommends using a support span length of (L-30) mm (Figure 3.25). However, the corners of some samples broke off at the supports and the span length was shortened to (L-40) mm, which solved the problem.

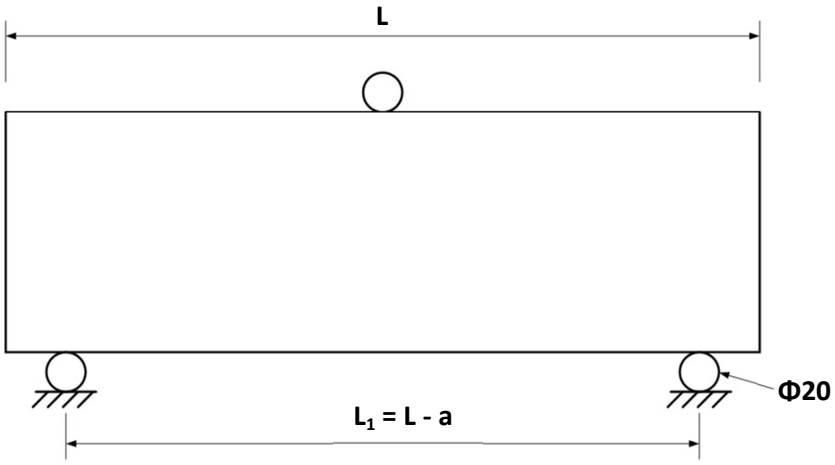

Figure 3.25: *Flexure test setup and spacing*

A Wykeham Farrance International flexure test machine (Figure 3.26) was used to conduct the flexure tests. The blocks were centred using a laser level. A displacement-based test was done at a rate of 0.1mm/min and the testing was allowed to continue well past the maximum applied force to capture the effect the fibres had on cracking during flexure. The applied force and LVDT mid span displacement were recorded versus time in intervals of 0.5 seconds (2 Hz).

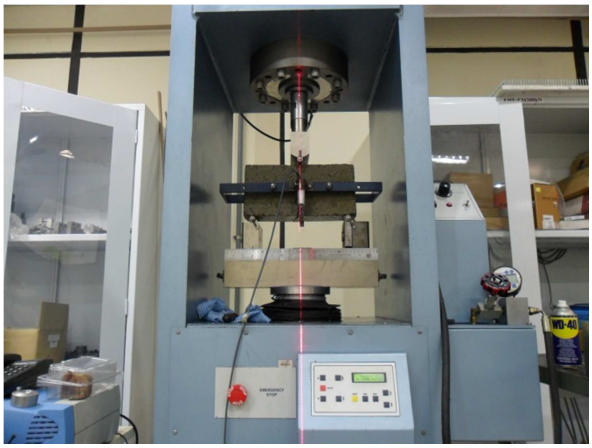

Figure 3.26: *Wykeham Farrance International flexure test machine*

3.4.3 Capillary water absorption

The capillary water absorption tests were performed in accordance with the method described in NBR 9779 (Associação Brasileira de Normas Técnicas, 1995)

Age and types of mixes

Table 3.8 shows the amount of blocks tested.

Table 3.8: *Number of blocks prepared for capillary suction testing*

	Number of blocks
Mix	**28 Day**
M1	5S, 4H
M2	5S, 4H
M3	5S, 4H
M4	5S, 4H
M5	5S, 4H
M6	5S, 4H

Note: The designation 'S' and 'H' in the mix name refer to 'Solid' and 'Hollow'

Sample preparation

All blocks of similar type and mix were dried in an oven at 60°C for 48 hours (at which time constant mass was reached), three days prior to reaching an age of 28 days. After drying the blocks were allowed to cool down to room temperature over a period of 24 hours, after which they were lightly wiped with a dry cloth to remove all loose material from the surface.

Test procedure

At the start of the test the dried blocks were weighed and the dimensions of each face to be in contact with water were measured using a vernier calliper. The blocks were then put in a large tank as shown in Figure 3.27. The bottom of the tank was lined with a thin rubber mesh to keep the blocks from resting on the flat bottom surface of the tank.

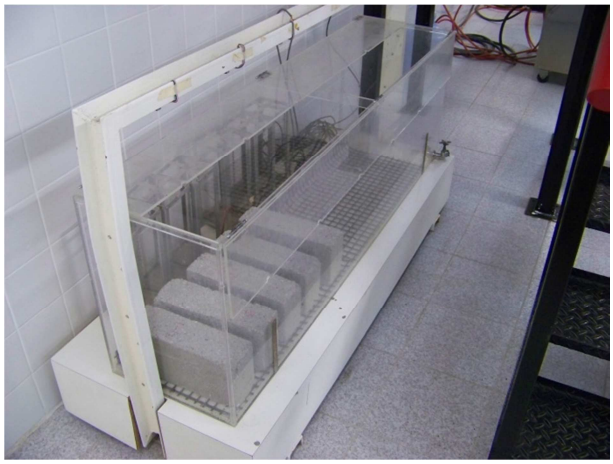

Figure 3.27: *Tank used for capillary suction test*

The blocks were spaced in such a way that, even with removal of a block, the sides would not touch. The solid blocks were arranged so that one of the 290x90 mm faces was in contact with the water, while the hollow blocks were arranged so that one of the 390x140 mm faces was in contact with the water. The tank was slowly filled with water until the water level was constant at 5±1 mm above the lower faces of the blocks. After one hour, the blocks were removed one by one, wiped with a damp cloth and weighed. This was repeated at times of 3h, 6h, 24h, 48h and 72h after the start of test. During the 3 day testing time, the water level was regularly checked and filled up to keep it constant at 5±1 mm above the lower faces of the blocks.

3.4.4 Density, absorption and void content

This test was performed in accordance with the method described in ASTM C-642 (1997). The following was determined from this test: absorption after immersion, absorption after immersion and boiling, dry bulk density and volume of permeable pore space.

Age and types of mixes

Three solid blocks were tested of each mix type.

Sample preparation

Three blocks of each mix type were tested at a time. Each block was sawn into three pieces with dimensions of roughly 95x140x90 mm. Each of the nine smaller blocks were dried for 48 hours at

60°C in an oven, three days prior to reaching an age of 28 days. After drying the blocks were allowed to cool to room temperature for 24 hours. The blocks were wiped with a dry cloth to remove any loose material at the surface.

Test procedure

At the start of the test, each small block was weighed and then immersed in water at approximately 23°C for 48 hours. After immersion, each block was quickly wiped with a damp cloth and weighed once more. Next, the samples were put in a large pot, covered with water and allowed to boil for 5 hours. After boiling, the blocks were allowed to cool to room temperature for 24 hours, wiped with a damp cloth and weighed once more. Lastly, the blocks were suspended by a wire and the apparent mass in water was determined. Figure 3.28 shows the whole process.

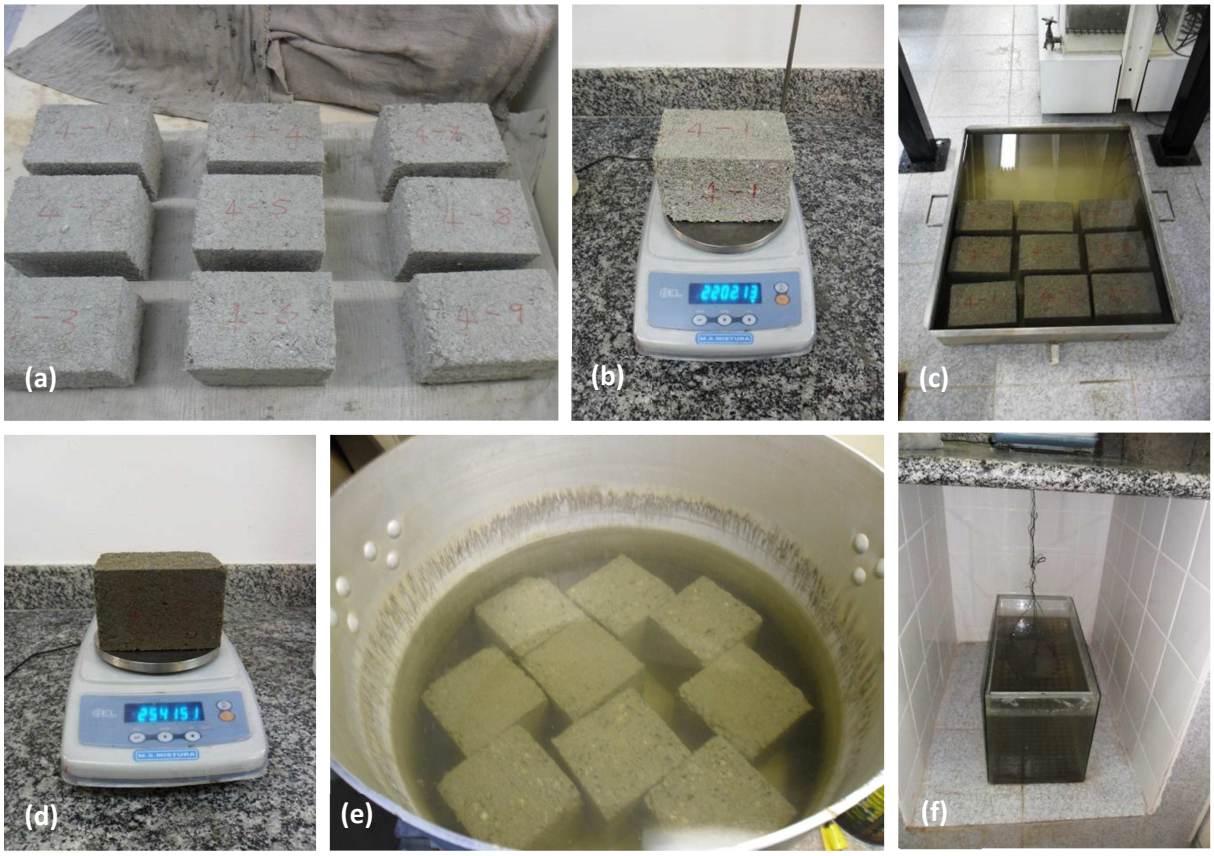

Figure 3.28: *Density, absorption and void test procedure: (a) dried and cut blocks; (b) being weighed; (c) immersed blocks; (d) immersed blocks weighed; (e) boiling; (f) apparent mass in water*

3.4.5 Dimensional stability

This test was aimed at measuring the dimensional stability of the blocks under various wet/dry cycles. This test was not performed according to any code or standard. After drying, the temperature of the blocks was held constant for the remainder of the test as to exclude change in temperature as a possible factor influencing dimensional change.

Age and types of mixes

Three samples of each solid block mix type were tested for dimensional stability.

Sample preparation

Since the available vernier caliper could only measure to a length of 280 mm, each block had to be cut to a length of 270 mm (from 290 mm). Three days prior to reaching an age of 28 days, the blocks were allowed to dry in an oven at 60°C for 48 hours. After drying, blocks were moved to a storage room at 34°C and allowed to cool down for 24 hours.

Using a permanent marker, each block was subdivided as shown in Figure 3.29.

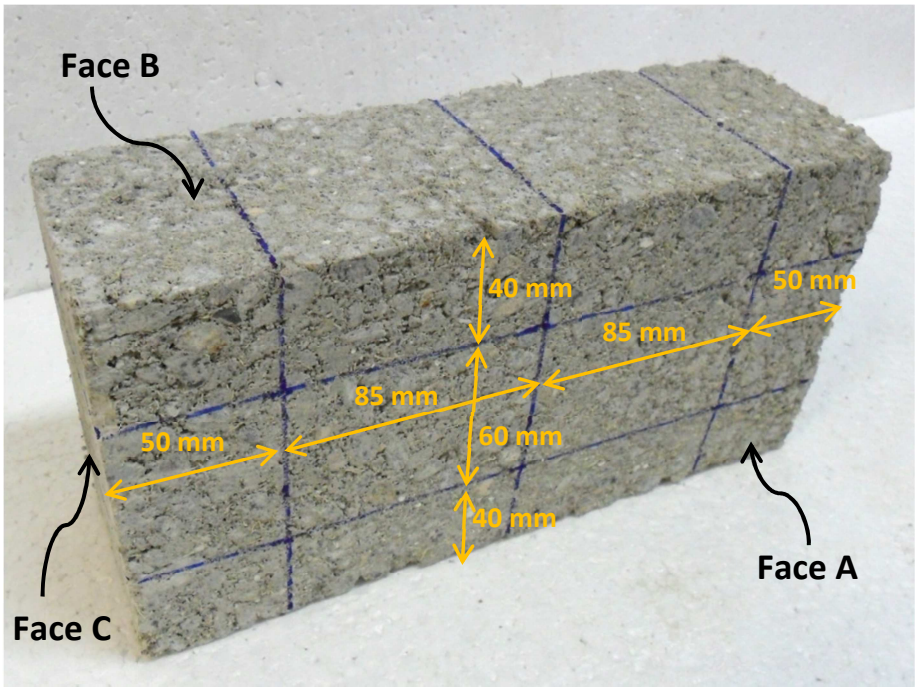

Figure 3.29: *Subdivision of block*

As shown in Figure 3.30, face A contained five width measurements (three lines and the two edges) as well as four length measurements (two lines and two edges). Similarly, face B contained five height measurements (three lines and two edges). The same was true for the opposite faces. All in all, each block delivered 10 height measurements, 10 width measurements and 8 length measurements.

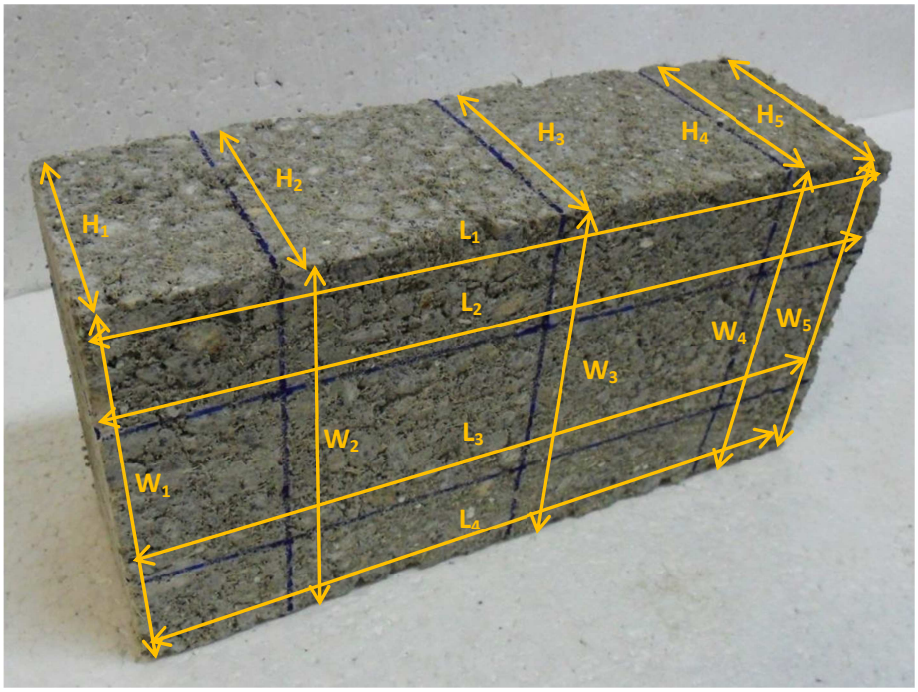

Figure 3.30: *Dimensions of block*

Test procedure

At the start of the test, each block was weighed. Using a Mitsutoyo vernier caliper, all of the abovementioned dimensions were measured and tabulated (Figure 3.31). The caliper used was accurate to 1/50 mm.

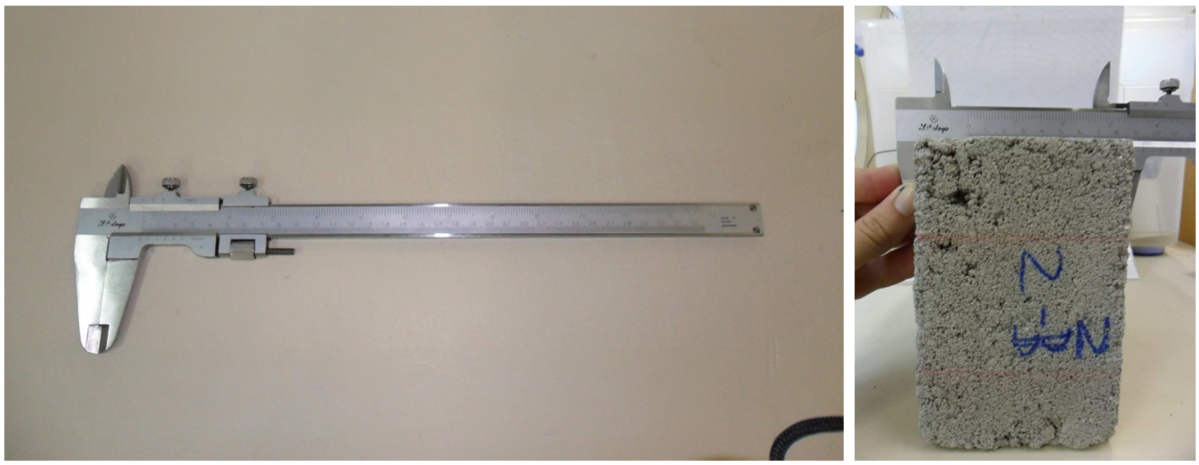

Figure 3.31: *(a) Vernier caliper; (b) Measuring height with vernier caliper*

Next, the blocks were soaked in water for 48 hours at 34°C. This was deemed sufficient time to completely saturate the blocks. After removal, the blocks were wiped with a damp cloth so as to remove any excess surface moisture. The dimensions and mass of the blocks were once again measured.

After measurements, the blocks were dried in a wind tunnel at 34°C for 48 hours (Figure 3.32). This was deemed sufficient to properly dry out the blocks.

Figure 3.32: *Blocks drying in wind tunnel*

After drying the dimensions and weight of the blocks were measured again and the whole process was repeated three more times. In total there were four wet and four dry values for each dimension.

3.4.6 Drying shrinkage

Drying shrinkage was performed over a two month period for all samples. The environment where storing and testing was done was held at a constant temperature of 23±1°C and relative humidity of 60±5%.

Age and types of mixes

Four samples of each solid block mix type were tested.

Sample preparation

As described in Section 3.3.4, all shrinkage samples were embedded with 25 mm steel pins in the middle of the two 70x70 mm faces that protruded the faces by approximately 5 mm. At an age of 28 days after moulding, samples were removed from the curing chamber and wiped with a damp cloth to remove any excess water and loose material.

Test procedure

Four samples of each mix type were tested at a time. After wiping, each sample was weighed. A shrinkage testing rig was set up and the measuring device was zeroed using a metal calibration rod with a length of 295 mm (Figure 3.33). Each sample was measured pin to pin and the results were tabulated. The samples were stored on a rack, resting on two thin metal wires to allow for free drying shrinkage with minimum friction. For the first two days, measuring was done each hour within

office hours. In the following 5 days samples were measured three times a day. In the next two weeks measuring was done once a day and over the remaining weeks, once every three days.

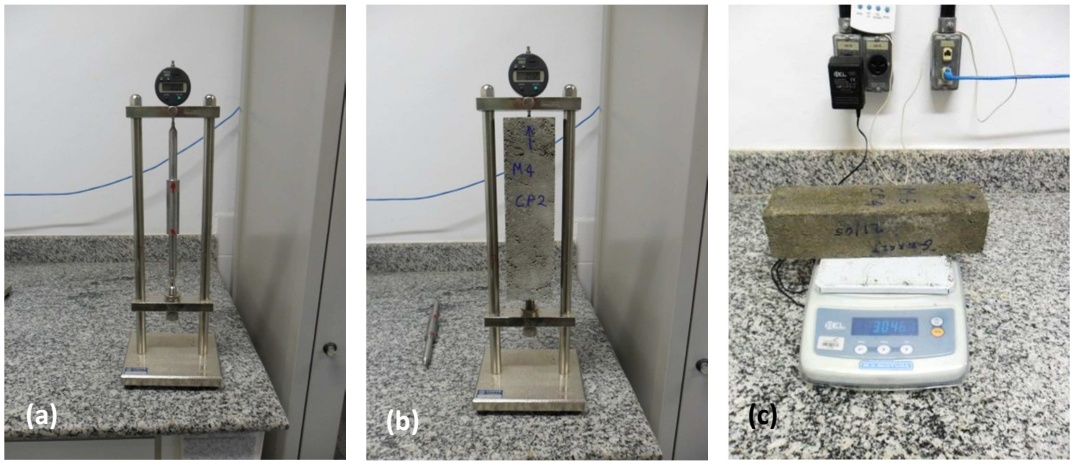

Figure 3.33: *Shrinkage measuring; (a) zeroing; (b) sample being measured; (c) weighing of sample*

3.4.7 Summary of tests performed

Table 3.9 shows the number blocks of each mix type tested. In total 126 solid blocks, 48 hollow blocks and 24 shrinkage beams were tested.

Table 3.9: *Summary of number of blocks of each mix type used for per test*

Test	Solid	Hollow
Compression	5	5
Flexure	5	-
Capillary water absorption	5	4
Density, water absorption and voids*	3	-
Dimensional stability	3	-
Drying shrinkage**	4	-

*Three blocks were cut into thirds, giving 9 samples to be tested
**Shrinkage beams were used, not blocks

4. Mechanical and volumetric test results

This section deals with the analysis and representation of results obtained from all the tests mentioned in Section 3.4. Tests were split into two categories: (i) mechanical and (ii) volumetric and durability.

Where results provided are the averages of the samples tested, the results are split into two groups: without CSF (referring to M1, M3 and M5) and with 10% CSF (referring to M2, M4 and M6). The dotted lines surrounding the curves represent the standard deviation band (distance between standard deviation above and below average). Also, the standard deviation (σ) and coefficient of variation (CoV) are displayed on graphs, where applicable. The standard deviation refers to the sample standard deviation using a normal distribution.

4.1 Mechanical test results

This section deals with the results of all mechanical tests (compression and flexure). Results are discussed briefly, but a more in-depth discussion where all test results are considered, follows in Chapter 5.

4.1.1 Compression test

The compression test results of the 7 day solid blocks, 28 day solid blocks and 28 day hollow blocks are shown graphically in this section. The force-displacement curves of the various mixes are provided for each block type and age, as well as the average stiffness of each mix.

As mentioned in Chapter 3.4.1, an LVDT was used to measure the vertical displacement of each block during compression testing. At a later stage, however, it was decided that one LVDT was insufficient to properly capture the vertical displacement due to possible non-uniform deformations. Therefore, the machine cross-head displacement was used for data representation rather than the LVDT displacement data. It must be noted that the cross-head displacement includes deformations in the loading frame (i.e. in the machine).

The maximum compressive strength was calculated by dividing the maximum applied force by the smaller of the two face areas of the block over which it was applied, as prescribed by SANS 1215 (2008). For the hollow blocks the smaller of the two gross areas of the faces were used (i.e. the area of the cavities were not subtracted). The solid blocks had an area of about 40 600 mm^2, while the smallest netto area of a hollow block was about 17 000 mm^2 (42% of that of a solid block). The gross area of a hollow block was about 54 600 mm^2 (3.2 times the netto area).

Solid block results (7 day)

Figure 4.1 shows the force-displacement graphs of the solid blocks at an age of 7 days. Due to human error, the displacement data for mixes M2 and M6 was not recorded; therefore the graphs for these two mixes cannot be shown.

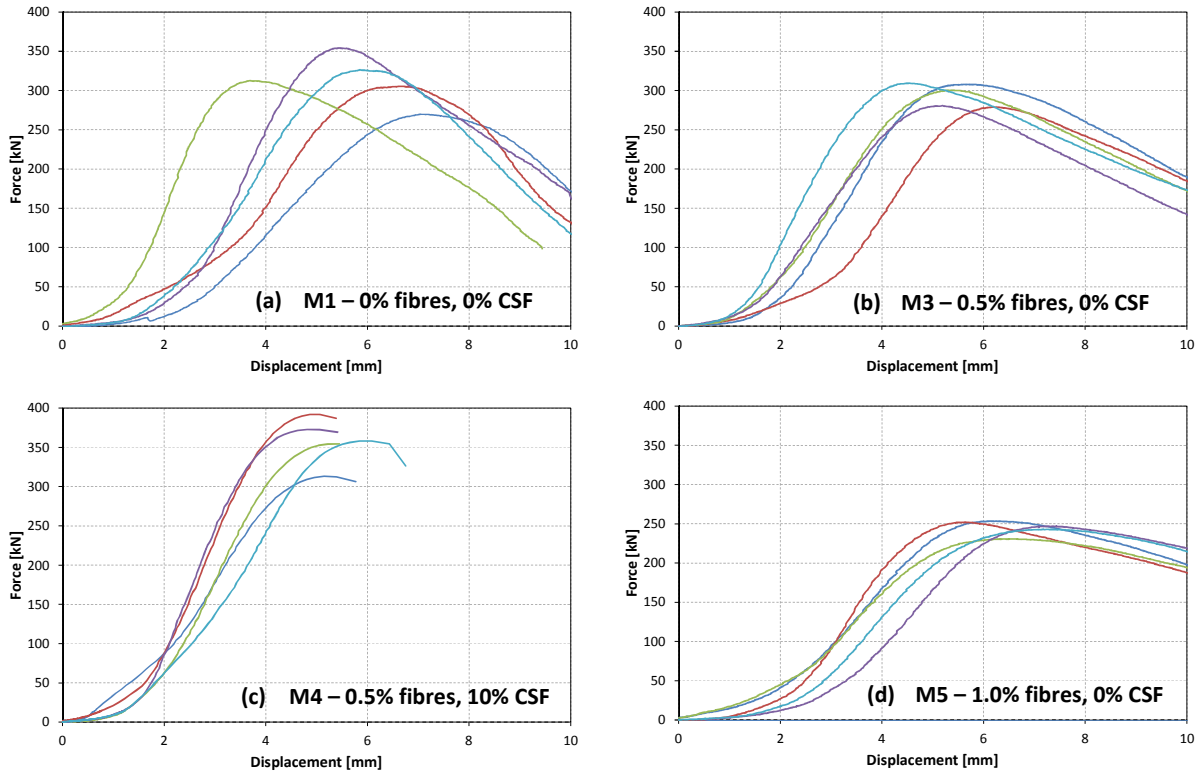

Figure 4.1: *Force-displacement graphs of solid blocks at 7 day age (a) M1; (b) M3; (c) M4; (d) M5*

Since the true deformation of the blocks was not known the strain could not be calculated. However, the cross-head displacement was used to determine the relative stiffness of each block. The stiffness of each sample tested was calculated as the gradient of the force-displacement diagram between one third and one half of the maximum force. Figure 4.2 shows the average stiffnesses of mixes M1, M3, M4 and M5 at an age of 7 days.

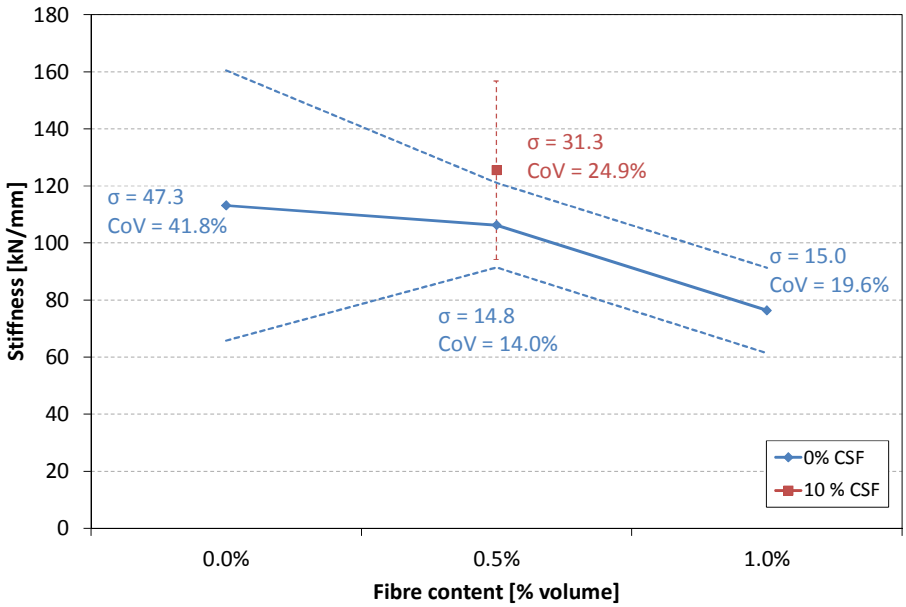

Figure 4.2: *Average stiffness of solid block mixes at 7 day age*

Figure 4.2 clearly shows that an increase in fibre content has a significant effect on the stiffness of a block. Also, if one considers the data points at 0.5% fibre content, it is clear that a higher CSF content increases the stiffness considerably (in this case by 18%). In all cases, especially at 0% fibre content, the variance of the results was high.

Figure 4.3 shows the average maximum compressive stress of each mix type.

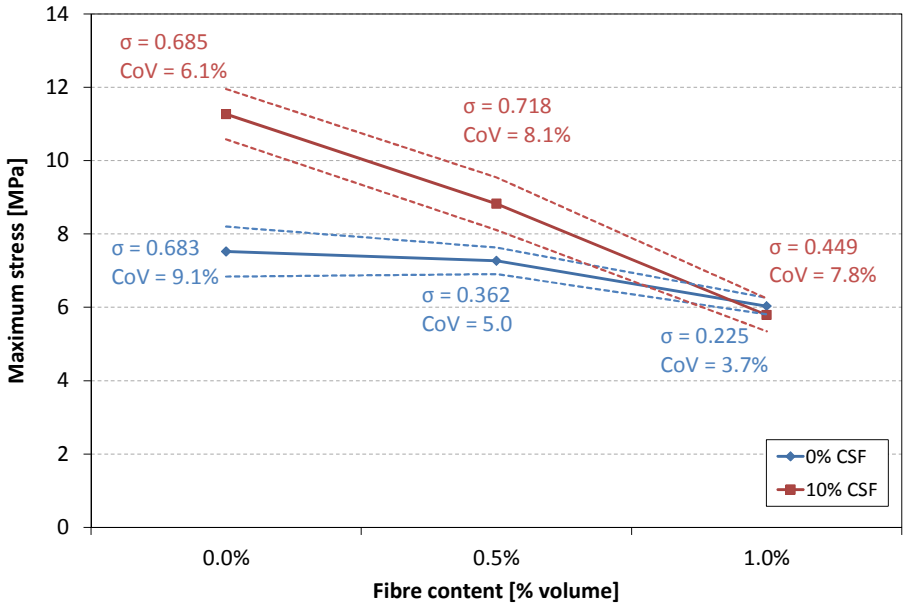

Figure 4.3: *Average maximum compressive stress of solid block mixes at 7 day age*

The effect of fibre and CSF content on the maximum compressive stress seems to mimic the effect on stiffness, although the variability of the compressive stress is considerably lower than that of the stiffness. Also, as fibre content increases, the extra strength provided by the addition of CSF seems to decrease until a point is reached at a fibre content of 1% where there is almost no difference between the compressive strength of mixes containing CSF and those not. For 0% CSF, the addition of 0.5% and 1% fibre reduced the stress by about 3 and 20%, respectively. Similarly, the reduction in stress of 10% CSF mixes was about 22 and 48%, respectively.

Solid block results (28 day)

Figure 4.4 shows the force-displacement graphs of the 28 day age solid blocks. The results for all six mixes are shown.

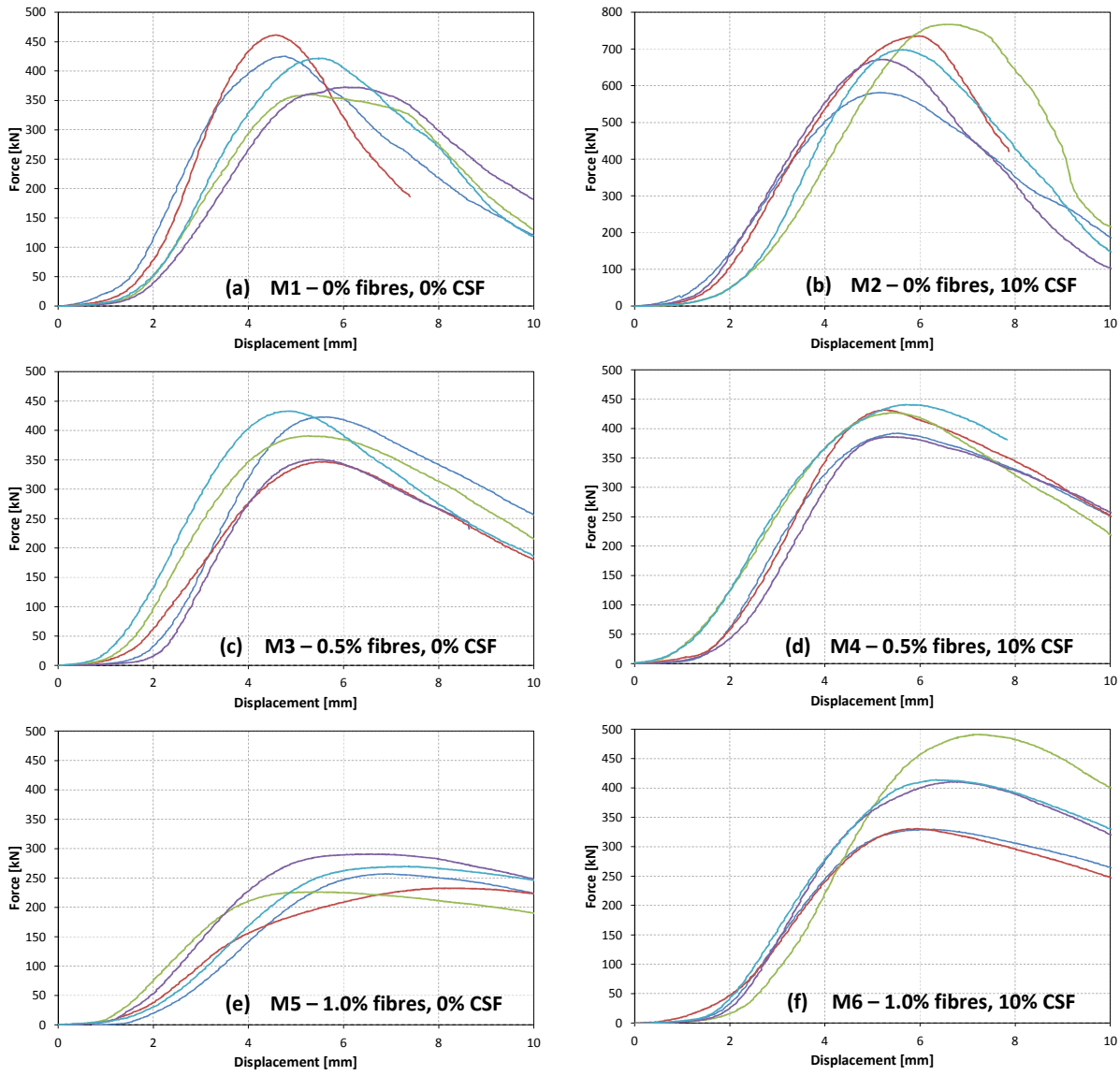

Figure 4.4: *Force-displacement graphs of solid blocks at 28 day age*

The stiffnesses of the various mixes at an age of 28 days were calculated similarly to that of the 7 day old blocks. The average stiffness of each mix is shown in Figure 4.5. It seems the fibre content has a strong influence on the stiffness of a block. Also, the addition of CSF increases the stiffness slightly. For the mixes without CSF, the average stiffness of the blocks containing 1% fibres is 52% lower than for the blocks with no fibre. For the mixes with 10% CSF, the difference is 43%.

Careful study of Figure 4.4 reveals that the initial slopes of the force-diplacement curves become less steep with the addition of fibre (as with the stiffnesses of the blocks). This initial lowering is indicative that there is a larger initial deformation and rearrangement of particles (due to a higher air content) before strength is gained.

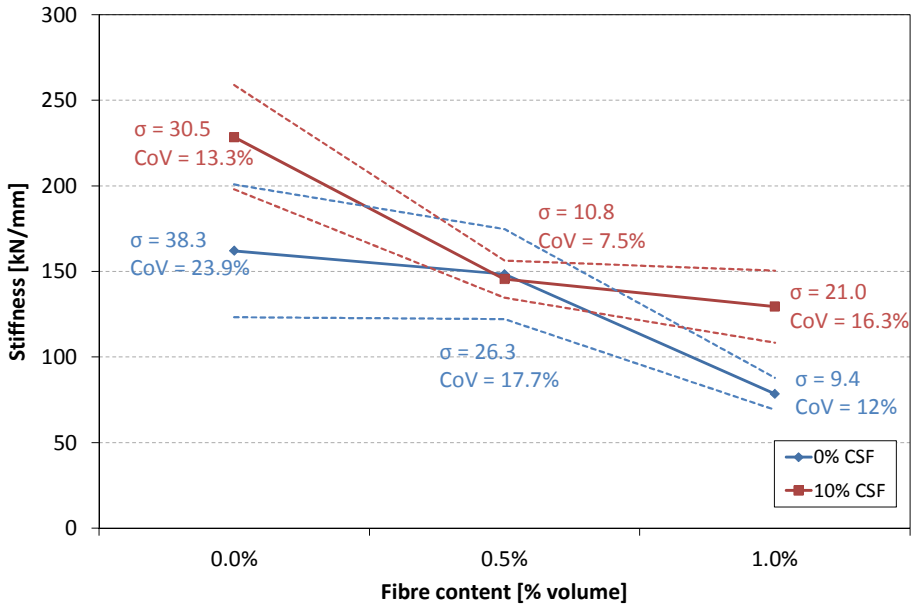

Figure 4.5: *Average stiffness of solid block mixes at 28 day age*

Figure 4.6 shows the average maximum stress for the various mixes.

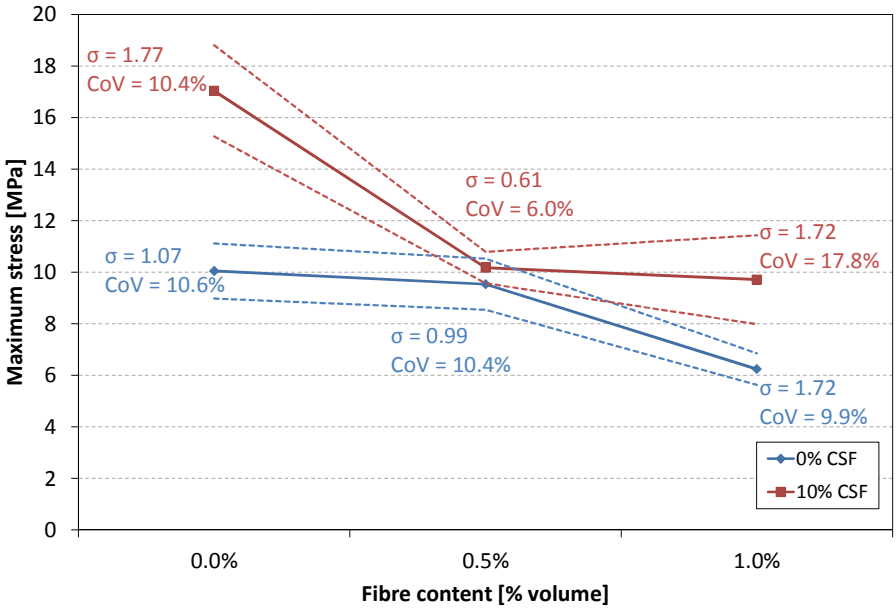

Figure 4.6: *Average maximum compressive stress of solid block mixes at 28 day age*

As expected, the shape of Figure 4.6 somewhat mimics that of Figure 4.5, once again indicating the strong relation between stiffness and compressive strength. The maximum stress of blocks containing no CSF decreases by 5 and 38% as fibre content increases to 0.5 and 1%, respectively. The same reduction due to fibre addition is 40 and 43%, respectively, for 10% CSF blocks.

Hollow block results (28 days)

Figure 4.7 shows the force-displacement graphs of the various hollow block mixes. Only three samples of mixes M1 and M2 were tested, due to poor sample quality (see Figure 4.10 and explanation).

Mixes M5 and M6 (1% fibre) showed promising post peak force behaviour, with a gentle decrease in force with a large increase in displacement. This is indicative of ductile behaviour of blocks containing 1% fibre. The other mixes showed a more sudden drop in strength after reaching maximum strength. This effect is most clearly visible in the results of M3 and M4 (0.5% fibre content).

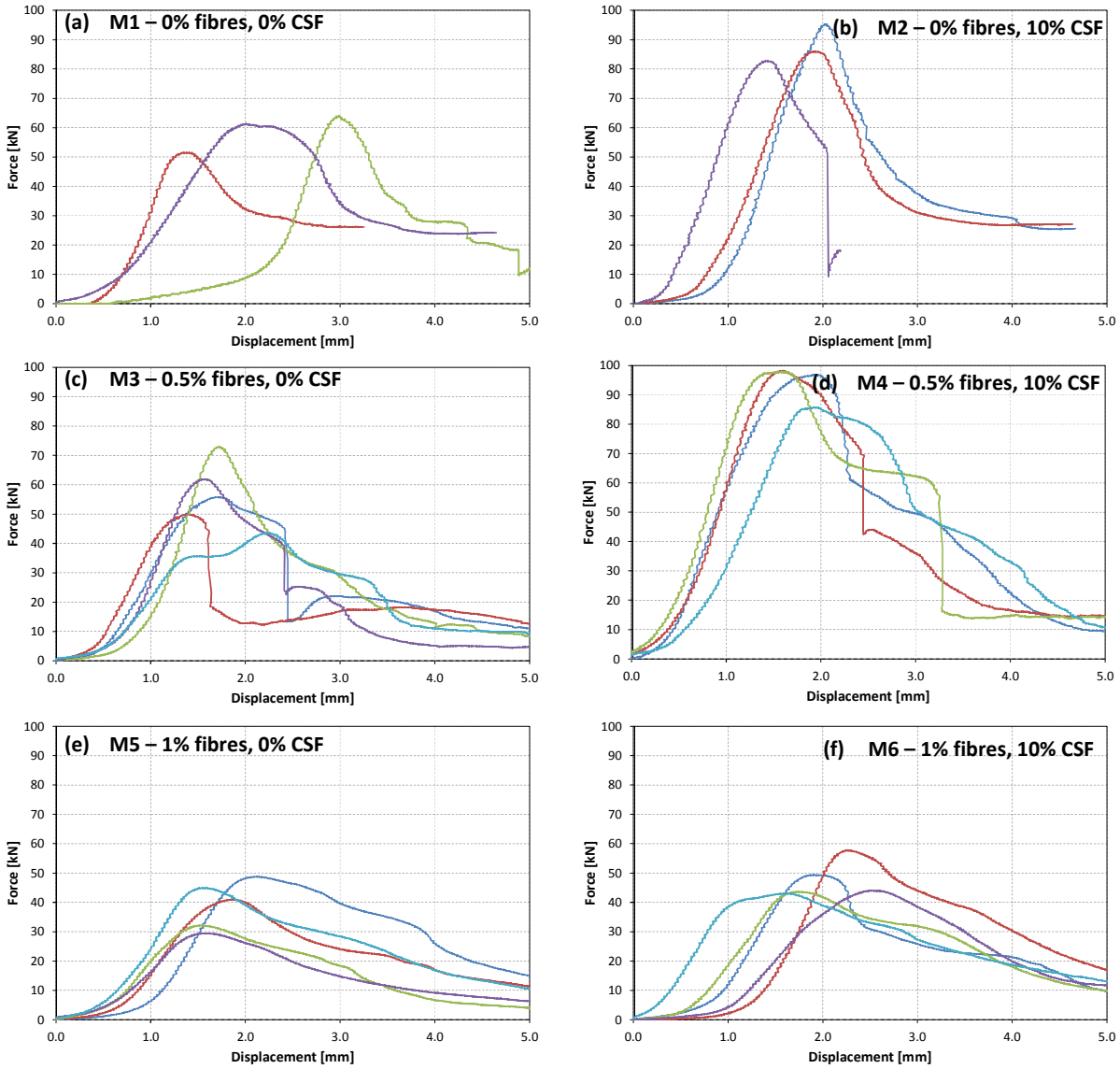

Figure 4.7: *Force-displacement graphs of hollow blocks at 28 day age*

The stiffnesses of the various hollow block mixes at an age of 28 days were calculated similarly to that of the solid blocks. The average stiffness of each mix is shown in Figure 4.8.

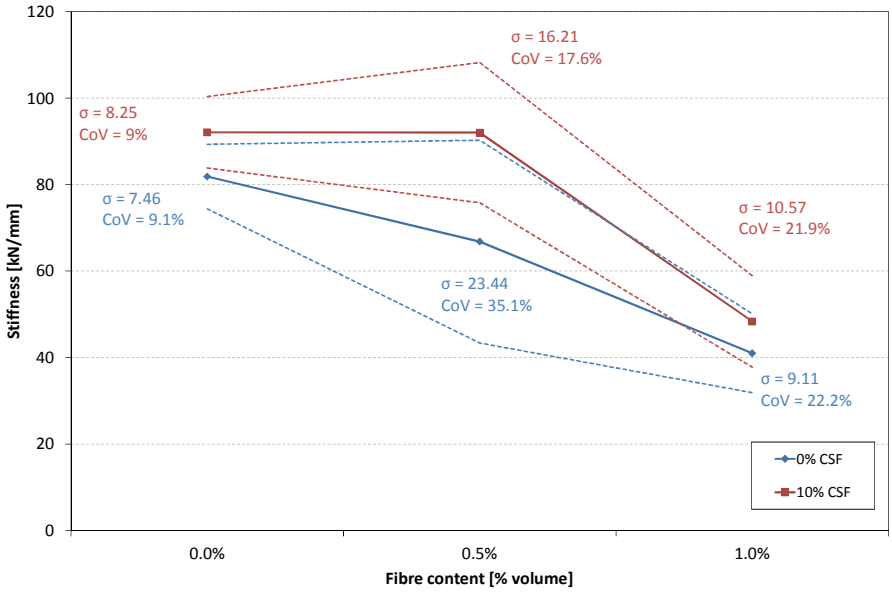

Figure 4.8: *Average stiffness of hollow block mixes at 28 day age*

The average maximum compressive strength of the various mixes is shown in Figure 4.9.

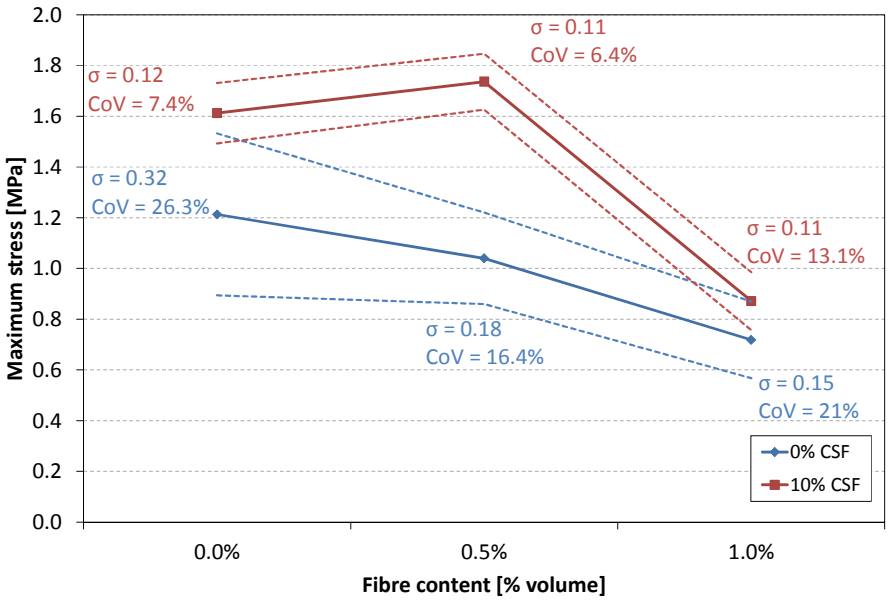

Figure 4.9: *Average maximum compressive stress of hollow block mixes at 28 day age*

It can be seen in Figure 4.8 and Figure 4.9 that for the blocks containing no CSF, the average stiffness and compressive strength decreases with an increase in fibre content. For the blocks containing 10% CSF, the stiffness and compressive strength increases slightly as the fibre content increases to 0.5%, and then sharply decreases as the fibre content is increased to 1%. This is contrary to the results obtained from the solid blocks.

A possible explanation can be that the mixes used were perhaps not entirely suited for blocks without fibres. The mixes with fibres showed better cohesion and many blocks that were produced (without fibres) tended to form small cracks in the upper middle web during moulding (Figure 4.10). The blocks with visible cracks were discarded, but it is possible that the blocks that were tested could have had smaller, less visible cracks.

Figure 4.10: *Cracking in top web of hollow block without fibre*

4.1.2 Flexure test

In this section the results from flexure testing of solid blocks at an age of 28 days are discussed. Figure 4.11 shows the applied force vs. midspan deflection curves of mixes M1, M2, M4, M5 and M6. Five samples of each mix type were tested, but due to human error only two or three sample's displacement data was properly recorded for each mix type. Due to a problem with the LVDT none of the displacement data of the M3 samples was recorded. The maximum applied force for all samples tested was captured.

Considering Figure 4.11, there is a clear difference in curve shape for results of M1 compared to results of M2-M6. This is due to an initial different test setup being used, one without an LVDT-holding brace (Figure 4.12). The setup used for testing M1 samples measured the total vertical midspan displacement at the bottom of the block, as opposed to the displacement relative to the connecting points of the LVDT frame. Also, the initial gentle slope of the curves in Figure 4.11 (a) shows that, during measuring, the setup used for M1 samples included the displacement caused by crushing at the supports and where the load was applied. The second setup used measured the displacement relative to the connecting points of the LVDT frame of the block and, therefore, does not include displacement caused by crushing at supports.

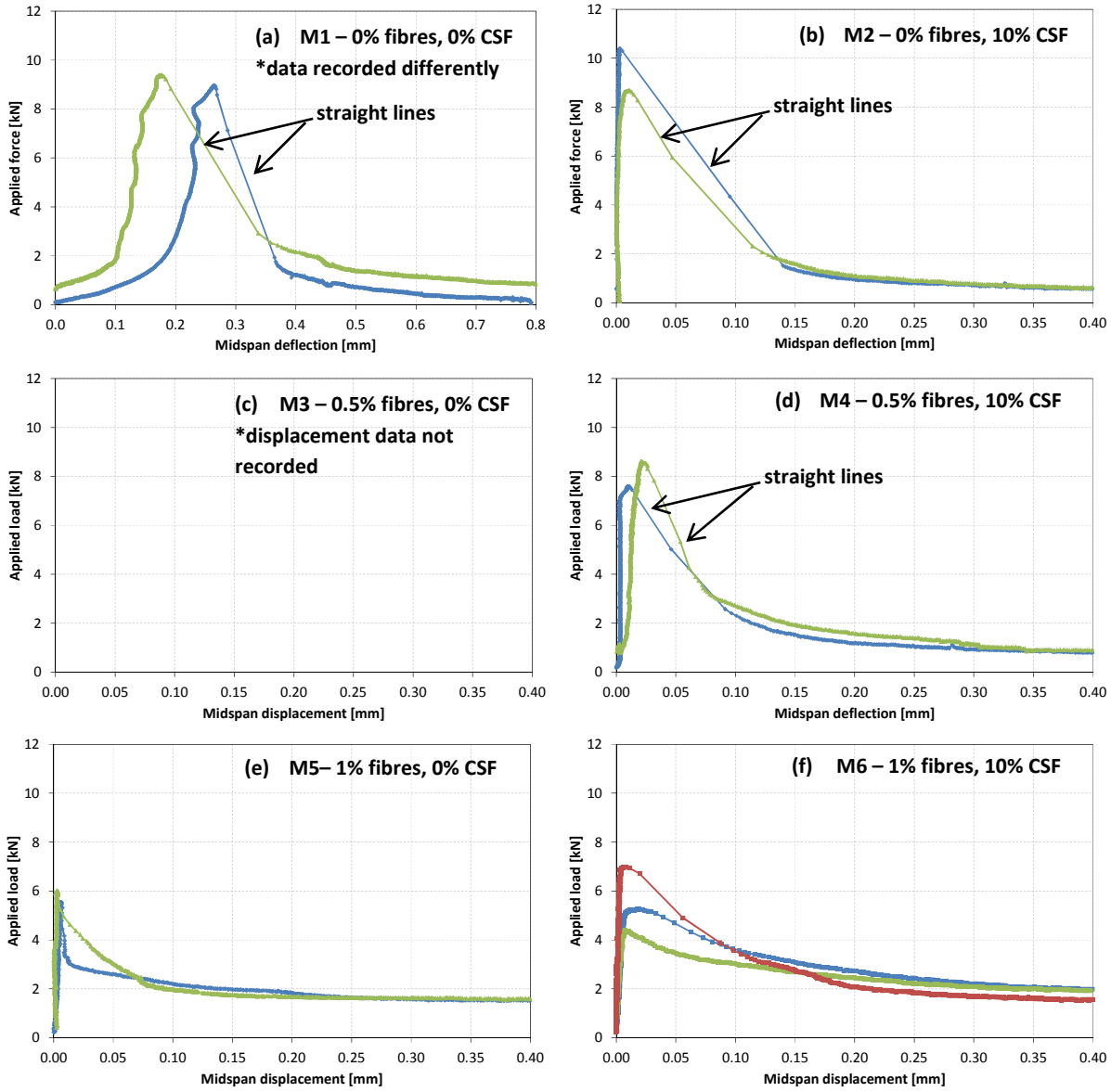

Figure 4.11: *Load-deflection curves of solid blocks at 28 day age*

Another observation to be made is the straight lines in the curves of Figure 4.11 (a), (b) and (d) immediately after reaching peak load. The shape of the curve is not necessarily representative of the deformation that occurred and had data logging taken place at a higher frequency, a better representation would have been attained.

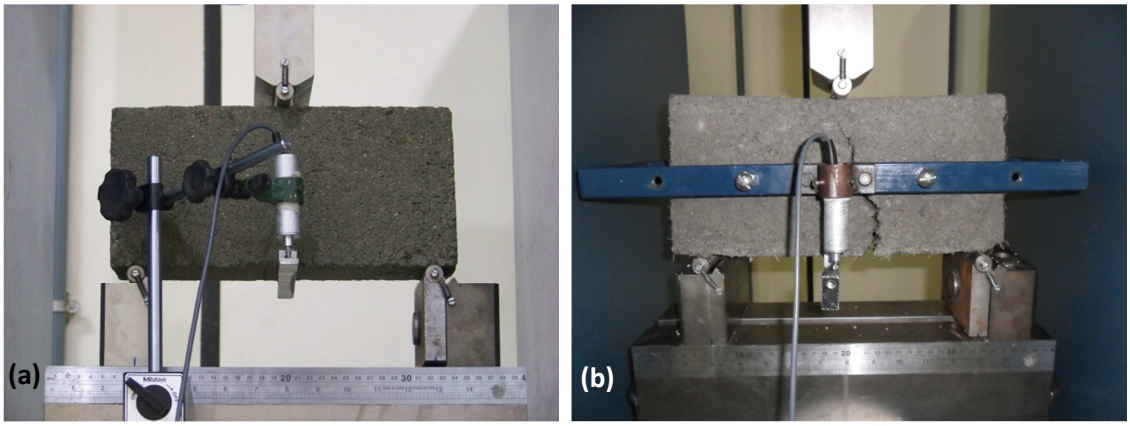

Figure 4.12: *Differing flexure test setups: (a) used for testing M1 blocks; (b) used for testing blocks of mixes M2-M6*

Since so few samples had acceptable displacement data, it was decided that calculating the average fracture energy of each mix type would give a poor representation of the actual fracture energy.

The maximum applied load was captured for all samples tested. Due to the corners of some samples breaking off at the bottom supports, only four of the five samples tested of mixes M1 and M2 delivered useable results.

The modulus of rupture (MOR) of each sample was calculated according to the method described in SANS 1575 (2007) and the following equation:

$$MOR = \frac{3L_1P}{2bd^2}$$

where,

L_1 = the span length (see Figure 3.25)

P = maximum applied load

b = width of beam/block (in this case 90 mm)

d = height of beam/block (in this case 140 mm)

The results are shown in Figure 4.13. For mixes both with and without CSF content there is a significant decrease in MOR. For 0% CSF mixes the addition of 0.5 and 1% fibre led to a decrease in MOR of 21 and 39%, respectively. The same increase in fibre content of 10% CSF mixes led to a decrease in MOR of 28 and 43%, respectively. At all fibre contents CSF mixes had a higher MOR (18, 7 and 8% higher for fibre contents of 0, 0.5 and 1%, respectively).

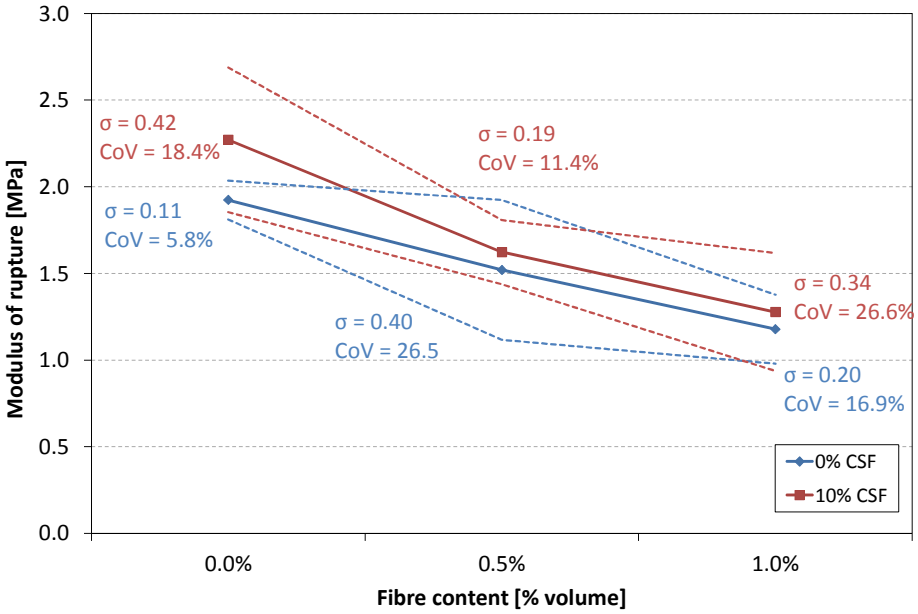

Figure 4.13: *Modulus of rupture of solid blocks at 28 days*

4.2 Volumetric and durability test results

This section covers the results obtained from testing for capillary water absorption, dimensional stability, drying shrinkage, density, total water absorption, porosity and void content.

4.2.1 Capillary water absorption

This section discusses the results of the capillary suction test of solid and hollow blocks at an age of 28 days. As described in Chapter 3.4.3, the mass of each block was determined at various time intervals. The capillary water absorption (g/cm^2) at each time interval was then calculated as follows:

$$water\ absorption\ at\ time\ t\ [g/cm^2] = \frac{mass\ of\ block\ at\ time\ t\ [g] - dry\ mass\ of\ block[g]}{face\ area\ of\ block\ in\ contact\ with\ water\ [cm^2]}$$

The water absorption of each block was plotted against time on a linear scale and as well as a natural logarithmic scale in order to better compare the rate of absorption of different mixes. Using natural logarithmic trendlines, the average slope (rate of absorption) of each block was determined.

Solid blocks

Figure 4.14 shows the water absorption over time of the different solid block mixes on a linear scale. The variability of the results of M6 is clearly the highest.

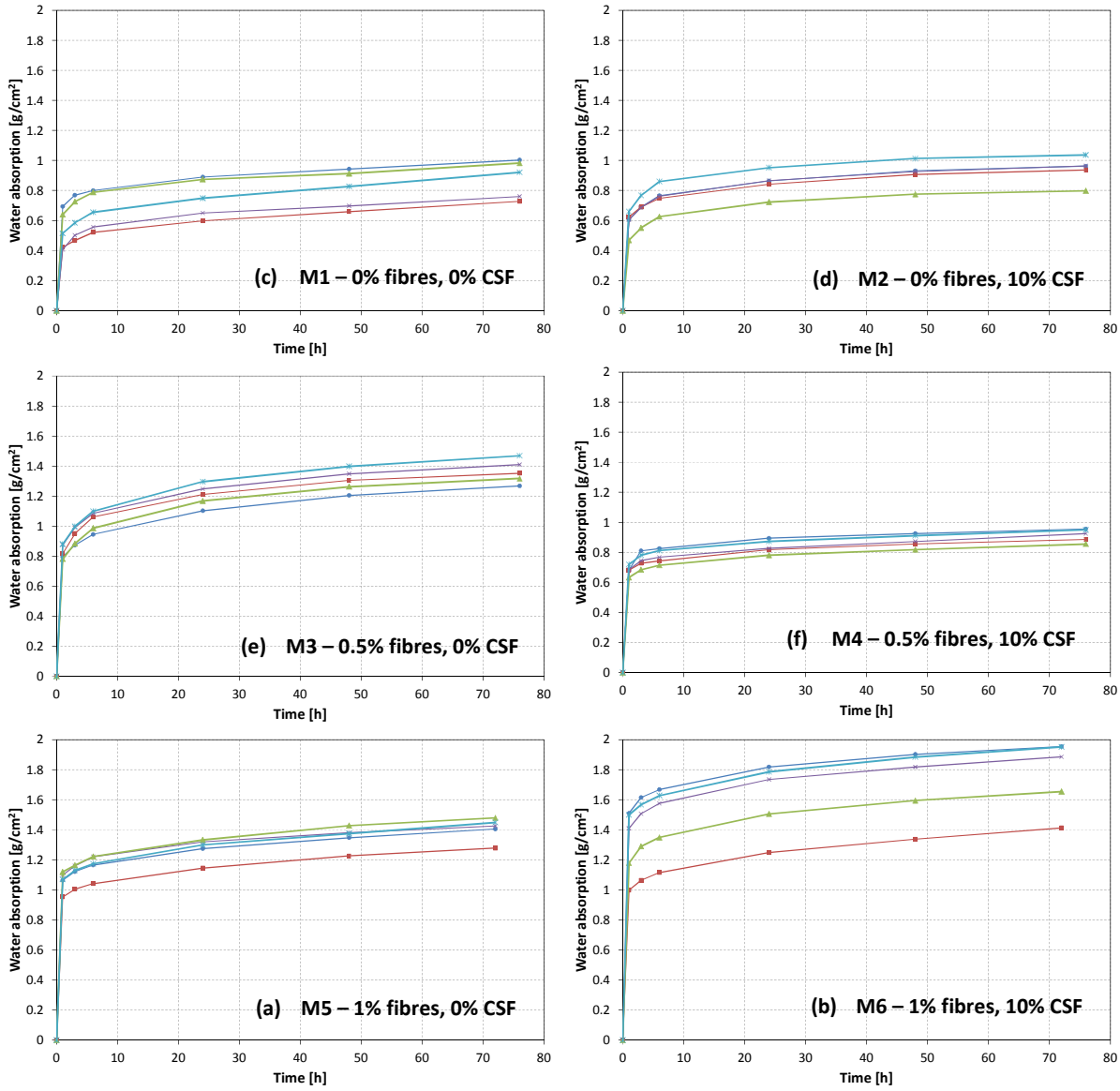

Figure 4.14: *Water absorption graphs of solid blocks (28 day age, linear time scale)*

The results show a very high initial absorption (within the first hour). Thereafter, the rate of absorption decreases significantly for all mixes.

There is a common trend between all the curves where the slope at 76 hours is not completely flat, indicating that the block is not saturated with regards to capillary absorption.

The average absorption after 1h is depicted in Figure 4.15. The values are also indicative of the initial rate of absorption. There seems to be a strong correlation between initial absorption and fibre content.

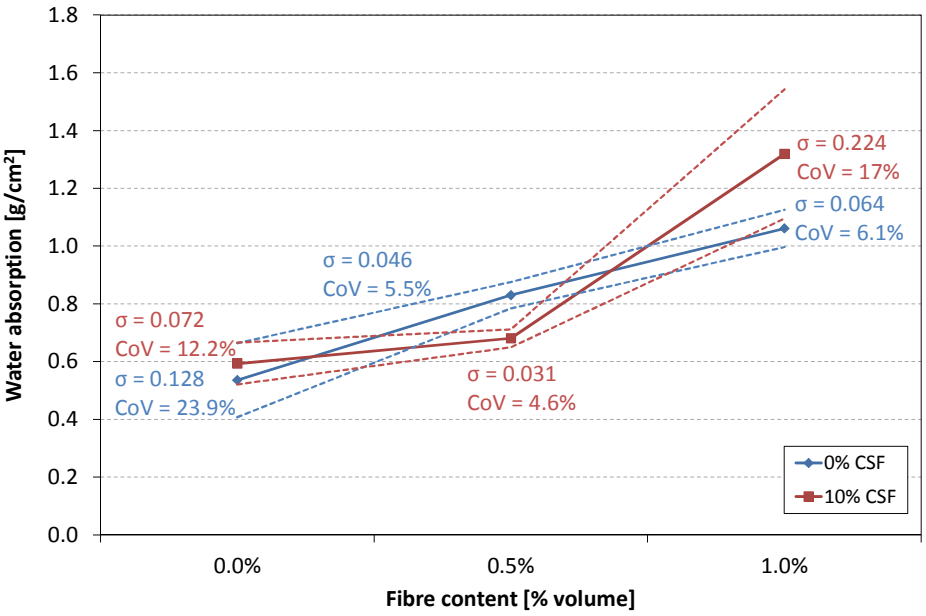

Figure 4.15: *Average water absorption of solid blocks after 1h (28 day age)*

Figure 4.16 shows the average water absorption after 72h, while Figure 4.17 shows the average absorption after 24, 48 and 72 h.

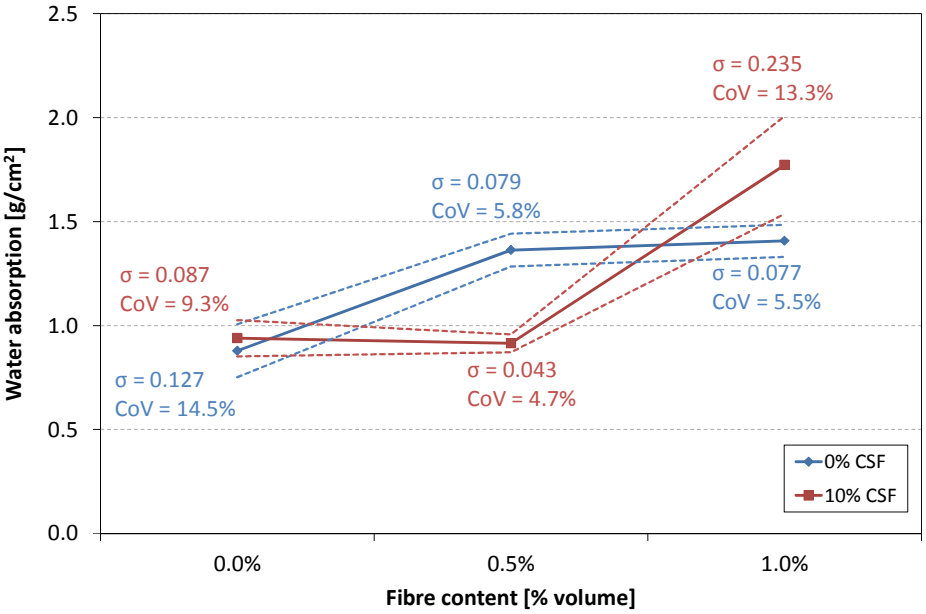

Figure 4.16: *Average water absorption of solid blocks after 72h*

At 0 and 1% fibre content the mixes with CSF have a higher water absorption than the mixes without CSF (7 and 26%, respectively). At 0.5% fibre content, however, the opposite is true with the 0% CSF blocks absorbing about 49% more. The 0% CSF blocks show a larger increase in absorption with the increase to 0.5% fibre, while the 10% CSF blocks show a larger increase with the increase to 1% fibre content.

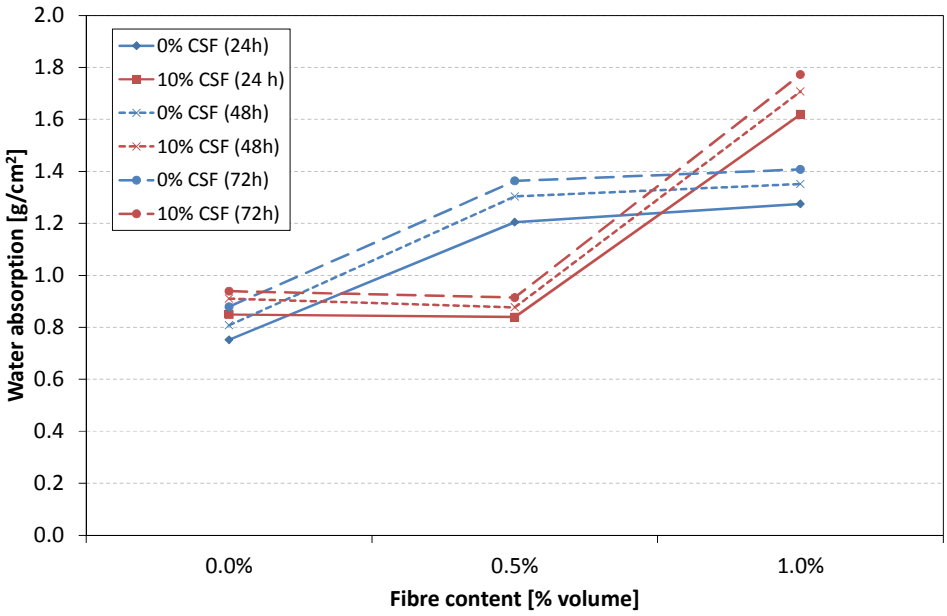

Figure 4.17: *Average water absorption of solid blocks after 24h, 48h and 72h*

As to be expected, the average absorption increases over time for all mixes. Also, at a fibre content of 0% and 1% the blocks containing CSF have a higher absorption than those without CSF, while the opposite is true for blocks with a fibre content of 0.5%.

The results have also been plotted on a natural logarithmic time scale as shown in Figure 4.18.

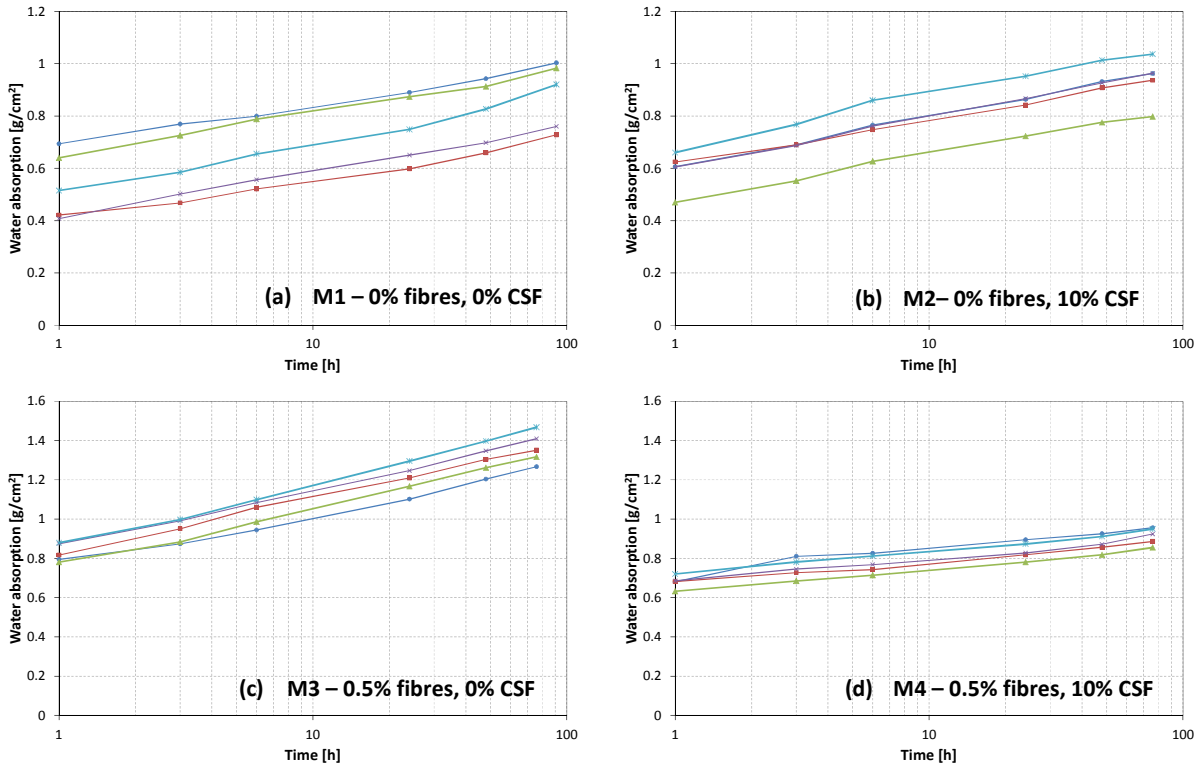

Figure 4.18: *Water absorption graphs of solid blocks (28 day age, natural log time scale)*

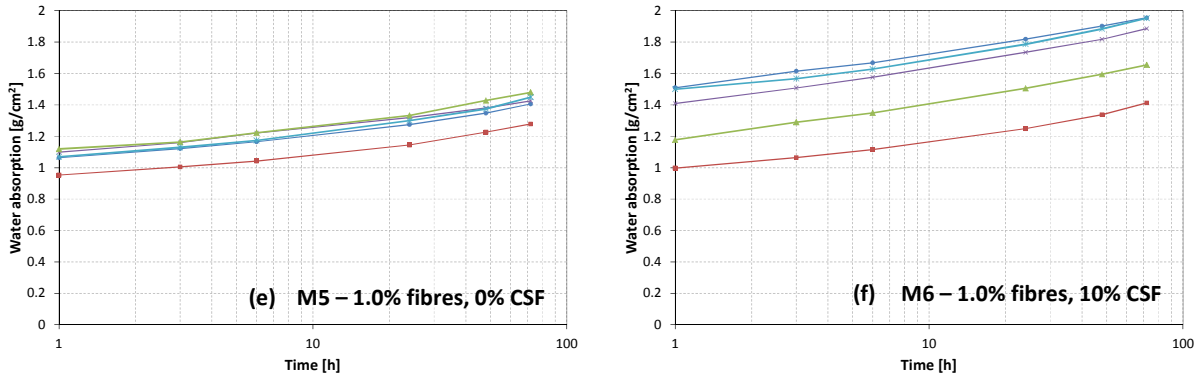

Figure 4.18 (cont.): *Water absorption graphs of solid blocks (28 day age, natural log time scale)*

The slope of the graphs (on a natural logarithmic scale) tends to be fairly constant. Using natural logarithmic trendlines, the slope of each curve was established. Figure 4.19 shows the average rate of absorption of the various mixes. The rates show the same relative trend as the actual absorption. It should be noted that the rate of absorption of the first hour of testing is not properly captured due to the nature of the natural logarithm.

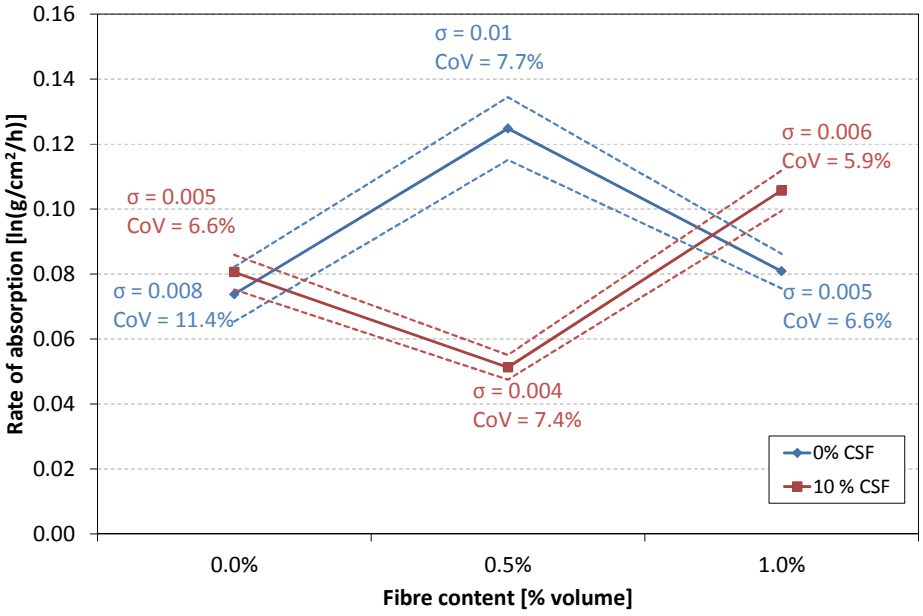

Figure 4.19: *Rate of water absorption of solid blocks (logarithmic)*

At 0 and 1% fibre content the mixes with CSF have a higher rate of absorption than the mixes without CSF (9 and 31%, respectively). At 0.5% fibre content, however, the opposite is true with the 0% CSF blocks absorbing at a rate of about 2.45 times more.

Hollow blocks

The capillary water absorption results for the hollow blocks are presented in a similar manner to the solid blocks. It is worth noting that this test was not performed by the author.

Figure 4.20 shows the absorption plotted on a linear time scale.

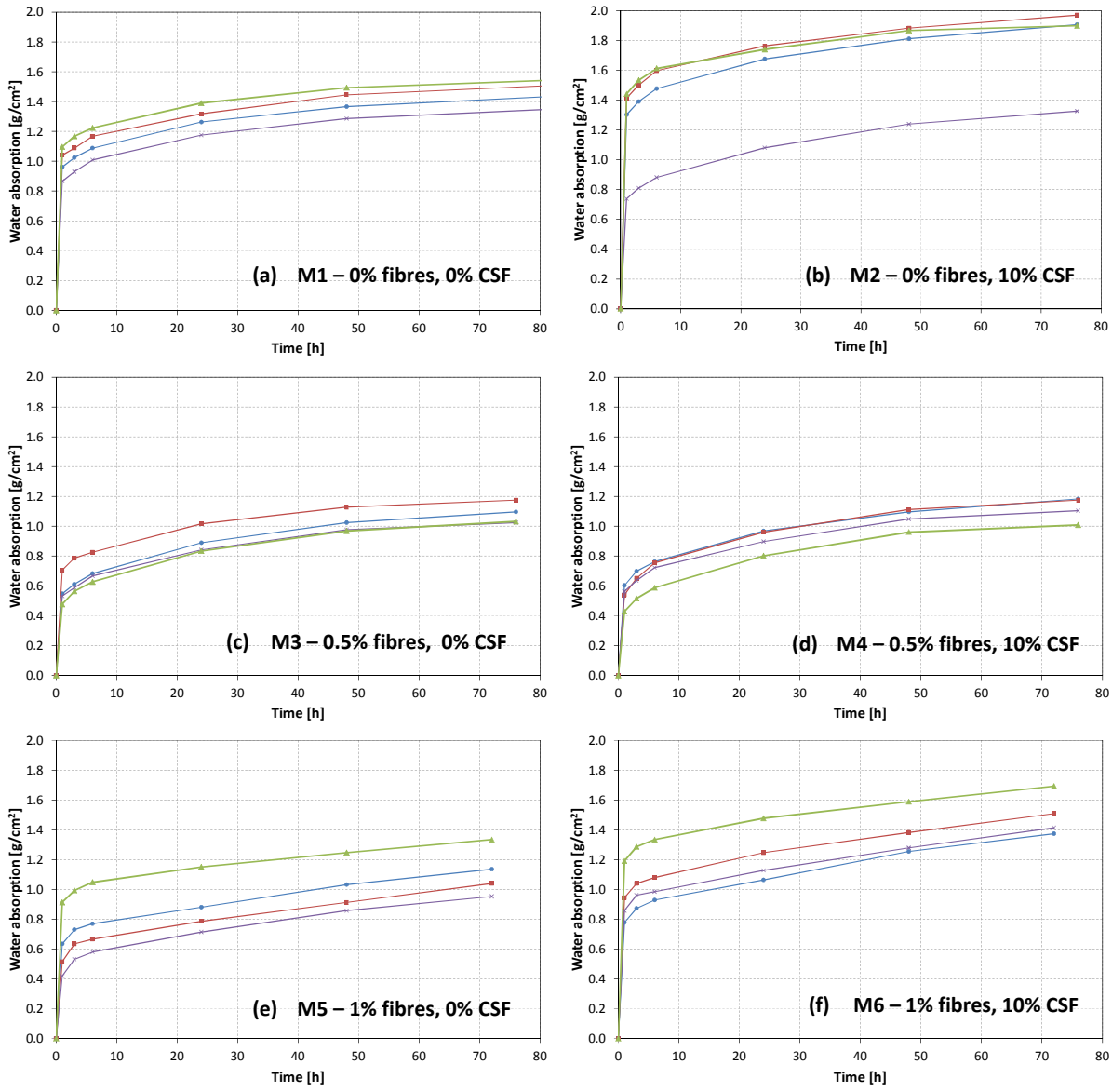

Figure 4.20: *Water absorption graphs of hollow blocks (28 day age, linear time scale)*

The trends regarding the rate of absorption are similar to that of the solid blocks.

Figure 4.21 shows the average water absorption after 1h. This is also indicative of the initial rate of absorption. Blocks without fibres seemed to have a higher initial absorption.

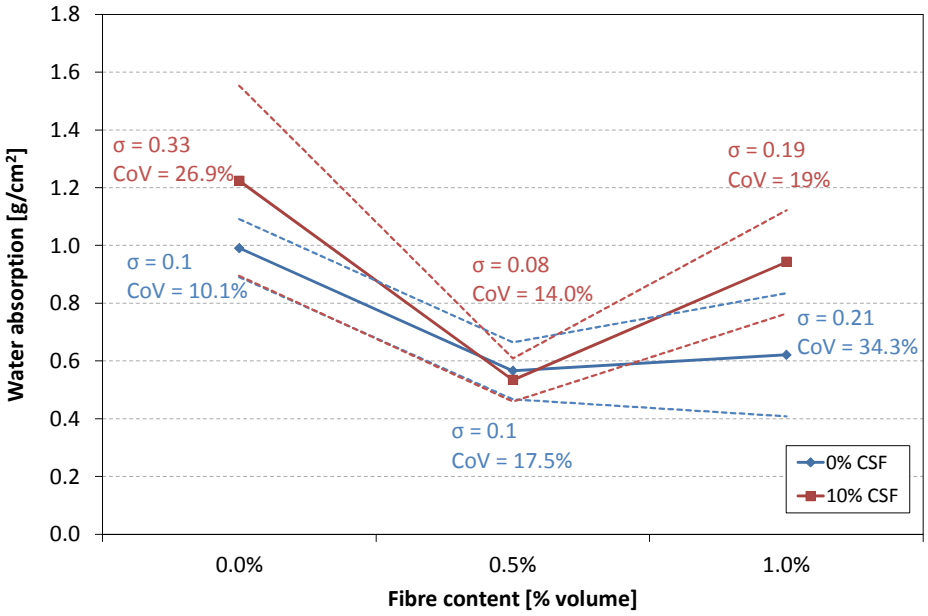

Figure 4.21: *Average water absorption of hollow blocks after 1h (28 day age)*

The average water absorption of the various mixes at 72h is shown in Figure 4.22, while Figure 4.23 shows the absorption at 24, 48 and 72h.

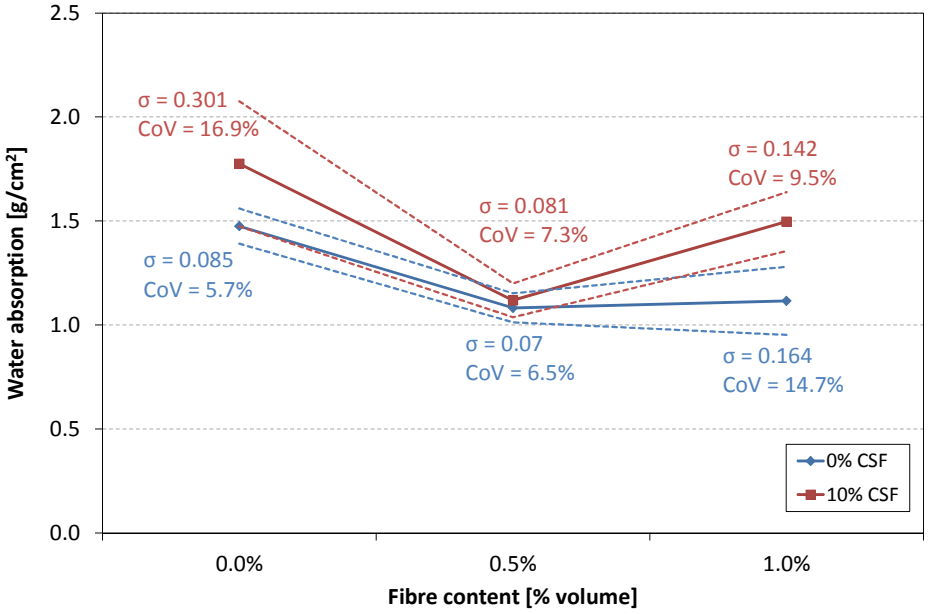

Figure 4.22: *Average water absorption of hollow blocks after 72h*

The absorption after 72h shows a somewhat unexpected trend whereby the absorption does not increase with fibre content. The mixes without CSF have a reduced absorption of 27% with an addition of 0.5% fibre, while the addition of 1% fibre shows a decrease 24% relative to the reference matrix. The mixes with CSF showed a similar decrease of 37 and 16%, respectively. The unexpected results could possibly be attributed to human error.

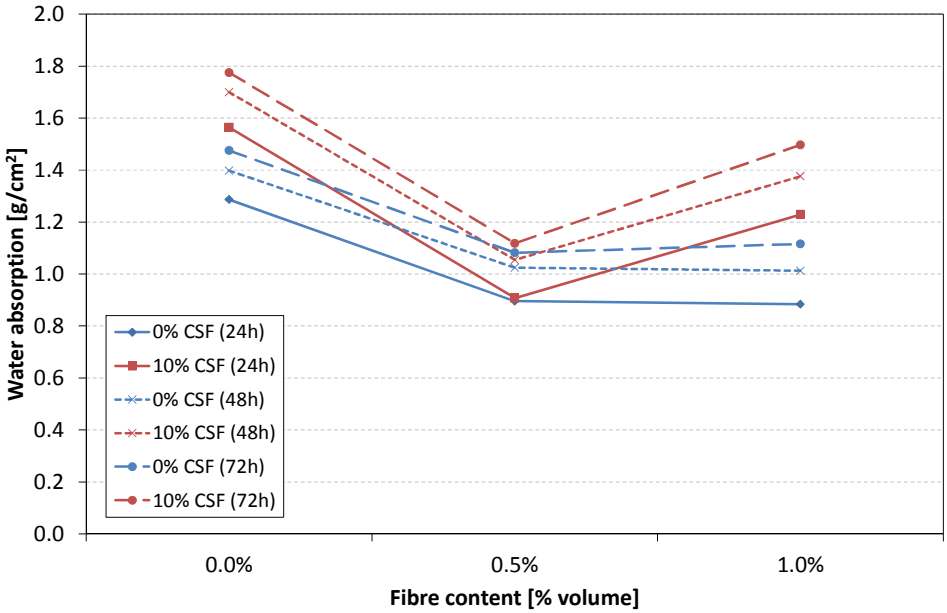

Figure 4.23: *Average water absorption of hollow blocks after 24h, 48h and 72h*

As to be expected, the average absorption increased over time for all mixes.

The water absorption over time (on a logarithmic scale) of the hollow blocks is presented in Figure 4.24. It should be noted that, due to the nature of a natural logarithmic curve, the initial rate (during the first hour) is not included in these graphs.

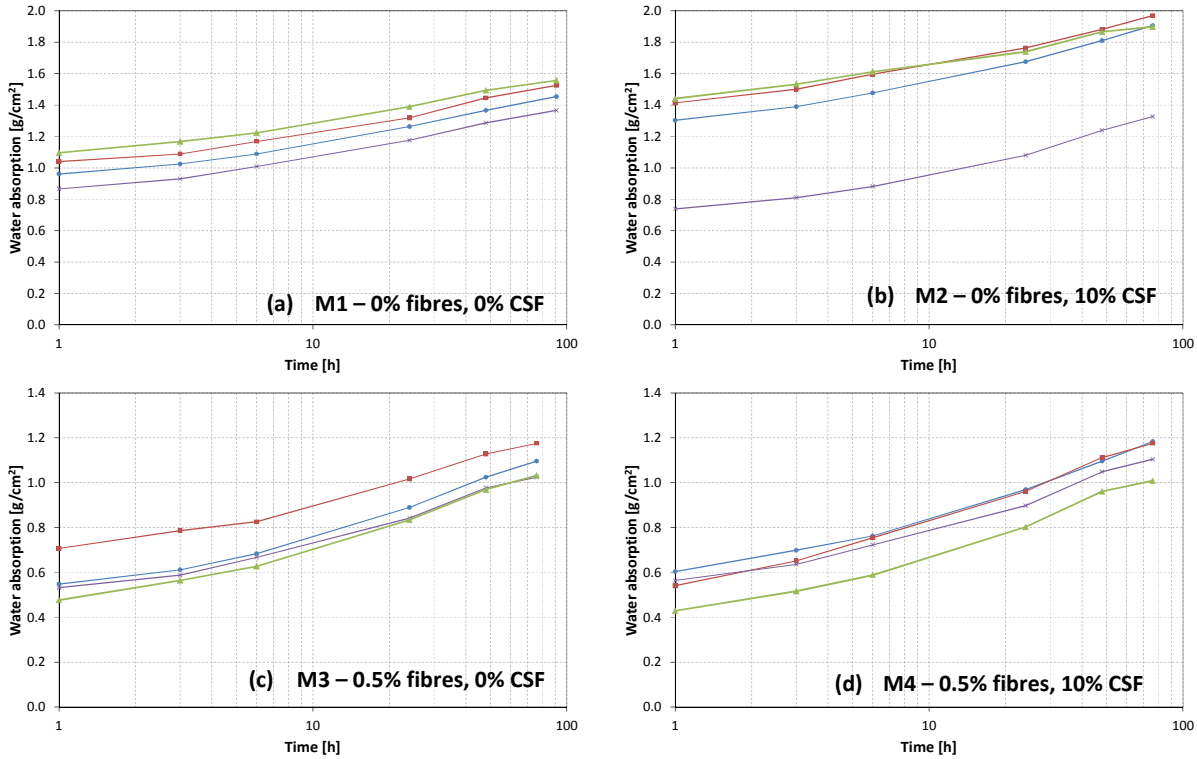

Figure 4.24: *Water absorption over time graphs of hollow blocks at 28 day age*

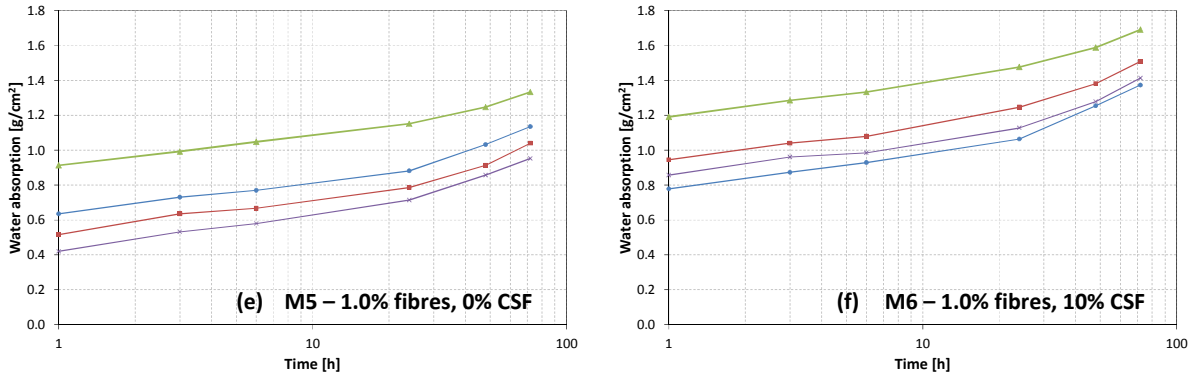

Figure 4.24: *Water absorption over time graphs of hollow blocks at 28 day age*

Similarly to the results of the solid blocks, the absorption over time, if plotted on a logarithmic scale, has a fairly constant rate. Using natural logarithmic trendlines, the slope of each curve was established. Figure 4.25 shows the average rate of absorption of the various mixes. The rates show the same relative trend as the actual absorption.

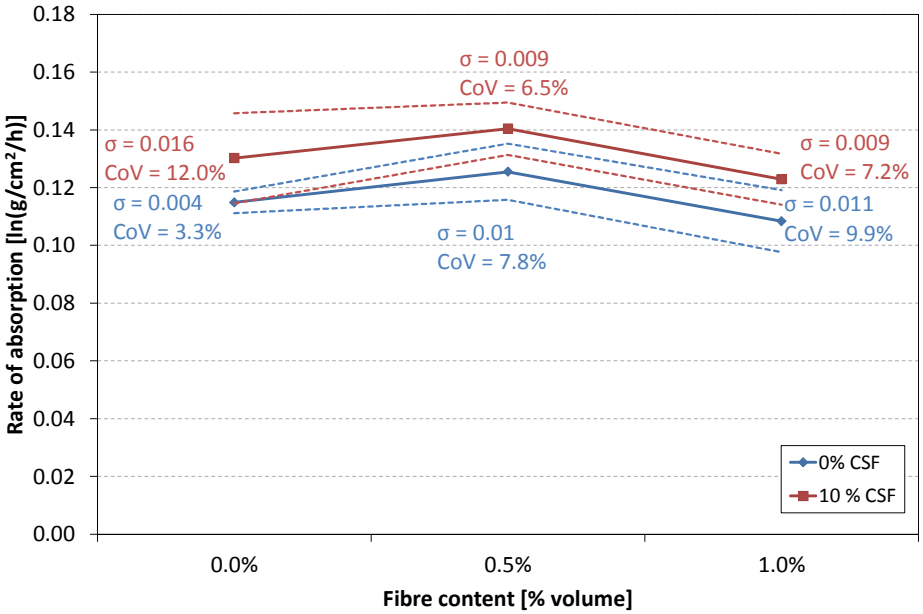

Figure 4.25: *Rate of water absorption of hollow blocks*

For both matrix types there is an increase in rate of absorption with the addition of 0.5% fibres. With the addition of 0.5% more, there is a decrease in rate of absorption that ends up being less than that of the reference matrix.

The rate for the 10% CSF blocks is between 11 and 14% than that of 0% CSF blocks.

4.2.2 Density, absorption and void content

The total immersion test was performed according to ASTM C642-97 (1997). The following properties were calculated:

$$\text{Absorption after immersion, \%} = [(B - A)/A] \times 100 \quad (1)$$

$$\text{Absorption after immersion and boiling, \%} = [(C - A)/A] \times 100 \quad (2)$$

$$\text{Bulk density, dry} = [A/(C - D)] \times \rho \quad (3)$$

$$\text{Volume of permeable pore space, \%} = [(C - A)/(C - D)] \times 100 \quad (4)$$

where,

A = mass of oven-dried sample in air, g

B = mass of surface-dry sample in air after immersion, g

C = Mass of surface-dry sample in air after immersion and boiling, g

D = Apparent mass of sample in water after immersion and boiling, g

This section discusses the abovementioned four properties that were calculated.

Figure 4.26 shows the water absorption after immersion. There is a significant increase in absorption with an increase in fibre content. For the 0% CSF mixes the absorption increased by 73% and 85% with the addition of 0.5% and 1% fibre, respectively. For the 10% CSF mixes the increase was slightly lower at 54% and 62%, respectively. On average the absorption for blocks without CSF was 5% higher than that for blocks with CSF, although the difference is much smaller for blocks without fibres. The blocks with no fibre showed the highest variability.

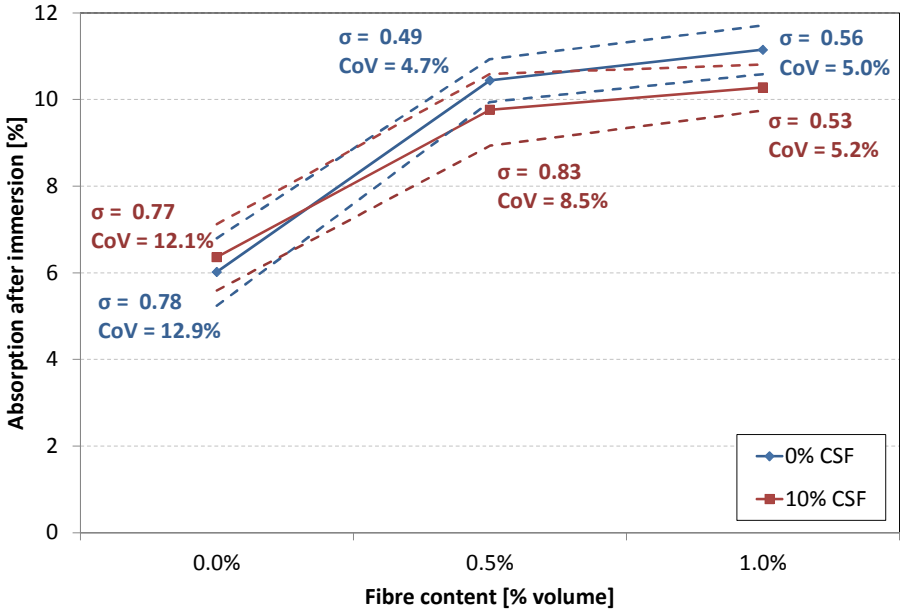

Figure 4.26: *Absorption after immersion*

Figure 4.27 shows the absorption after immersion and boiling. As with absorption after immersion, the results show a substantial increase in absorption with the addition of fibres to the matrix. For the blocks containing no CSF the absorption increased by 55% and 70% with the addition of 0.5% and 1% fibres, respectively. For the block with CSF the increase was 40% and 47% respectively. Once again, the blocks without fibre showed 6% lower absorption, on average.

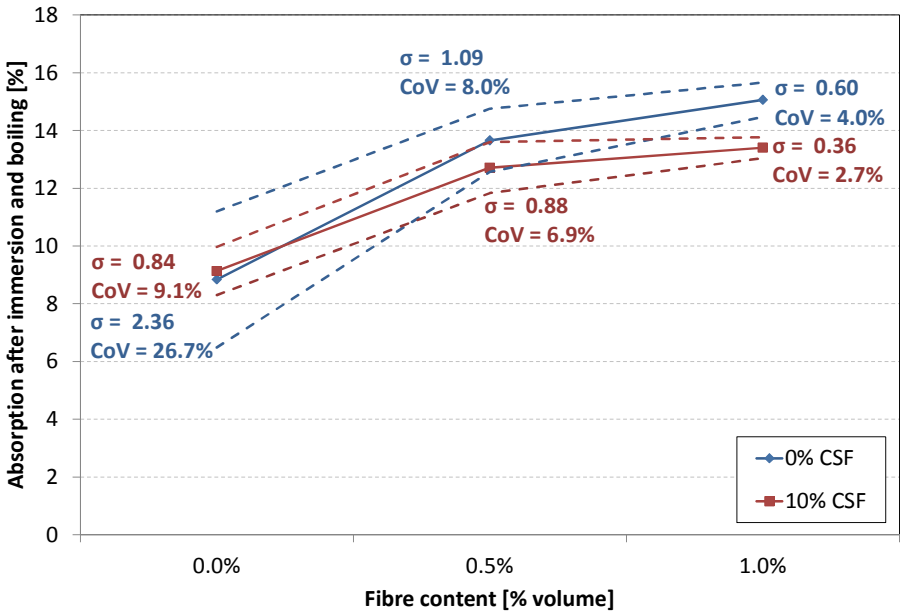

Figure 4.27: *Absorption after immersion and boiling*

After boiling, absorption increased significantly. For blocks with 0% fibre, the increase was 43%. For blocks with 0.5% fibre the increase was 30% on average, while blocks with 1% fibre had an increased absorption of 32%. The blocks without fibres showed the highest variability.

The calculated average dry bulk densities of the blocks are shown in Figure 4.28. The graph shows a sharp decrease in dry bulk density with the addition of fibres for both mix types (0% and 10% CSF). The 0% CSF blocks showed a 6% decrease with the addition of 0.5% fibre and a decrease of 8% with the addition of 1% fibre. For the 10% CSF blocks the decrease was 5% and 6%, respectively.

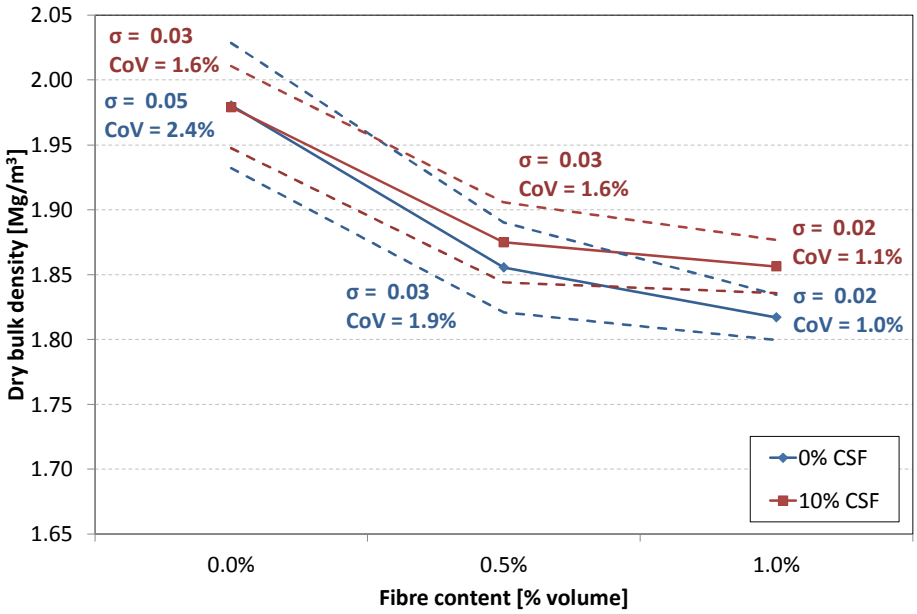

Figure 4.28: *Dry bulk density*

The average volume of permeable void space of each block type was calculated as well (Figure 4.29). The curves show a large increase in pore space (or porosity). The matrices without CSF showed an increase in void space of 45% and 57% with the addition of 0.5% and 1% sisal fibres, respectively. The increase was 32% and 38%, respectively, for mixes with CSF. With no fibres the addition of 10% silica increased the porosity by 3.5%. With fibres added the samples without CSF had a higher porosity than those with CSF (6.2% for 0.5% fibre and 10% for 1% fibre).

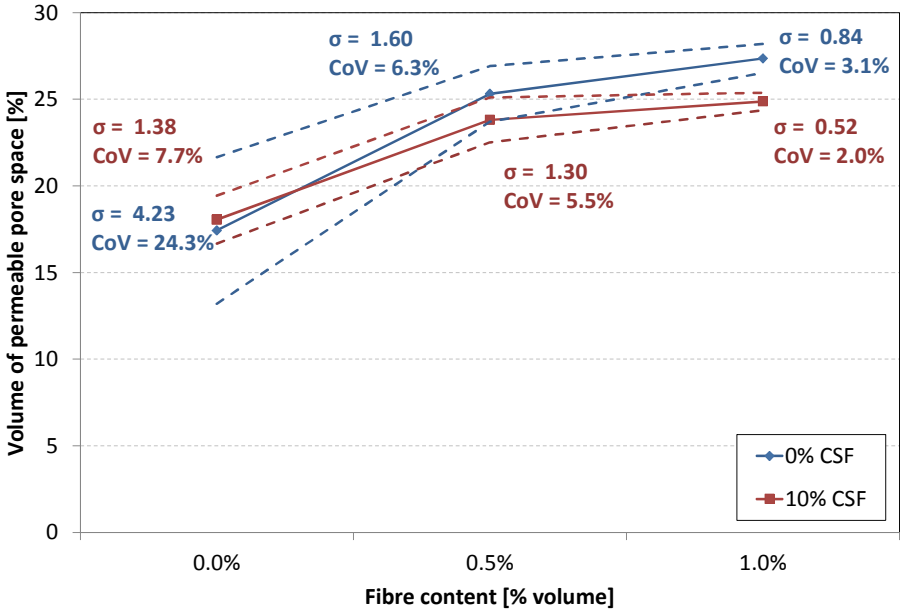

Figure 4.29: *Volume of permeable pore space*

The mixes without any fibre had an average pore space volume of 17.4% (0% CSF) and 18.1% (10% CSF).

4.2.3 Dimensional stability

This test was set up and performed as described in Section 3.4.5. Each block was subjected to 4 cycles of wetting and drying and the various dimensions (as described in Section 3.4.5) were measured after each cycle.

After testing each block was virtually broken into twelve smaller segments along the lines where the dimensions were measured, as shown in Figure 4.30.

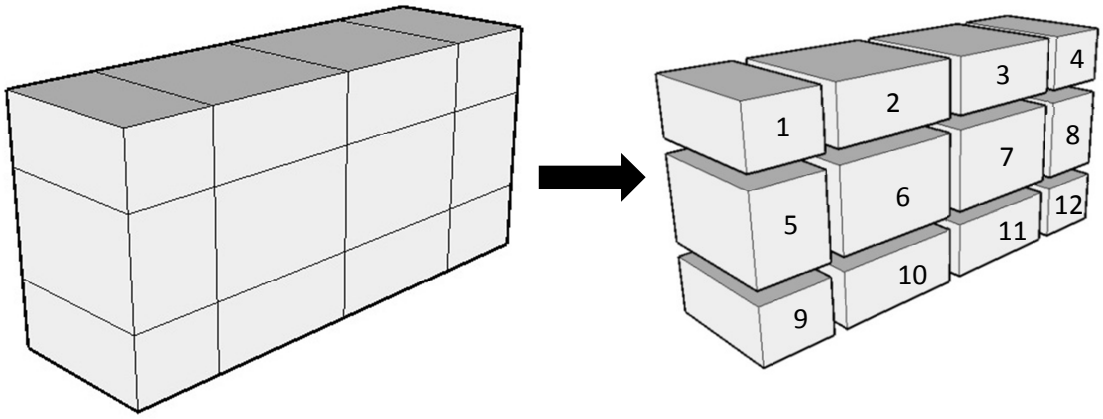

Figure 4.30: *Solid block splitting into segments*

Some segments did not have dimensions that were measured. For example, looking at segments 2, 6 and 10 (Figure 4.31) only the height dimensions H2, H3, H7 and H8 are known. To establish a value for $H_{2/6}$, linear interpolation was used between H2 and H7, using the ratio of 40/140 (the ratio according to which the block was originally split up over its width, Figure 3.29). Similarly, $H_{6/10}$ was calculated by linearly interpolating between H2 and N7 and using the ratio of 100/140.

The width dimensions were calculated by using the ratio of where lines were drawn on the original blocks. For example $W_{2/2}$ was calculated by multiplying the measured width (W_2) with the ratio of 40/140. Using this method, width $W_{2/10}$ would have the same length as $W_{2/2}$. Similarly $W_{2/6}$ was calculated using a ratio of 60/140.

The length dimensions were calculated similarly to the width, by multiplying the measured length with the ratios according to which the measuring lines were drawn on the blocks.

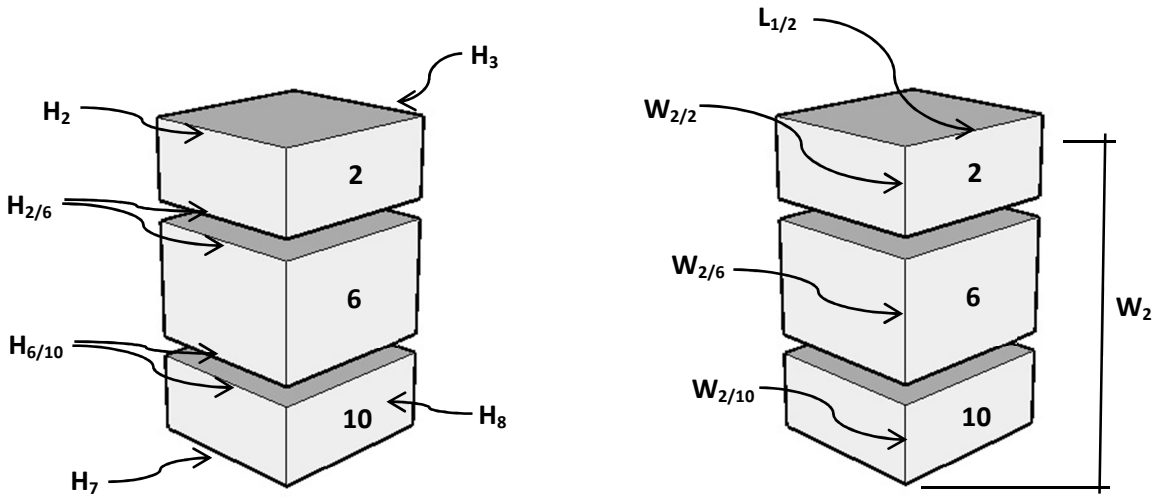

Figure 4.31: *Interpolation of dimensions*

For every wet/dry cycle the volume of each segment was calculated. The volume of all the segments for each cycle was added up to get to the final volume of the entire block.

The volume of each segment was calculated using the *convhulln* function found in Matlab. The convhulln function is based on the Qhull algorithm used for calculating the surface area and volume of a convex hull (Qhull.org, 2012).

The volumes of the bricks were also calculated using a method developed by Turner (2012). This method breaks each block segment into six tetrahedrons. It then calculates the volume of each tetrahedron by taking the determinant of the scalar triple product between the vectors that make up

the sides. Table 4.1 shows a comparison between results found using the convhulln function and the method developed by Turner.

Table 4.1: *Comparison between volume results of convulln and Turner's function*

Cycle	*convulln* function [mm^3]	Turner [mm^3]	Difference [%]
Dry 1	3516201	3520220	0.11%
Wet 1	3451387	3448206	-0.09%
Dry 2	3453363	3450128	-0.09%
Wet 2	3460684	3456668	-0.12%
Dry 3	3457540	3453994	-0.10%
Wet 3	3462389	3458488	-0.11%
Dry 4	3458006	3454130	-0.11%
Wet 4	3460965	3456965	-0.12%

Results obtained using Turner's differ by less than 0.12% than the results obtained from the *convulln* function. This difference was deemed small enough and it was decided to use the *convulln* function for volume calculations.

Three blocks of each mix type were tested. The volume for each block during each cycle was calculated and the results are represented as a percentage change in volume compared to the original dry volume (D1). The results are presented in Figure 4.32.

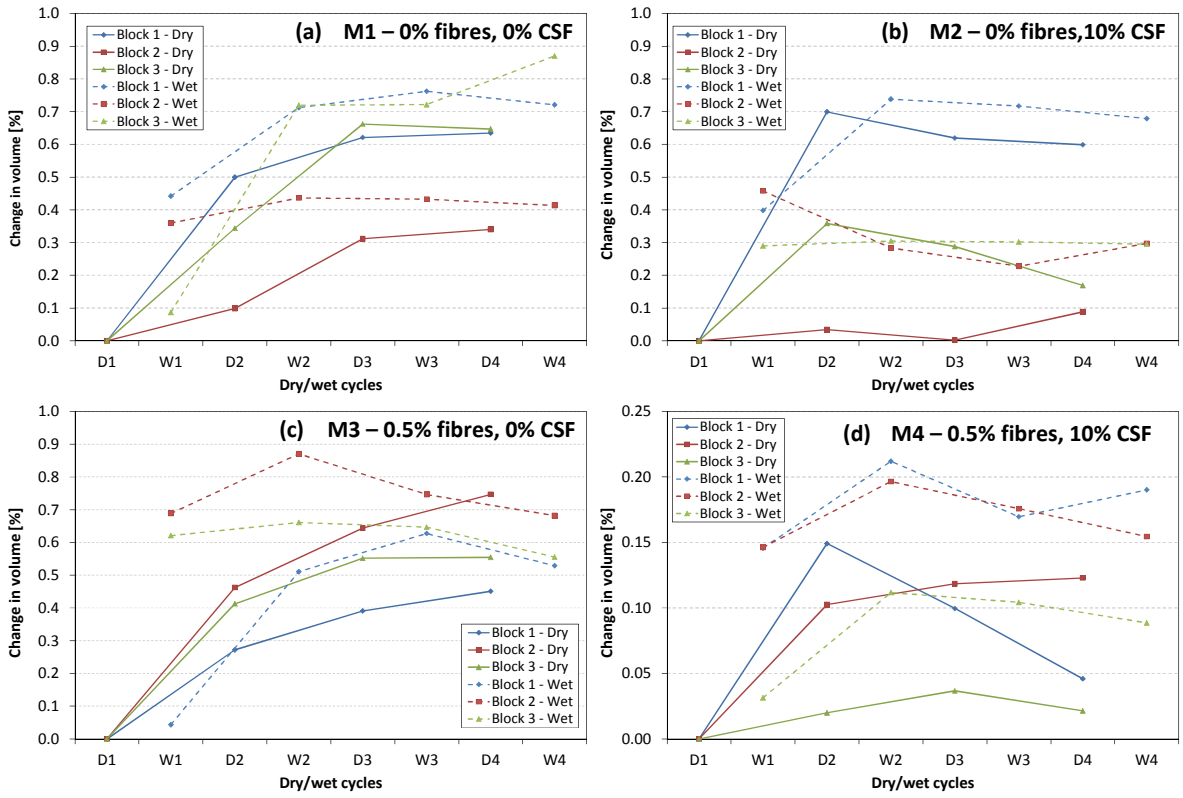

Figure 4.32: *Change in volume during wet/dry cycles*

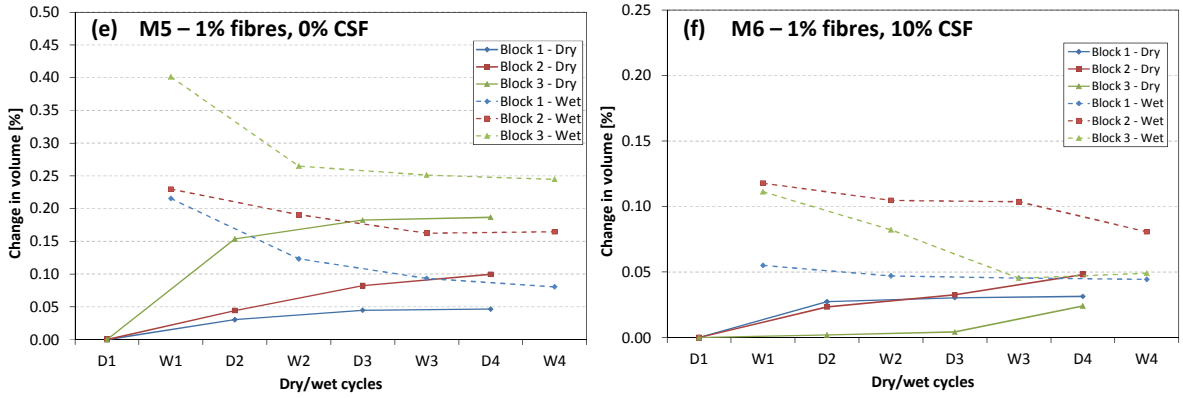

Figure 4.32 (cont.): *Change in volume during wet/dry cycles*

The results represented in Figure 4.32 show a high variability. This could be a result of the high level of difficulty of measuring changes in length accurately using a Vernier calliper. In some cases the change in length between a wet and dry cycle was 0.04mm, for example, but the Vernier calliper used was only accurate to within 0.02 mm. The results could, therefore, reflect a somewhat inaccurate representation of the changes in length between cycles. Also, measuring at exactly the same spots during all cycles proved to be very difficult and even slight deviations from the measuring spots could lead to relatively large changes in length.

The results show a trend where both wet and dry volumes initially increase and after about two cycles, start to stabilise.

For each mix the average of the dry and wet cycle volumes of the three blocks were determined. Figure 4.33 shows the average results for mixes containing no CSF.

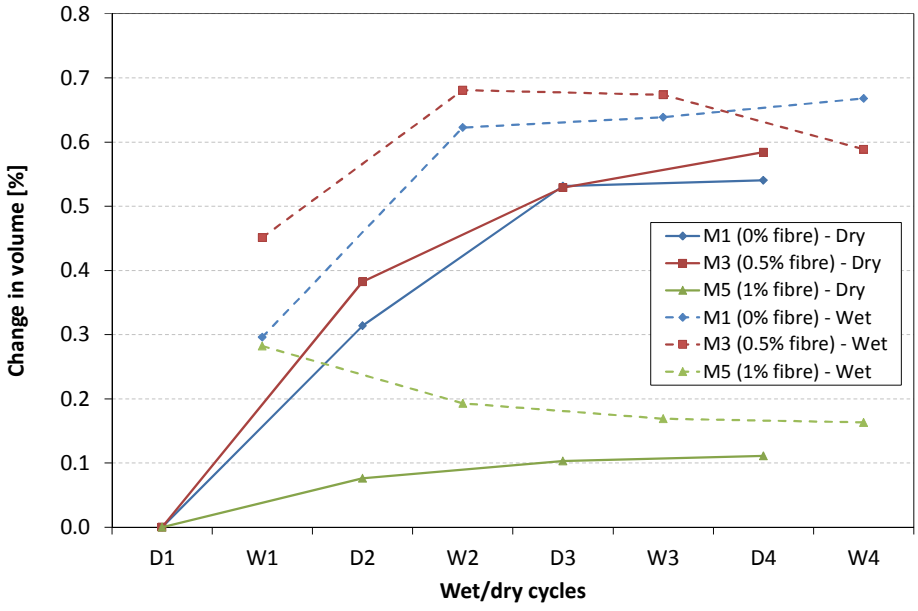

Figure 4.33: *Average change in volume during wet/dry cycles (mixes with 0% CSF)*

Average results for mixes M1 and M3 shows a similar shape for both wet and dry cycles, although the initial change in volume of M3 after the first wetting cycle was about 52% higher than that of M1. Both dry and wet cycle volume changes increased rapidly during the first couple of cycles, but stabilised soon after.

The results of M5 (1% fibre) showed a very different trend. The initial increase in volume change was slower for dry cycles and for wetting there was a decrease in volume change. After a couple of cycles the curves stabilised somewhat. After four cycles there was a difference in change in volume between wet and dry cycles of about 0.05%.

The final average wet change in volume of M5 was 0.163%. For M3, this value was 0.589% (3.6 times more) while the value for M1 was 0.668% (4.1 times higher).

For the average dry volume changes the final value for M5 was 0.111%, for M3 it was 0.584% (5.3 times higher) and for M1 it was 0.541% (4.9 times higher).

Figure 4.34 shows the average change in volume of mixes with 10% CSF. The blocks containing CSF showed a trend where there was an initial increase in volume during wet cycles, but a decrease as cycles continued. There is a clear decrease in change in volume as the fibre content of the blocks increases. The final average wet change in volume of M6 was 0.058%. For M4, this value was 0.144% (2.5 times more) while the value for M2 was 0.423% (7.3 times higher).

For the average dry volume changes the final value for M6 was 0.034%, for M4 it was 0.063% (1.8 times higher) and for M2 it was 0.285% (8.3 times higher).

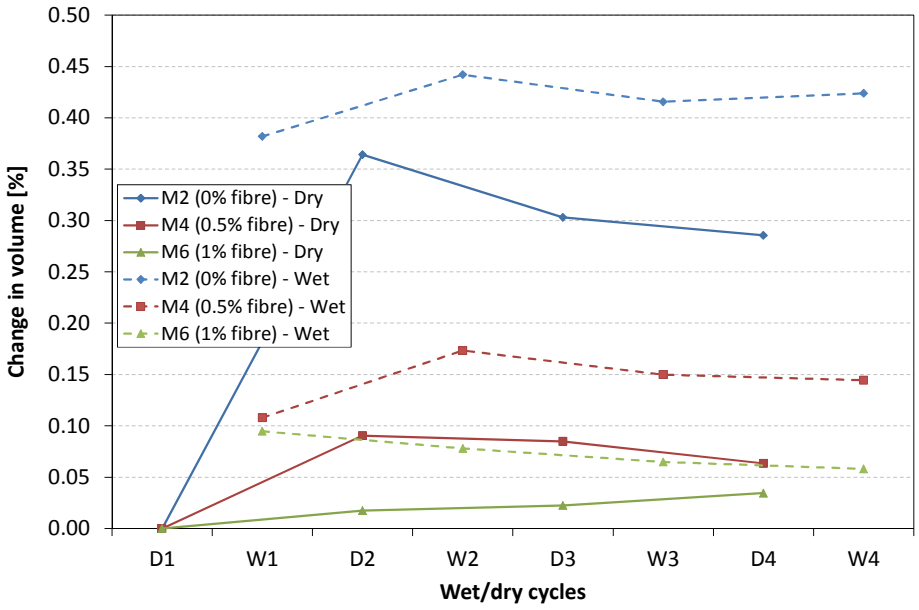

Figure 4.34: *Average change in volume during wet/dry cycles (mixes with 10% CSF)*

4.2.4 Drying shrinkage

This section discusses the results obtained from drying shrinkage testing of the solid block mixes. Each different mix consisted of four samples and the test was run for just short of two months. Drying shrinkage and mass loss were measured over time and the results are discussed separately.

Shrinkage

Figure 4.35 shows the shrinkage strain-time curves for the six mixes, presented on a natural logarithmic time scale. Appendix B contains the results presented on a linear time scale. The shrinkage strain was calculated by dividing the change in length at each time interval by the original length between the two metal pins (see Chapter 3.4.6). It should be noted that one sample data of mixes M1 and M4 each was rejected due to a high variation (data more than three standard deviations away from the average).

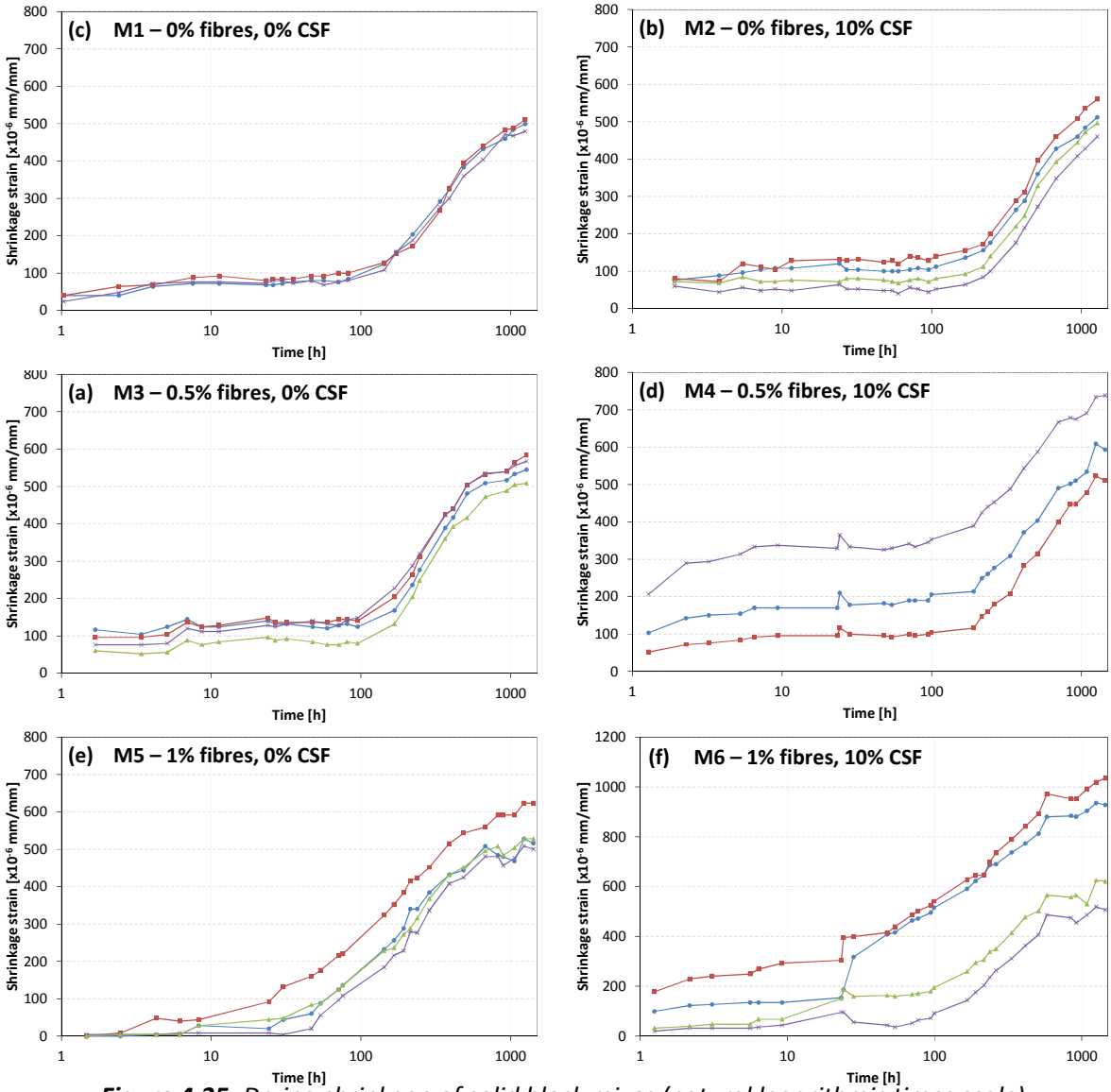

Figure 4.35: *Drying shrinkage of solid block mixes (natural logarithmic times scale)*

Considering the shrinkage graphs for M4, M5, and M6, it is clear that the samples exhibited a larger variation in shrinkage strain. This could possibly be attributed to these three tests being performed by a different person.

Closely studying Figure 4.35, it becomes clear that they tend to have three different average slopes. Figure 4.36 shows how natural logarithmic trendlines have been fitted to a shrinkage curve of one of the M1 samples. For all six mixes the change in slope tended to occur at different time intervals, but for the different samples in each mix the slope changes tended to happen more or less at the same time.

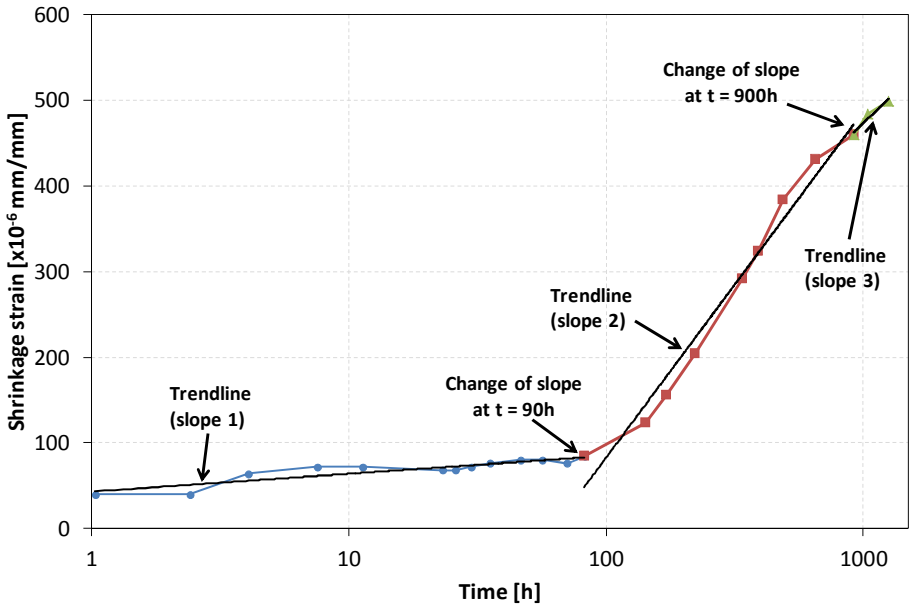

Figure 4.36: *Trendlines fitted to shrinkage curve*

To test the validity of the assumption that each shrinkage curve can be broken into three regions, the theoretical drying shrinkage of the mixes without fibres was modelled using the methods described by the CEB-FIP in the Model Code 2010 (Euro-International Committee for Concrete, 2010). The average compressive strength of the blocks was used as input and it should be noted that the Model Code 2010 requires cube compressive strength as input. Also, the Model Code does not make provision for concrete mixes containing fibres.

Figure 4.37 shows a comparison between two actual sample shrinkage curves (M1 and M2) and the theoretical curves, as predicted by the Model Code 2010. Even though the shrinkage values do not compare well, the CEB-FIP curves do show a similar three slope trend over a two month period. A notable difference in the slopes is that for the actual sample curves, the time until the first slope change occurs is considerably longer.

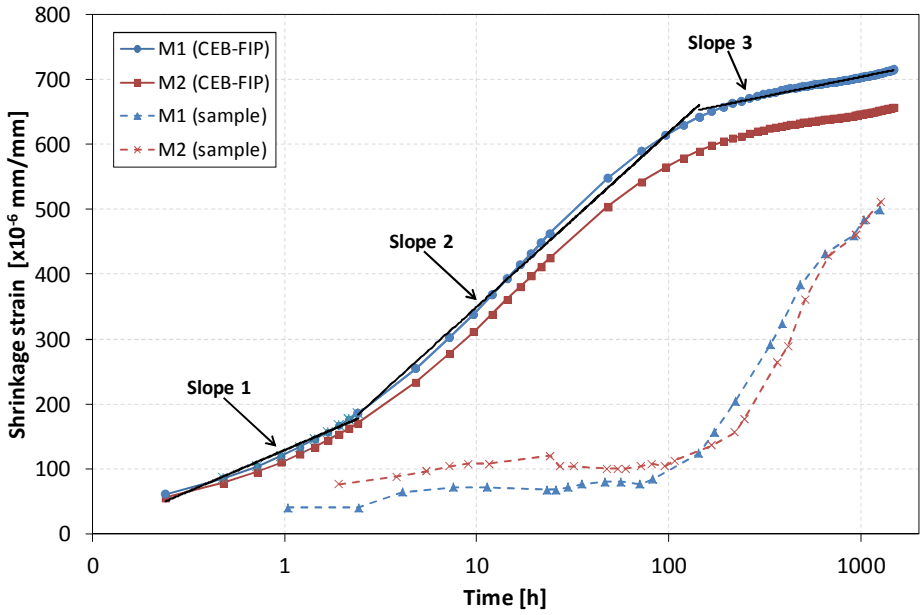

Figure 4.37: *Comparison between CEB-FIP and actual shrinkage curves.*

The average shrinkage slope and time of slope change was determined for each mix. Table 4.2 shows the approximate time at which these slope changes occur for each mix, while Figure 4.38 shows the average logarithmic slopes of the drying shrinkage strain of the various mixes.

Table 4.2: *Average drying shrinkage natural logarithmic slope changes*

	M1	M2	M3	M4	M5	M6
Slope change 1 [h]	90	160	100	190	50	50
Slope change 2 [h]	900	940	680	1000	680	480

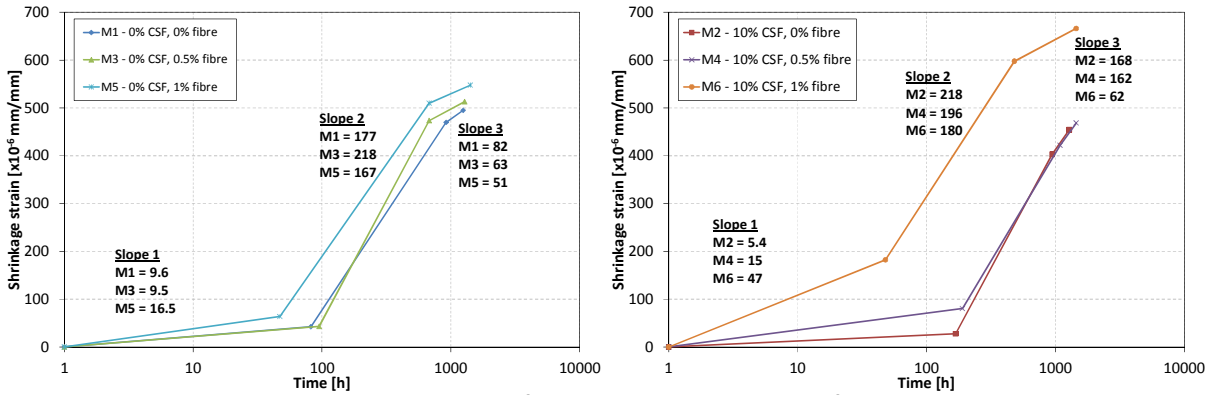

Figure 4.38: *Average slopes of drying shrinkage strain of solid block mixes*

The above shows that the blocks containing 1% fibres had the highest initial shrinkage rate. For the blocks with no CSF this rate was, on average, 74% higher than that of blocks with 0 and 0.5% fibre content. For the blocks containing CSF, the initial rate for 1% fibre blocks was 870% higher than 0% fibre blocks and 310% higher than 0.5% fibre blocks.

The blocks with the 1% fibre changed slope sooner (about 50% sooner for blocks without CSF and about 70% sooner for blocks with CSF), although the second slope is more or less the same for all mixes.

The next slope change occurs soonest, once again, for blocks with the highest fibre content. The slope after the change is somewhat lower than before the change for all mixes and the slope is inversely affected by the fibre content.

In all cases the shrinkage graphs had a gentle initial slope. After the first slope change the slope increased greatly (in the order of 4-23 times for blocks without CSF and 4-40 times for blocks with CSF). The second slope change led to a reduction in slope (20-90% for blocks without CSF and 20-65% for blocks with CSF.

The total drying shrinkage after two months is shown in Figure 4.39. Considering blocks without CSF, an addition of 0.5% of fibres leads to an increase of 11% in drying shrinkage after two months. Increasing the fibre content to 1% had no significant effect on the total drying shrinkage.

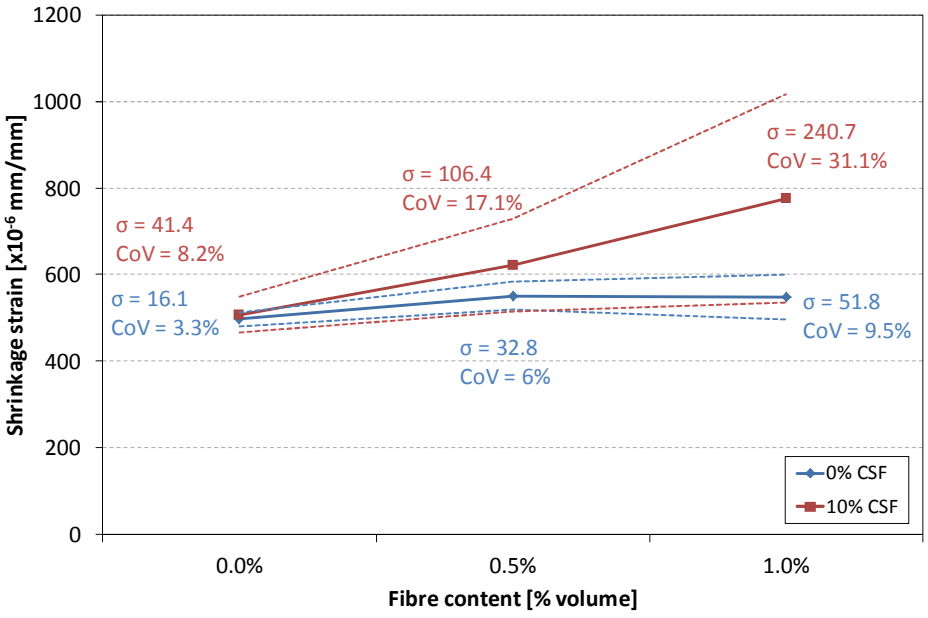

Figure 4.39: *Drying shrinkage after two months*

For the blocks containing CSF, an addition of 0.5% fibre led to an increase in drying shrinkage of 22%. Similarly, increasing the fibre content to 1% led to a further increase in shrinkage of 24%. Furthermore, the blocks containing CSF showed a considerably higher variation in total shrinkage than the blocks without CSF.

Mass loss

The mass loss of each shrinkage sample was measured at the same time intervals as the shrinkage and plotted against shrinkage strain. The results were analysed and plotted as mass loss against drying shrinkage. Furthermore, the average slopes of mass loss over time can calculated and plotted.

Figure 4.40 shows weight loss of the samples of each mix type as a percentage, plotted against the shrinkage.

The results of M4, M5 and M6, as with the shrinkage results, showed a larger variation at a later time than the other mixes and this can, once again, possibly be attributed to the tests being performed by another person.

It is clear from Figure 4.40 that all of the samples experienced an initial mass loss that resulted in a large drying shrinkage. This could possibly be a result of sudden change in humidity (from 100% RH in the curing chamber to 60% RH in the test room. For mixes M1, M2, M3 and M4, this was followed by a large mass loss without a significant increase in shrinkage, after which there was another sharp increase in shrinkage.

The curves for M5 and M6 did not exhibit the same shape. M5 showed a large initial mass loss with virtually no increase in shrinkage, followed by a sharp increase in shrinkage. The results for M6 showed a very high variability, but a similar shape to M5.

The mass loss was also plotted against time on a natural logarithmic time scale. This can be seen in Appendix B.

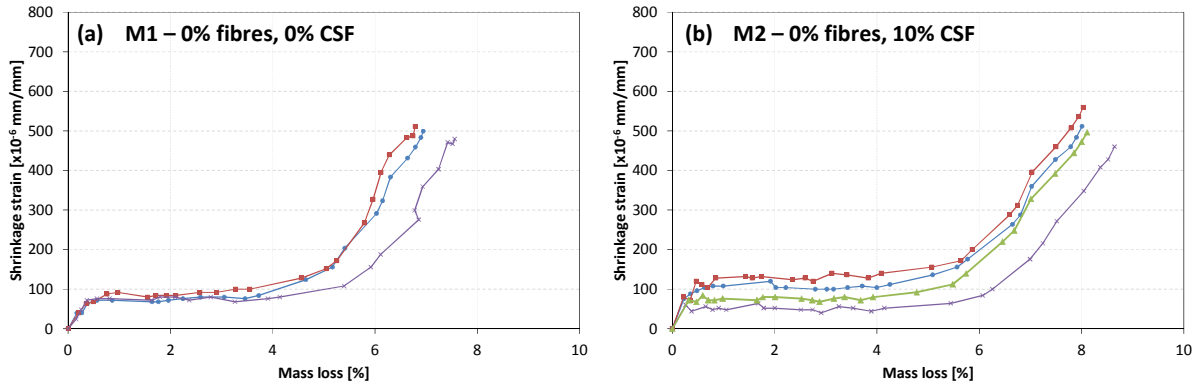

Figure 4.40: *Mass loss of solid block mixes*

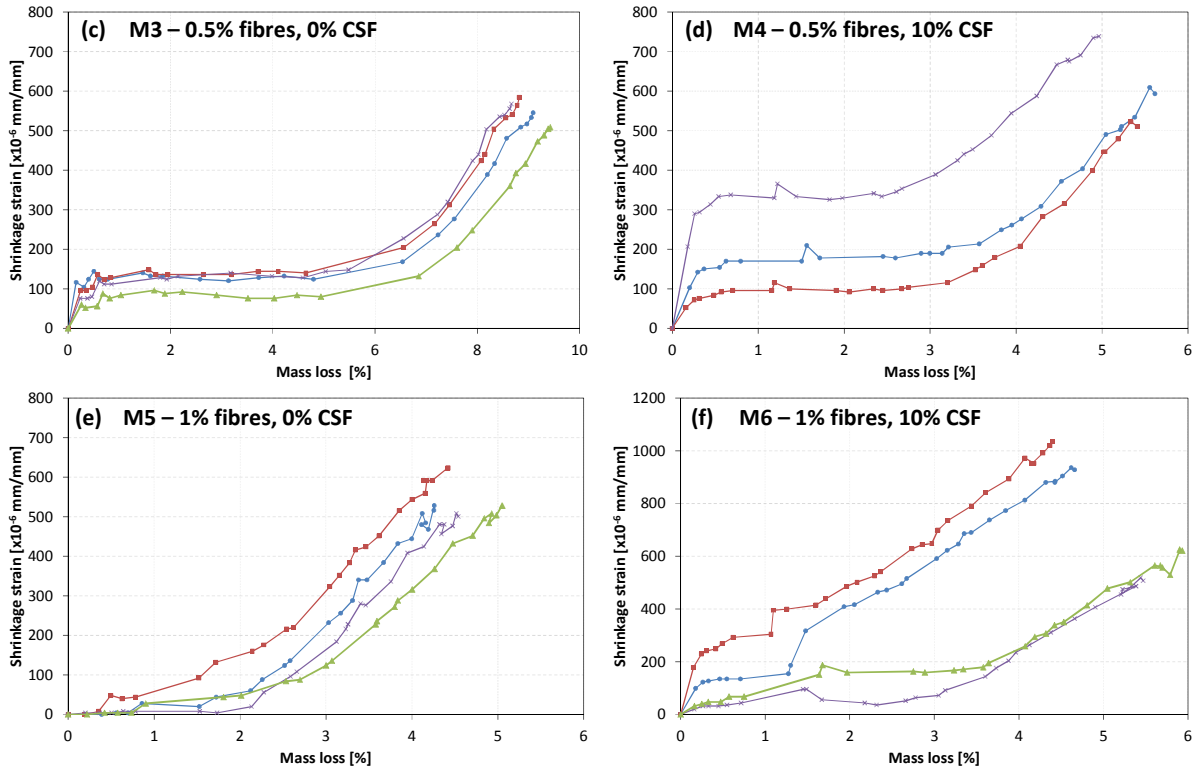

Figure 4.40 (cont.): *Mass loss of solid block mixes*

The average slopes were determined for each mix and are shown in Figure 4.41. This was done in a similar way as was used for the shrinkage-time curves.

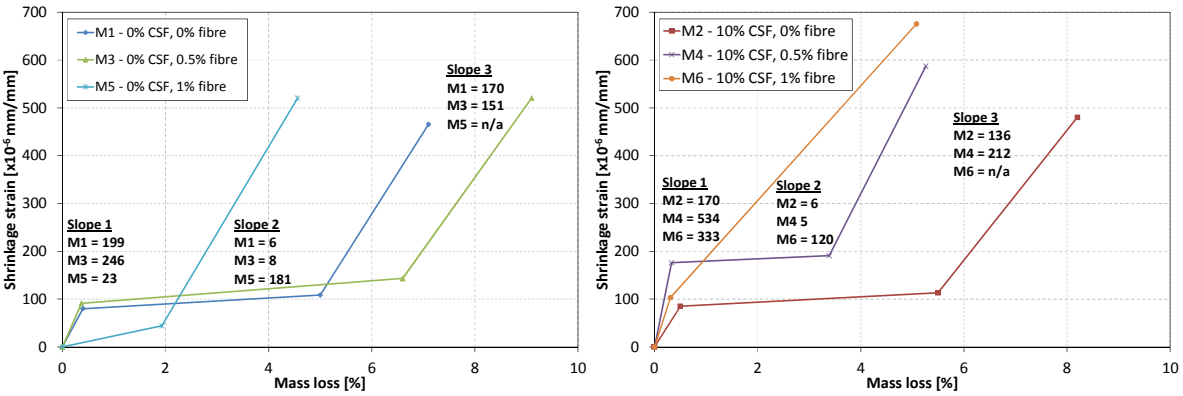

Figure 4.41: *Average slope of shrinkage vs. mass loss of solid block mixes*

It seems like the fibre content has a larger effect on the shape of the shrinkage-mass loss curves than the CSF content. Mixes with similar fibre content showed similar behaviour.

The average slopes of mass loss-time graphs were also plotted. Similarly to the shrinkage-time graphs, the curves showed two slope changes. Table 4.3 shows the rough times at which changes in slopes occur for the different mixes, while Figure 4.42 shows the average slopes of each mix.

For mixes containing CSF, as shown in Figure 4.42, the mix with no fibre content had the highest initial slope (0.396), while the slopes of the mixes with 0.5% and 1% fibre content was close to 45% lower (0.217 and 0.22, respectively). After the first slope change, the slope of M2 was 1.8 while the slopes of M4 and M6 were once again very similar (at 47% lower). After the last slope change, M2 once more had the highest slope, followed by M4 and M6.

Studying the results of the mixes without CSF, the same trends do not appear. The slope of M3 (0.5% fibre) is highest in all three sections, while the slopes of M1 (0% fibre) and M6 (1% fibre) are initially very similar. The first slope change of M3 also occurs at a much later time.

After the first slope change M3 clearly has the highest slope (2.599), followed by M1 (40% lower) and M5 (68% lower). After the last slope change, M1 had the highest slope, followed by M3 (26% lower) and M5 (64% lower).

Clearly, the mixes with 1% fibre had the lowest rate of weight loss. The difference between 0% and 0.5% was the opposite for mixes with and without CSF. Also, on average, mixes without CSF tended to have a slightly higher slope.

Table 4.3: *Average weight loss natural logarithmic slope changes*

	M1	M2	M3	M4	M5	M6
Slope change 1 [h]	8	12	24	5	6	6
Slope change 2 [h]	173	510	360	850	680	580

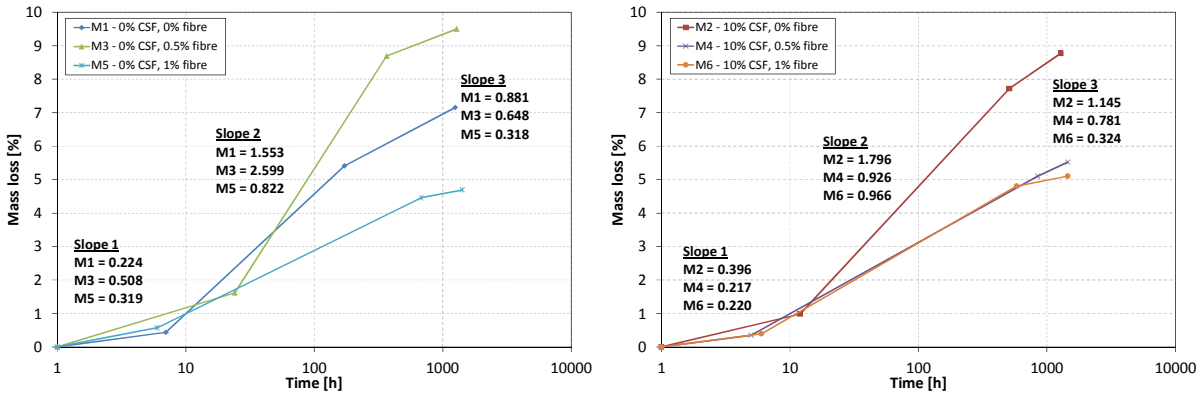

Figure 4.42: *Average slopes of mass loss during drying shrinkage of solid block mixes*

The total average weight loss after two months is shown in Figure 4.43. The results for mixes with CSF show a reduction in mass loss with an increase in fibre content. Adding 0.5% fibre resulted in a decrease of 36% while the addition of 1% fibre resulted in a decrease of 38%.

Contrary to expectations, the results for mixes without CSF did not follow the same trend as those with CSF. An addition of 0.5% fibre led to an increase in total weight loss of 27%, while the addition

of 1% fibre led to a decrease of 36% in weight loss. The unexpected spike in weight loss at 0.5% fibre might be attributed to poor testing, natural variability of the concrete or poor manufacturing.

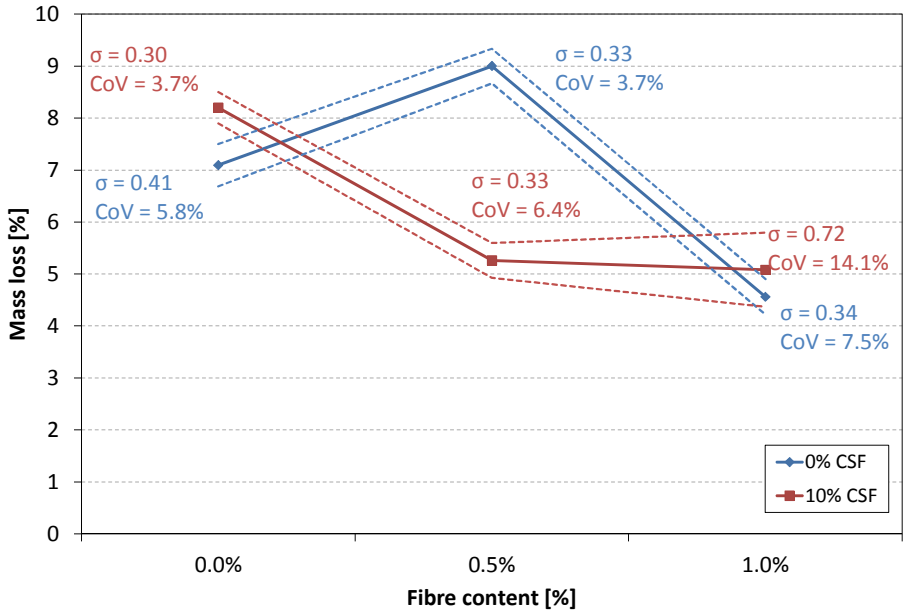

Figure 4.43: *Mass loss after two months*

5. Discussion of experimental results

In this chapter the results obtained in Chapter 4 are discussed at length. The tests have been categorized similarly to what has been done in Chapter 4 ((i) mechanical test and (ii) volumetric and durability test results).

5.1 Mechanical test results

5.1.1 Compression test

The general trends of 7 and 28 day solid block and 28 day hollow block compression results are discussed in this section. Also, a comparison is drawn between 7 and 28 day results to investigate the effect of curing age. Similarly, a comparison is drawn between 28 day solid and hollow block results to investigate the effect of block type.

Solid block (7 day)

At an age of 7 days, 10% CSF blocks had a higher stiffness and strength than those without CSF. However, as fibre content increased, the effect of silica content reduced to a point where, at 1% fibre content, there was no significant difference between 0% CSF and 10% CSF strengths. The strength and stiffness results for the 0% CSF blocks showed a considerably higher variance.

Solid block (28day)

As mentioned in Section 4.1.1, as fibre content increased there was an increase in initial displacement caused by rearrangement of particles before strength was gained. This was caused by a higher volume of permeable pore space.

There seemed to be a strong correlation between fibre content and strength, as well as stiffness. As fibre content increased, strength and stiffness values decreased by between 38 and 43% (1% fibre). The stiffness and strength of CSF containing samples were higher for all fibre contents tested.

At 28 days the compressive strength variance was slightly higher than at 7 days.

Hollow block (28 day)

Similarly to the solid blocks, the hollow blocks showed a decrease in stiffness and strength with an increase in fibre content. The force-displacement graphs (Figure 4.7) indicated a greater ductility in blocks with 1% fibre content. Interestingly, the blocks with 0.5% fibre content showed the most brittle behaviour. However, as discussed in Section 4.1.1, the validity of the M1 and M2 results (0% fibre) is questionable.

Comparison between solid block ages

The stiffness and average maximum compressive strengths of the solid blocks at ages of 7 days and 28 days are shown in Figure 5.1 and Figure *5.2*. It can be seen that the stiffness tends to increase with age. However, as the fibre content increases, the effect of age becomes smaller (for 0% CSF mixes). The stiffnesses of blocks with no CSF at 28 days were 43, 40 and 3% higher for fibre contents of 0%, 0.5% and 1%, respectively. Therefore, at a fibre content of 1% there seems to be almost no difference between stiffnesses.

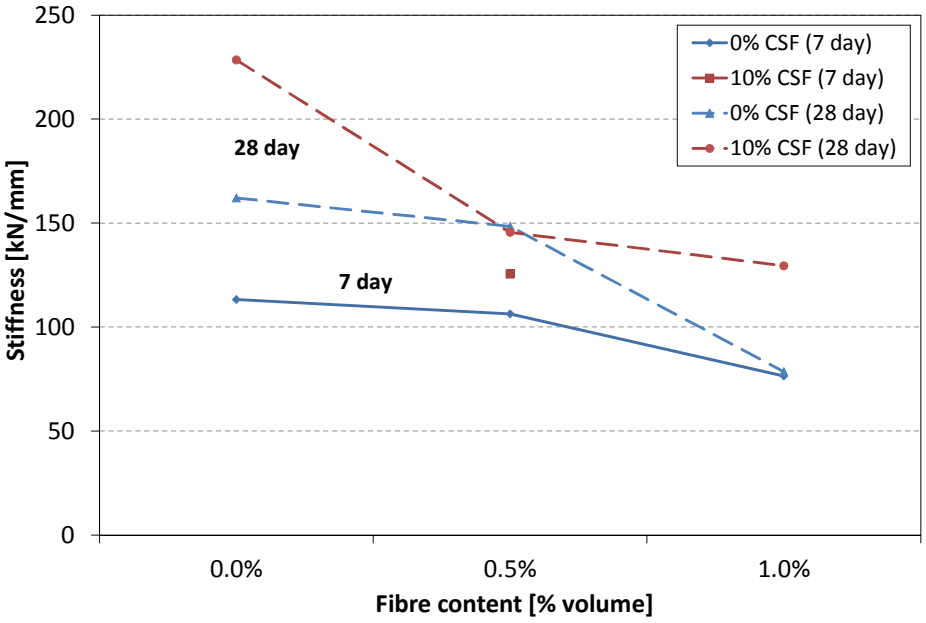

Figure 5.1: *Average stiffness of solid blocks at ages 7 and 28 days*

As with the stiffness, the compressive strength of the blocks with no CSF tends to be higher at 28 days (33%, 30% and 3% for fibre contents of 0%, 0.5% and 1%, respectively). With 1% fibre content, once again, there is no significant difference between 7 day and 28 day compressive strength as fibre content is increased.

The blocks containing CSF do not show the same tendency. There is a smaller difference between 7 and 28 day strength at a fibre content of 0.5% (16%) than at 0% fibre content (51%). With a fibre content of 1% the difference rises again to 67%.

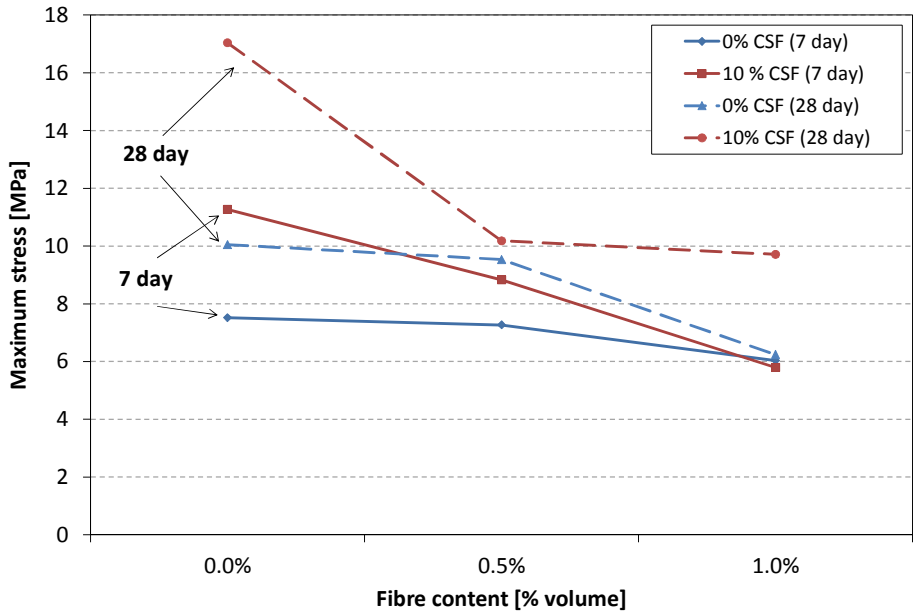

Figure 5.2: *Average maximum compressive strength of solid blocks at ages 7 and 28 days*

The reduction in strength is caused by an increase in volume of voids which, in turn, is caused by an increase in fibre content. This phenomenon is further discussed in Section 5.2.2.

Comparison between solid and hollow blocks

Figure 5.4 show the stiffnesses and maximum compressive strengths of the solid and hollow blocks at 28 days. On average, the hollow blocks containing CSF had stiffnesses of 36-60% lower than that of the solid blocks, while those with no CSF had stiffnesses of 48-55% lower.

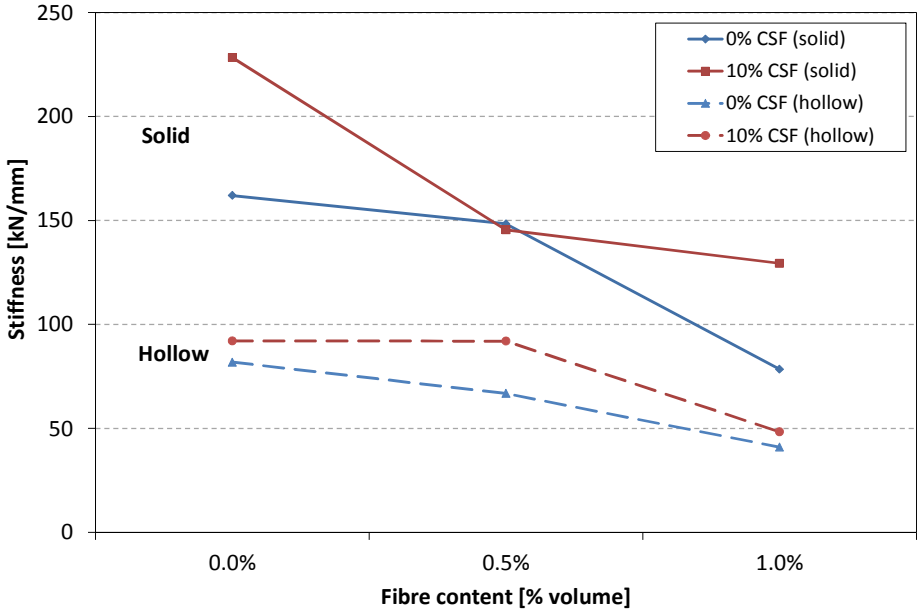

Figure 5.3: *Average stiffness of solid and hollow blocks at 28 day age*

On average, the compressive strength of hollow blocks with no CSF was about 88% lower than that of similar solid blocks, while the difference was between 83 and 91% for hollow blocks with 10% CSF. When comparing the true compressive strength of the hollow blocks (i.e. the area of the cavities was excluded) with that of the solid blocks the difference becomes between 61 and 65% lower for blocks without CSF and between 45 and 71% lower for block containing CSF.

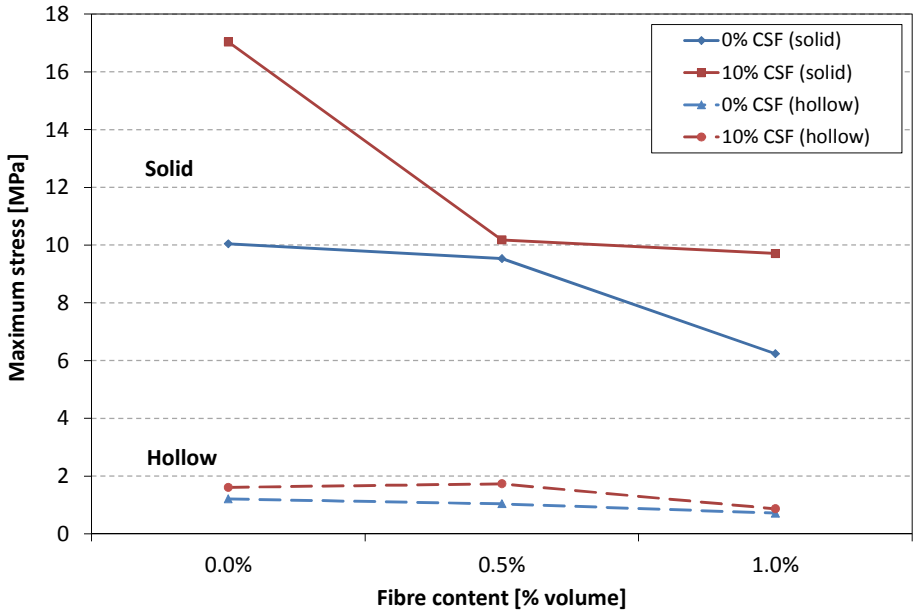

Figure 5.4: *Average compressive stress of solid and hollow blocks at 28 day age*

SANS 1215 (see Table 2.1) requires 3.5 MPa blocks, for use in South Africa, to have a minimum individual nominal compressive stress of 3 MPa and an average compressive (for 5 samples) of 4 MPa. The solid blocks all lie comfortably above this threshold. The hollow blocks, however, all underperformed in this regard.

A better approach could, perhaps, have been followed during the mix design where similar mixes were developed for both solid and hollow blocks. Each hollow block used about 12% less material than a solid block, but provided a wall surface (surface exposed if a wall was built with the block) of 2.8 times that of a solid block. Therefore, on a (wall area)/(volume material required) basis, the hollow blocks were considerably less expensive to produce. However, given the poor mechanical performance of the hollow blocks it would have made sense to increase the cementitious content of the mix.

On average the 0% CSF and 10% CSF solid blocks (1% fibre) had compressive strengths of 1.8 and 2.8 times that of what is required according to the SANS 1215 requirements, respectively. If fibre-

reinforced blocks were to be developed that simply had to comply with the requirements of SANS 1215, the cementitious content of the mixes could be reduced somewhat to make a more economic mix. However, the fine aggregate content would have to be increased to make up for the loss of cementitious fines and therefore reduce porosity.

Given the results it can be concluded that fibre and CSF content have a significant effect on the compressive strength and stiffness of NFRC blocks. The general trend is that an increase in fibre content leads to a reduction in strength and stiffness. Also, an increase in CSF content leads to an increase in strength and stiffness.

5.1.2 Flexure test

As discussed in Section 4.1.2 , an increase in fibre led to a significant decrease in MOR for both mix types. For 0% CSF mixes the addition of 0.5 and 1% fibre led to a decrease in MOR of 21 and 39%, respectively. The same increase in fibre content of 10% CSF mixes led to a decrease in MOR of 28 and 43%, respectively. For all fibre contents, CSF mixes had a higher MOR (18, 7 and 8% higher for fibre contents of 0, 0.5 and 1%, respectively) than those without CSF.

Awwad et al. (2012) found a similar decrease in MOR with an increase in hemp fibre content in concrete cube samples. They recorded a 14-31% decrease with the addition of 0.5% fibre and an 11-57% decrease with the addition of 1% fibre at an age of 28 days.

Agopyan et al. (2005) tested cementitious composites containing 2% coir fibre and found that, only after 28 days, there was a decrease in MOR relative to a reference matrix without fibres.

According to Illston and Domone (2011) the reinforcing of concrete beams with up to 0.44% polypropylene fibres (by volume) does not significantly affect the MOR and compressive strength, but can increase the toughness and ductility in the post-cracking zone.

The gentler slopes of the force-displacement curves, after reaching the maximum applied force, of the M5 and M6 results (Figure 4.11, p69) are indicative of a higher ductility. As stated in Section 4.1.2, this ductility could not be quantified due to poor displacement data.

To conclude, it can be stated that an increase in fibre content leads to a decrease in flexural strength, but an increase in CSF content leads to an increase thereof. Also, the addition of fibres does tend to increase ductility.

5.2 Volumetric and durability tests results

The results obtained from capillary water absorption, dimensional stability, drying shrinkage, density, total water absorption and void content tests are discussed in this section.

5.2.1 Capillary water absorption

This section discusses the results obtained from testing solid and hollow blocks at an age of 28 days. The results of both block types are discussed and a comparison is drawn between them.

Solid blocks

The results, as shown in Section 4.2.1, indicate that an increase in fibre content leads to an increase in capillary water absorption. Also, in general, blocks with a 10% CSF content tended to absorb more water.

The results for the logarithmic rate of absorption showed a less clear pattern. For both matrix types there was a slight increase in rate of absorption with 1% fibre content relative to the reference matrices. However, at 0.5% fibre content the mixes with CSF showed a sharp decrease in rate, while the mixes without CSF showed a sharp increase. This is somewhat contrary to the expectation of a slight increase in rate with an increase in fibre content. This could possibly be attributed to human error, although both the absorption and rate of absorption results for M3 and M4 (0.5% fibre content) showed a fairly low variability.

Hollow blocks

Once again, contrary to expectations, the absorption results of the hollow blocks did not show an increase with an increase in fibre content, although both matrix types followed the same trend. There was a sharp decrease in total absorption with the addition of 0.5% fibres. With 1% fibre content, the absorption was more than with 0.5% fibre content, but less than with 0%. At all fibre contents the mixes with CSF had a higher absorption.

The rate of absorption showed a slight increase with the addition of 0.5% fibre, but a slight decrease with the addition of 1% fibre. The rate of CSF-containing blocks was consistently higher than that of blocks without CSF.

Comparison between block types

The absorption of the solid blocks followed a trend as to be expected whereby absorption increases with fibre content (Figure 5.5). However, the hollow blocks do not follow this trend, since the maximum water was absorbed by the blocks containing no fibres. This unexpected behaviour can possibly be attributed to the solid and hollow block tests being performed by different people.

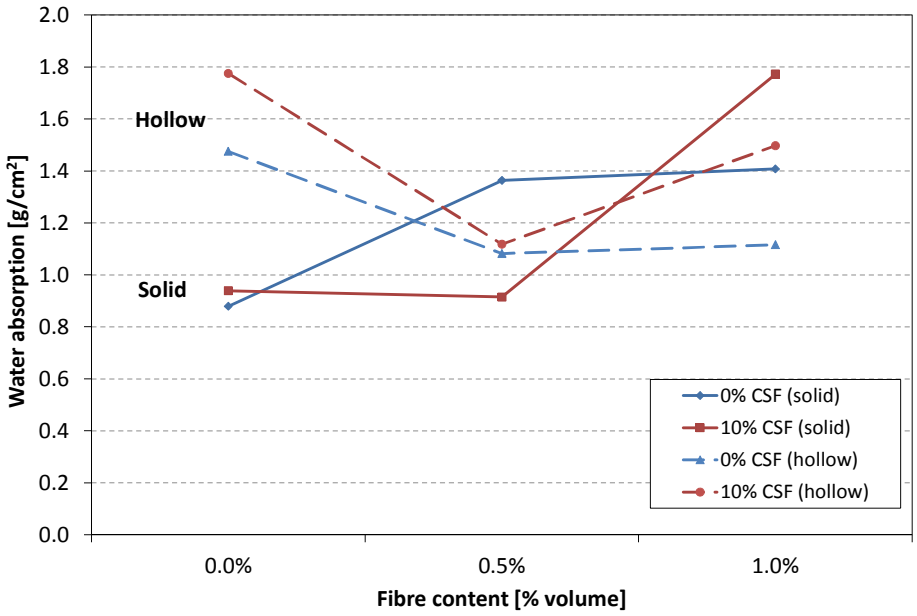

Figure 5.5: *Average water absorption of solid and hollow blocks after 72h*

The average rate of absorption of the solid and hollow block mixes are shown in Figure 5.6. For the hollow blocks, the rate of absorption was highest for the blocks containing 10% CSF and a fibre content of 0.5%. The absorption rates of the hollow blocks were consistently higher than that of the solid blocks. This can possibly be attributed to the following: a smaller face area in contact with the water, a larger height and a higher density due to higher compaction pressure during production. The densities of the hollow blocks, however, were not determined and can, therefore, not be compared.

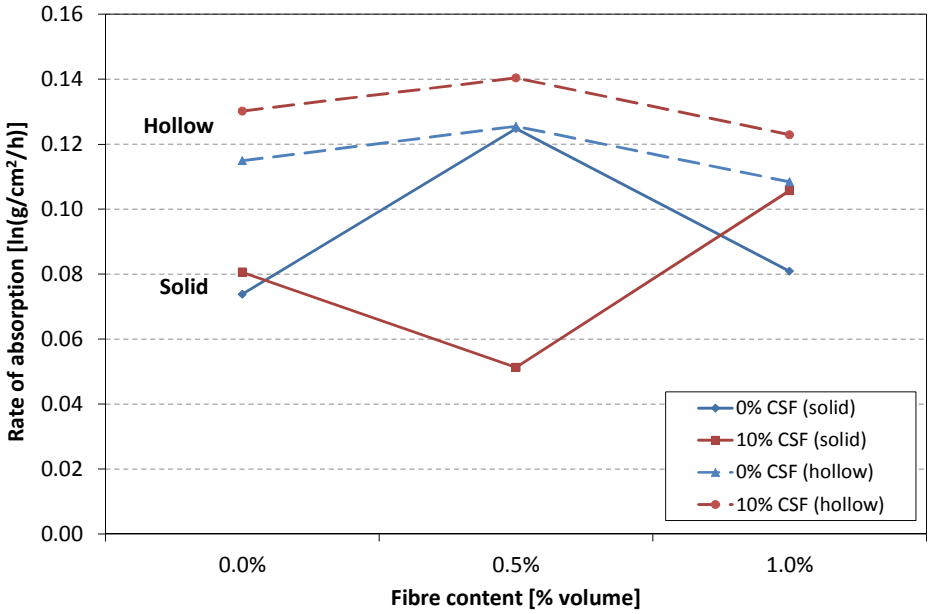

Figure 5.6: *Rate of water absorption of solid and hollow blocks*

After testing, all solid blocks were broken in half to visually inspect how the water had moved up in the block. Many blocks were wet up to the top and in some instances the top face was wet (Figure 5.7), possibly indicating that the height of the block had a limiting effect on the water absorption, especially at later stages.

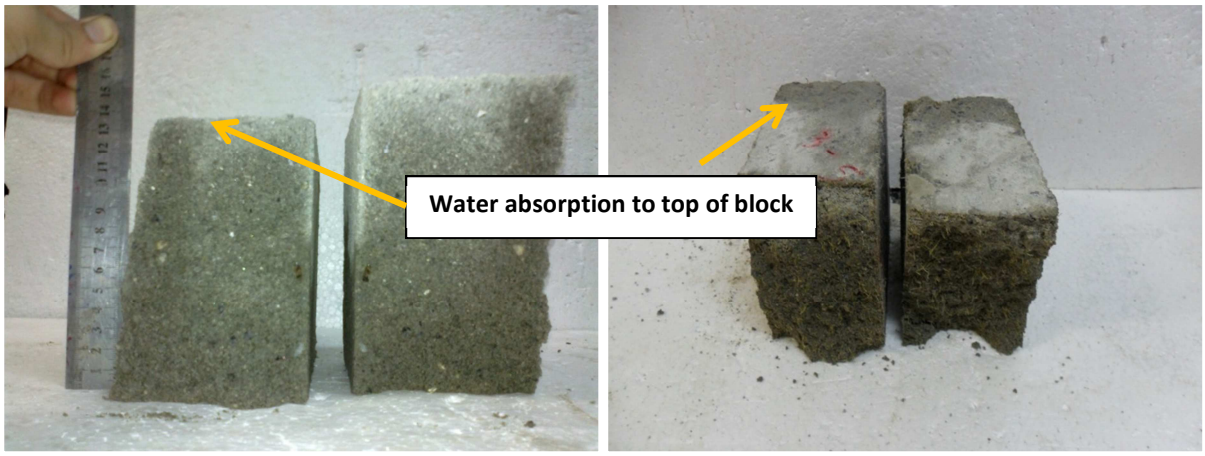

Figure 5.7: *Block with water absorbed to top face after 72h*

De Gutierrez et al. (2005) tested concrete samples with added CSF and fly-ash, as well as different sisal fibre contents. They found that the addition of CSF decreased the absorption drastically relative to a reference matrix (for both samples with and without fibre), although the capillary absorption of samples with fibre was still much higher than those without. The samples with fly-ash showed no change in capillary absorption when fibre was present.

Due to its filler effect, silica fume is often recommended as a means to reduce porosity and capillary water absorption. However, the trend found in this research is that the addition of CSF increased capillary water absorption of blocks, with and without sisal fibres.

It can be concluded that block type does play a significant role, not only in the magnitude of absorption, but also on the effect of fibre and CSF content. The solid blocks showed a trend where an increase in fibre content led to an increase in capillary absorption. At some fibre contents, blocks containing CSF tended to have a higher absorption, but there was no clear trend.

The hollow blocks tended to have a higher absorption with no fibre content, relative to the solid blocks, but the addition of fibres led to a decrease in absorption.

The rate of capillary absorption is a function of mainly pore size and shape. These two properties caused a capillary suction in cement matrices that, when partially saturated, assists in the uptake of moisture and hinders the release of moisture. Therefore, a matrix with smaller pores would have a

higher rate of absorption than one with larger pores (Yaremko, 2012). It was found, however, that the blocks containing fibres had a higher porosity and higher rate of absorption. The higher rate could be directly attributed to the hygroscopic properties of sisal fibres.

5.2.2 Density, absorption and void content

The results from the water absorption test showed a trend that was expected. An increase in fibre content led to an increase in absorption. Also, the blocks with CSF tended to have a lower absorption than those without CSF. The absorption results depicted in Figure 4.26 presented the results in terms of % mass increase. Smith (1973) has noted that the Portland Cement Association limits the maximum water absorption to 240 kg/m^3, or 12% of the mass. All the results fell below this limit.

Rawi and Khafagy (2009) found a significantly lower increase in absorption with the addition of 0.5% and 1% sisal fibres to a standard concrete mix. They found an increase of 16% (0.5% fibres) and 23% (1% fibres). They used a mix proportion of 1:1.16:2.0 (cement:sand:stone) and a w:c ratio 0.4.

The density results also showed a trend as was expected. With the addition of fibre the dry bulk density decreased by 5-8%.

Awwad et al. (2012) tested the density of concrete cubes made with a cement-sand-stone matrix and reinforced with hemp fibres. The results of the tests showed a reduction in density of 3% (0.5% fibres) and 5% (1% fibres) compared to a reference matrix with no fibres. One contributing factor to the slightly lower density reduction of the hemp fibre samples could possibly be attributed to hemp fibres being 11% more dense than sisal, on average.

Both 0% CSF and 10% CSF batches had the same dry bulk density with no fibre content. Siddique and Khan (2011) and Chung (2002) have stated that the addition of CSF lowers the density of concrete. Ajileye (2012) has found that the replacement of cement with 10% CSF (by weight) in a normal concrete mix can lead to a reduction in density of about 4.5%. However, the lack of a decrease in the density results could possibly be attributed to the very low CSF content (1.2% by total volume). Contrary to expectations, there was a slight increase in density with the addition of CSF in the blocks containing fibres (1% for 0.5% fibres and 2.3 % for 1% fibres).

The mixes without any fibre had an average pore space volume of 17.4% (0% CSF) and 18.1% (10% CSF). The pore space volume of samples increased by about 32-57% with the addition of 1% fibre. Also, the mixes without CSF displayed the greatest increase.

Owens (2009) has stated that conventional grade concrete has an overall porosity of about 16%. The slightly larger results found in this study can be attributed to the low cementitious material content of the mixes tested, compared to conventional concrete.

According to Chung (2002) the addition of CSF does tend to increase the air void content of concrete. Siddique and Khan (2011) have stated similar views, but only up to an age of 28 days, after which the void filling effect of CSF becomes more apparent.

From the results it can be concluded that the addition of sisal fibre to a cementitious matrix does increase the air void content significantly. Also, the substitution of cement with 10% CSF showed a slight increase in air void content in matrices without fibres, but a significant decrease in air void content in matrices containing fibre.

5.2.3 Dimensional stability

Figures 4.33 and 4.34 represent the volumetric change results in such a way that the effect of fibre content can be investigated. For both matrix types (0 and 10% CSF content) there seemed to be a decrease in change of volume between wet and dry cycles with an increase in fibre content. Also, the initial change in volume decreased with an addition of fibre content.

The results of Figures 4.33 and 4.34 are represented in a slightly different manner in Figure 5.8. Here the data is arranged according to the fibre content of the blocks in order to compare the effect of the addition of CSF at different fibre contents.

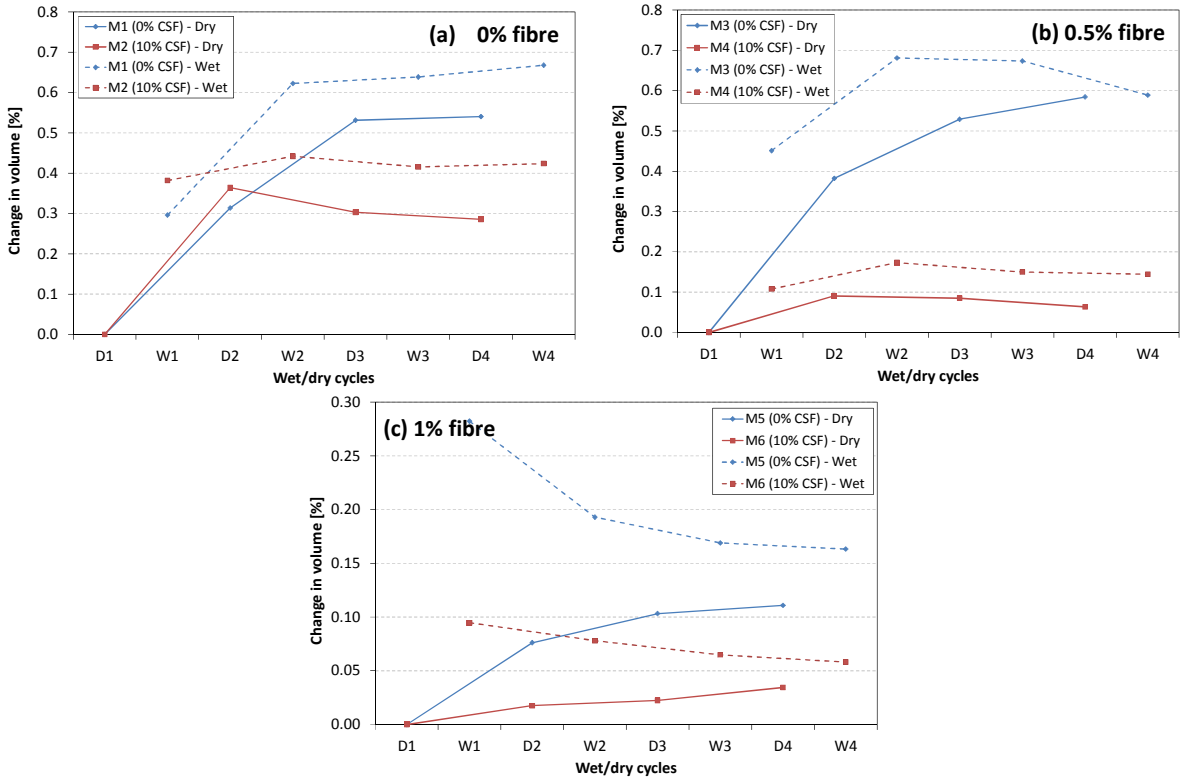

Figure 5.8: *Average change in volume during wet/dry cycles for mixes with (a) 0% fibre; (b) 0.5% fibre; (c) 1% fibre*

Figure 5.8 shows clearly that at all fibre contents blocks with CSF displayed a smaller initial volume change, as well as a smaller difference between wet and dry blocks. The blocks without CSF and fibres had a 1.9 times higher change in volume for dry cycles than the blocks containing CSF. The final change in volume was about 1.6 times higher for wet cycles.

Similarly, at 0.5% fibre content the blocks without CSF had a 9.2 times higher change in volume for dry cycles and 4.1 times higher change for wet cycles. For blocks containing 1% fibre, the changes were 3.2 and 2.8 times higher, respectively.

It can be concluded that both an addition of fibre and CSF has a significant effect on the change in volumes during wet/dry cycles. Both additives tended to decrease the initial change in volume as well as the difference between wet and dry volumes, indicating that they improved dimensional stability.

As stated in Section 5.2.1 matrices with larger pores tend to absorb water at a lower rate and dry out more quickly than those with smaller pores. Yaremko (2012) has stated that, when exposed to repeated wet-dry cycles, which causes a constant intake and release of moisture, the pore system of a matrix runs the risk of being damaged. This might lead to a longer time needed to absorb water. In

this study, however, moisture absorption was not tested after wet-dry cycles and this could be a possible prospect for future research.

5.2.4 Drying shrinkage

The results obtained from testing for drying shrinkage are shown in Section 4.2.4. From Figure 4.39 it can be concluded that the addition of fibres led to an increase in drying shrinkage. The addition of CSF increased shrinkage as well.

It was also found that over a two month period there tended to be three distinct shrinkage rates for most samples tested. This is discussed in Section 4.2.4 and shown in Figure 4.37 and Figure 4.38. The conclusion to be made from inspection is that the addition in fibre content increased the initial rate of shrinkage. After the first rate change, the effect of added fibres diminished and there seemed to be no significant difference between shrinkage rates. Similarly, the addition of CSF only significantly increased the initial rate of shrinkage, but after the first rate changes the effect became substantially less.

The mass loss was plotted against shrinkage as well (Figure 4.40). These graphs show most clearly how the loss of water caused shrinkage. This was discussed in Section 4.2.4 and it can be concluded from the results that mixes with higher fibre content tended to shrink more, but at a lower mass loss (i.e. water loss). These results are mimicked in Figure 4.42, where mass loss is plotted against time.

Interestingly, the mass loss showed an unexpected trend when plotted against fibre content (Figure 4.43). Mixes with CSF showed a decrease in mass loss with an increase in fibre content. The mixes without CSF, however, showed an increase in mass loss with the addition of 0.5% fibres, but a decrease with the addition of 1% fibres. This could possibly be attributed to poor block production.

Silva et al. (2010) have stated that the drying shrinkage of a cement matrix is related to the magnitude of its porosity and to the size, shape and continuity of the capillary system in the hydrated cement paste. The porous nature of the fibres creates more paths through which moisture can escape. The addition of sisal fibres, therefore, increases the porosity of the matrix which leads to higher shrinkages, while the addition of CSF does the same.

It has been mentioned by Siddique and Khan (2011) that the substitution of up to 15% of cement (by weight) for CSF in a cement matrix does not have a significant effect on drying shrinkage. This corresponds to the results for matrices without fibres, where the difference in shrinkage between M1 and M2 was less than 2%. However, with the addition of fibres the difference between matrices

with and without fibres becomes larges. At 0.5% fibre content the shrinkage was 13% more for the samples containing CSF and the difference increased to 41% at 1% fibre content.

According to Siddique and Khan (2011) there are four mechanisms for drying shrinkage: capillary tension, surface tension, disjoining tension and movement of interlayer water. Capillary tension describes the transfer of tension from the meniscus of capillary pore water to the walls of the pore as water evaporates. Surface tension of solid particles is reduced by the absorption of water. Disjoining pressure is comparable to the phenomenon that occurs as clay swells as water is drawn in between adjacent particles forcing them apart. These three mechanisms are applicable to free and absorbed water and can be associated with the second slope of mixes M1, M2, M3 and M4 in Figure 4.41. These three mechanisms clearly led to a large loss of mass (due to free and absorbed water evaporating) and a small increase in shrinkage.

As stated by Illston & Domone (2011) the last mechanism (movement of interlayer water) requires a steep hygrometric energy gradient to remove water and it is believed that this mechanism causes a much higher shrinkage than that of the removal of free and absorbed water. The steeper slopes in Figure 4.41 (slope 3 for M1-4; slope 2 for M5 and M6) can be attributed to this mechanism.

5.3 Summary of results

A short summary of the effect of the addition of fibre and substitution of cement with CSF is presented in Table 5.1. The effect of fibre is based on the results for matrices with both CSF contents (0 and 10%). Furthermore, the effect of CSF is based on results for all fibre contents of mixes containing CSF, relative to the results of those mixes without CSF (with and without fibres).

Table 5.1: *Summary of effect of addition of fibre and CSF*

Test perfomed	Effect (increase or decrease) of addition of:	
	Fibre	**CSF**
Compression strength	Decrease	Increase
Flexural strength	Decrease*	Increase
Capillary water absorption	Increase	Increase
Density	Decrease	Increase
Total water absorption	Increase	Decrease
Air content	Increase	Decrease
Dimensional stability	Increase**	Increase**
Drying shrinkage	Increase	Increase

*Flexural strength was reduced, but ductility was increased

**The dimensional stability refers to the initial volume change due to wetting as well as the difference in volume change between subsequent dry and wet cycle volumes. An increase in stability, therefore, refers to a small initial change in volume and difference between wet and dry cycles

In general, it can be stated that the addition of natural fibres decreases the strength of a concrete block, although a partial substitution of cement with CSF, in conjunction with fibres, does increase the strength relative to blocks without CSF content.

Interestingly, the addition of CSF to fibre containing matrices led to an increase in capillary water absorption, but a decrease in absorption through immersion. This shows that the addition of CSF does significantly alter the pore system of a cementitious matrix reinforced with natural fibres.

Also, the dimensional stability increases with the addition of CSF and fibres. The same can be said for drying shrinkage. Therefore, even though an increase in fibre and CSF caused samples to shrink more under drying, they were more stable under cycles of wetting and drying.

6. Conclusions and recommendations for future work

This chapter discusses the conclusions that can be drawn following the study. Recommendations for future work are discussed as well.

6.1 Conclusion

The objective of this study was to investigate the mechanical and volumetric properties of SFRC blocks, with regards to its possible use in the LCH sector in South Africa. A particular focus was on developing a matrix with a reduced CH content to improve durability.

In order to evaluate the mechanical performance of the blocks, compression and flexure tests were performed and it was concluded that there was a decrease in both compression and flexural strength with an increase in fibre content. The addition of fibre, however, did lead to a higher ductility. The addition of CSF to matrices did increase both compression and flexural strength, but the extent of the effect was lowered as fibre content increased.

Regarding the volumetric properties of blocks, mixed results were achieved. The addition of fibres decreased the density and increased the porosity, which in turn led to a higher absorption and rate of absorption. Drying shrinkage was increased as well. The dimensional stability of blocks, after repeated wet-dry cycles, was significantly improved with the addition of fibres.

The partial substitution of cement with CSF led to a slight increase in capillary absorption and rate of absorption. Absorption through immersion, however, was reduced somewhat. The density and air void content was reduced, with the biggest reductions at the highest fibre contents. Due to the reduced pore sizes, drying shrinkage and dimensional stability was increased significantly.

From the results the use of sisal fibre as reinforcement in concrete blocks is questionable. All mechanical properties were reduced significantly, apart from the increase in ductility. The volumetric properties were reduced as well, although all still fell within the allowable limits for concrete blocks, where applicable. Nevertheless, sisal fibre does seem to have a use as a means of dimensional stabilisation.

It was also shown that the use of sisal fibre as a cement content reducing material cannot be recommended. The study investigated blocks with fibre contents of 0.5 and 1% by volume and it was found that even at these low volumes the adverse effect on strength was significant. With respects

to the results obtained in this research, the positive effects of volume that is added to concrete through the addition of fibre is diminished through the negative effect the fibre has on strength.

Furthermore, sisal is not as widely available in South Africa as in Brazil and the economic advantages of using it as reinforcing material is difficult to assess.

As a possible new technology for use in LCH, much more research is needed to quantify the durability of SFRC blocks.

6.2 Recommendations for future work

Much research is still needed before natural fibres can be considered as a durable concrete reinforcing material.

The following recommendation can be made with regard to the fibre type used and sustainability:

- Hemp is a fibre similar to sisal and perhaps more suited to cultivation conditions in South Africa. The possibility of the use of hemp fibre in South Africa should be further investigated.
- It is important to quantify the environmental sustainability of sisal (or other natural fibres) in terms of carbon footprint, life cycle assessment, etc. This, however, lies outside the scope of an engineering study.

The following recommendations can be made with regard to the matrix type used:

- The partial substitution of cement with CSF as a means of lowering the CH content and alkalinity does improve the strength and durability of NFRC. The amount of CSF needed for a CH-free matrix requires investigation.
- Since CSF is very expensive in South Africa, other pozzolans with the same CH-reducing effect need to be researched to find a more economically viable alternative.

The following recommendations can be made with regard to the durability and strength:

- Similar tests as were performed in this study could be performed over longer periods (perhaps up to two years) to properly investigate the durability and the effect of CSF over longer periods.
- The effect of fibre length could be studied. Longer fibres might improve the mechanical performance of blocks. However, it should be noted that longer fibre will increase the possibility of fibre balling during mixing and it might not work with hollow blocks, due to its small wall thicknesses.

- The effects when using finer aggregates need to be researched. The matrices used in this research could have made use of a higher fine aggregate content. This is contrary to suggestions in literature regarding the production of low cost concrete blocks with reasonable strength, but perhaps a less porous matrix could enhance the positive effects of the added natural fibres.
- The fibre-cement interface in a porous matrix requires further investigation in order to better understand how the fibre interacts with cement in such an environment.
- The moisture absorption of NFRC blocks after various wet/dry cycles could make for an interesting research topic. This would shed some light on the effect of wetting/drying on the pore system of a porous matrix.

7. References

AGOPYAN, V., SAVASTANO, J., H., JOHN, V.M. and CINCOTTO, M.A., 2005. Developments on vegetable fibre-cement based materials in Sao Paulo, Brazil: an overview. *Cement and Concrete Composites,* 27(5), pp. 527-536.

AGRICULTURAL RESEARCH COUNCIL, 2010. *Annual Report 2009/2010.* Agricultural Research Council.

AGRICULTURAL RESEARCH COUNCIL, n.d. (a). *Cotton*. [Online] Available: http://www.arc.agric.za/home.asp?pid=372&toolid=63&itemid=1462 [Accessed 24 February 2012].

AGRICULTURAL RESEARCH COUNCIL, n.d. (b). *Cultivating flax fibre in South Africa.* [Online] Available: http://www.arc.agric.za/home.asp?pid=372&toolid=63&itemid=1473 [Accessed 26 February 2012].

AGRICULTURAL RESEARCH COUNCIL, n.d.(c). *Indigenous fibre plants of South Africa*. [Online] Available: http://www.arc.agric.za/home.asp?pid=372&toolid=63&itemid=1518 [Accessed 26 July 2011].

AJILEYE, F.V., 2012. Investigations on Microsilica (silica fume) as Partial Cement Replacement in Concrete. *Global Journal of Researches in Engineering,* 12(1), pp. 16-23.

ANANDJIWALA, R.D., 2006. *The role of research & development in the global competitiveness of natural fibre products.* Port Elizabeth: CSIR Materials Science and Manufacturing.

ASH RESOURCES, 2012. *Price of fly-ash in South Africa*. Personal communication on 26 November 2012 with Randburg office (+27 11 657 2300). Randburg.

ASH RESOURCES, 2009. *DuraPozz – Product guide*. Randburg: Ash Resources.

ASH RESOURCES, n.d. *Pozz-fill – Product guide*. Randburg: Ash Resources.

ASSOCIAÇÃO BRASILEIRA DE NORMAS TÉCNICAS, 1995. *NBR 9779 - Argamassa e concreto endurecidos - Determinação da absorção de água por capilaridade.* Rio de Janeiro: Associação Brasileira de Normas Técnicas.

ASTM C 642, 1997. *Standard Test Method for Density, Absorption and Voids in Hardened Concrete.* West Conshohocken: American Society for Testing and Materials.

AWWAD, E., MABSOUT, M., HAMAD, B., FARRAN, M.T. and KHATIB, H., 2012. Studies on fiber-reinforced concrete using industrial hemp fibers. *Construction and Building Materials,* 35, pp. 710-717.

BAXTER, W.J. and SCHEIFELE, G., 2009. *Growing Industrial Hemp in Ontario*. [Online] Available: http://www.omafra.gov.on.ca/english/crops/facts/00-067.htm#fertility [Accessed 23 February 2012].

BENTUR, A. and MINDESS, S., eds, 2007. *Fibre reinforced cementitious composites.* 2 edn. Oxon: Taylor & Francis.

BERHANE, Z., 1994. Performance of natural fiber reinforced mortar roofing tiles. *Materials and Structures,* 27, pp. 347-352.

BOS, H., 2004. *The Potential of Flax Fibres as Reinforcement for Composite Materials*, Technische Universiteit Eindhoven.

BRITS, J., COETZEE, G., DE VILLIERS, W.I. and IMMELMAN, D.W., 2011. *Sustainability of Low Cost Housing in South Africa, and Related Aspects.* Stellenbosch: Institute of Structural Engineering.

BROSENS, C.A., 1982. *Natural fibres for fibre reinforced concrete*, Stellenbosch University.

BROUWER, W.D., 2000. *Natural Fibre Composites in Structural Components: Alternative Applications for Sisal.* Rome: Food and Agriculture Organization.

BUDDEN, T., 2007. Industrial Hemp coming to a field near you. *CAPE Environment,* 2, pp. 1-2.

CAPE CEMENT PRODUCTS, Bricks & Blocks. [Online]
Available: http://www.capecement.co.za/cape_cement_products.html [Accessed 21 March 2012].

CATLING, D. and GRAYSON, J., 1982. *Identification of vegetable fibres.* 1 edn. New York: Chapman and Hall.

CAWDRY, F., 2012. *Vegetable fibre cultivation and availability in Africa.* Message from F. Cawdry (fredc@kenaf.co.za). Sent Wednesday 15 February 2012. Stellenbosch: Sustainable Fibre Solutions.

C&CI, 2011. *Sustainable Concrete.* 1st edn. Midrand: Cement & Concrete Institute.

CHIEF DIRECTORATE: RESEARCH, 2010. The Use of Alternative Technologies in LCH Construction: Why the slow pace of delivery? *Human Settlements Review,* 1(1), pp. 266-270.

CHM, 2007. C*learing house mechanism*. [Online] Available: http://chm-thai.onep.go.th/chm/alien/IAS/detail.aspx?alienID=228 [Accessed 4 January 2013].

CHUNG, D.D.L., 2002. Improving cement-based materials by using silica fume. *Journal of Material Science,* 37, pp. 673-681.

CIMENTO.ORG, n.d. *CP V-ARI - Cimento Portland de alta resistência inicial* [Homepage of Cimento.org]. [Online]
Available: http://www.cimento.org/index.php?option=com_content&view=article&id=109&Itemid=154 [Accessed 16 April 2012].

COOK, D.J., 1980. Concrete and cement composites reinforced with natural fibres. *Fibrous Concrete.* 1 edn. Lancaster: The Construction Press, pp. 99-109.

COOK, J.G., 1984. *Handbook of textile fibres.* 5 edn. Durham: Merrow Publishing.

DAVIS, C., 2011. *Climate Risk and Vulnerability: A Handbook for Southern Africa.* Pretoria: Counsil for Scientific Research.

DE BEER, H., 2012. *Bricks and blocks commonly used in South Africa.* Cape Town: Cape Cement Products.

DE GUTIERREZ, R.M., DIAZ, L.N. and DELVASTO, S., 2005. Effect of pozzolans on the performance of fiber-reinforced mortars. *Cement and Concrete Composites,* 27, pp. 593-589.

DEPARTMENT AGRICULTURE, FORESTRY AND FISHERIES, 2010. *A profile of the South African hemp market value chain.* Arcadia: Department Agriculture, Forestry and Fisheries.

DEPARTMENT OF HUMAN SETTLEMENTS, 2004-last update, *The Extent of Usage of Alternative Building Technologies in Low-Cost Housing and their Socio-Economic Impact on Beneficiaries* [Homepage of Department of Human Settlements], [Online]. Available: http://www.dhs.gov.za [Accessed 13 March 2011].

DEVELOPMENT INSTITUTE: GOVERNMENT OF INDIA, 2011. *Project profile on cement concrete hollow blocks.* Chennai: Ministry of MSME.

EURO-INTERNATIONAL COMMITTEE FOR CONCRETE, 2010. *fib Model Code 2010.* 3 edn. CEB/FIP.

FERREIRA, S.R., 2012. *Preparation of sisal fibre.* Message from S.R. Ferreira (ferreira.sr@hotmail.com>). Sent Tuesday 17 April 2012. Rio de Janeiro: COPPE/UFRJ.

FOOD AND AGRICULTURE ORGANIZATION, 2009. *Jute, kenaf, sisal, abaca, coir and allied fibres - Statistics.* Food and Agriculture Organization of the United Nations.

GRABOIS, T.M., 2012. *The chemical compostion and particle size distribution of CP V-ARI cement.* Message from T.M. Grabois (thiagomgrabois@yahoo.com.br). Sent Tuesday 17 April 2012. Rio de Janeiro: COPPE/UFRJ.

GRAM, H.E., 1988. Durability of natural fiber in concrete. In: R.N. SWAMY, ed, *Natural Fiber Reinforced Cement and Concrete.* Glasgow and London: Blackie, pp. 143-172.

HARDWICK, G.B., 1992. *The replacement of glass fibre with South African grown sisal in fibre reinforced polyester panels*, Stellenbosch University.

HOLCIM, 2004. The manufacture of concrete masonry units. *Masonry Book.* Holcim, pp. 80-91.

HUNTER, L., 2012. *Vegetable fibre cultivation and availability in Africa.* Message from L. Hunter (lhunter@csir.co.za). Sent Monday 13 February 2012. Stellenbosch: Council for Scientific and Industrial Research.

HYDRAFORM, 2006. *Vibraform Manual.* Hydraform.

ILLSTON, J.M. and DOMONE, P.L.J., eds, 2001. *Construction materials - Their nature and behaviour.* 3rd edn. Oxon: Spon Press.

JACOBSZ, M.J. and VAN DER MERWE, W.J.C., 2010. *Production guidelines for flax.* Pretoria: Department of Agriculture, Forestry and Fisheries.

JACOBSZ, M., 2012. *Vegetable fibre cultivation and availability in Africa.* Message from M. Jacobsz (jacobszm@arc.agric.za). Sent Monday 13 February 2012. Agricultural Research Council.

JUSTICE, J.M., KENNISON, L.H., MOHR, B.J., BECKWITH, S.L., MCCORMICK, L.E., WIGGINS, B., ZHANG, Z.Z. and KURTIS, K.E., 2005. Comparison of Two Metakaolins and a Silica Fume Used as Supplementary Cementitious Materials. *Seventh International Symposium on Utilization of High-Strength/High Performance Concrete* .

KAITH, B.S., KALIA, S. and KAUR, I., eds, 2011. *Cellulose fibers: Bio- and nano polymer composites.* 1 edn. Heidelberg: Springer.

KALIA, S., DUFRESNE, A., CHERIAN, B.M., KAITH, B.S., AV'EROUS, L., NJUGUNA, J. and NASSIOPOULOS, E., 2011.
Cellulose-Based Bio- and Nanocomposites: A Review. *International Journal of Polymer Science,* 2011, pp. 1-35.

KARUS, M., 2004. European Hemp Industry 2002: Cultivation, Processing and Product Lines. *Journal of Industrial Hemp,* 9(2), pp. 93.

KHOLIYA, R., GOEL, A. and KHOLIYA, D., 2011. Unconventional fibre plants: A source of sustainable livelihoods. *International Journal of Science Technology & Management,* 2(1). pp. 27-35.

KIRBY, R.H., ed, 1963. *Vegetable fibres: Botany, cultivation and utilitization.* 1st edn. New York: Leonard Hill Books Limited.

KURUVILLA, J., TOLÊDO FILHO, R.D., JAMES, B., THOMAS, S. and DE CARVELHO, L.H., 1999. A review of sisal fiber reinforced polymer composites. *Revista Brasileira de Engenharia Agricola e Ambiental,* 3(3). pp. 367-379.

KVAVADZE, E., BAR-YOSEF, O., BELFER-COHEN, A., BOARETTO, E., JAKELI, N., MATSKEVICH, Z. and MESHVELIANI, T., 2009. 30,000-Year-Old Wild Flax Fibers. *Science,* 325, pp. 1359.

LAING, H., 2011. The “CMA House” - Bringing Detail and Durability to Affordable Housing, *International Housing & Construction Conference & Exhibition 2011*, 11-14 September 2011, Concrete Manufacturers Association.

LANE, J.W., ed, 2007. *Concrete Masonry Manual.* 8 edn. Midrand: Concrete Manufacturers.

MARTINS, A.P.S., 2012. *The chemical composition and particle size distribution of Pozofly fly-ash.* Message from A.P.S. Martins (adrianapsmartins@globo.com). Sent Tuesday 17 April 2012. Rio de Janeiro: COPPE/UFRJ.

MCKENZIE, R.R., 2006. *Flax stem cross-section*.

MOHANTY, A.K., MISRA, M. and DRZAL, L.T., eds, 2005. *Natural fibres, biopolymers and biocomposites.* Florida: Taylor & Francis Group.

MOHR, B.J., EL-ASHKAR, N.H. and KURTIS, K.E., 2004. Fiber-Cement Composites for Housing Construction: State-of-the-Art Review, M. SYAL, M. MULLINS and M.V. HASTAK, eds. In: *NSF Housing Research Agenda Workshop*, 12-14 February 2004.

MOHR, B.J., NANKO, H. and KURTIS, K.E., 2005. Durability of kraft pulp fiber-cement composites to wet/dry cycling. *Cement & Concrete Composites,* 27, pp. 435-448.

MÜSSIG, J., ed, 2010. *Industrial Application of Natural Fibres - Structure, Properties and Technical Applications.* 1 edn. West Sussex: Wiley.

MYFUNDI,2010. *Cotton: Agriculture and Economics*. [Online] Available: http://myfundi.co.za/e/Cotton_Agriculture_and_Economics [Accessed 24 February 2012].

NATIONAL COTTON COUNCIL OF AMERICA*, 2012. Production Ranking 2011.* [Online] Available: http://www.cotton.org/econ/cropinfo/cropdata/rankings.cfm [Accessed 24 February 2012].

NEVELL, T.P. and ZERONIAN, S.H., 1984. *Cellulose Chemistry and its Applications.* Chichester: Ellis Horwood.

NEVES JR, A., TOLÊDO FILHO, R.D., FAIRBAIRN, E.M.R. and DWECK, J., 2012. Early stages hydration of high initial strength Portland cement. *Journal of Thermal Analysis and Calorimetry,* , pp. 725-731.

NI, Y., 1995. *Natural fibre reinforced cement composites*. Victoria University of Technology.

NORCHEM, n.d. *Silica Fume & Sustainability.* [Online]. Available: http://www.norchem.com/applications-sustainability.html [Accessed 29 November 2012].

OWENS, G., ed, 2009. *Fulton's concrete technology.* 9 edn. Midrand: Cement & Concrete Institute.

PACHECO-TORGAL, F. and JALADI, S., 2011. Cementitious building materials reinforced with vegetable fibres: A review. *Construction and Building Materials,* 25, pp. 575-581.

PPC, 2012. *Price of cement in South Africa*. Personal communication on 26 November 2012 with Milnerton branch (+27 21 550 2100). Milnerton: Pretoria Portland Cement.

QHULL.ORG, n.d*. Qhull.* 18 February, 2012. [Online] Available: http://www.qhull.org/ [Accessed 1 December 2012].

RAJI, J.A., 2007. Intercropping kenaf and cowpea. *African Journal of Biotechnology,* 6, pp. 2807-2809.

RAMASWAMY, H.S., AHUJA, B.M. and KRISHNAMOORTHY, S., 1983. Behaviour of concrete reinforced with jute, coir and bamboo fibres. *International Journal of Cement Composites and Lightweight Concrete,* 5(1), pp. 3-13.

RAWI, K.H.A. and KHAFAGY, M.A.S.A., 2009. *Effect of adding sisal fiber and Iraqi bauxite on some properties of concrete.* Babylon: Technical Institute of Babylon.

RECREGARDEN, n.d. *Agave Sisalana*. [Online] Available: http://recregarden.blogspot.com/2011/03/agave-sisalana.html [Accessed 4 January 2013].

RONG, M.Z., ZHANG, M.Q., LIU, Y., YANG, G.C. and ZENG, H.M., 2001. The effect of fiber treatment on the mechanical properties of unidirectional sisal-reinforced epoxy composites. *Composites Science and Technology,* 61, pp. 1438-1447.

SANS 10400, 1990. *The application of the National Building Regulations.* 1 edn. Pretoria: Standards South Africa.

SANS 1083*, 2002. *Aggregates from natural sources - Aggregates for concrete.* 2.1 edn. Pretoria: Standards South Africa.

SANS 1215, 2008. *Concrete masonry units.* 1.4 edn. Pretoria: Standards South Africa.

SANS 1575, 2007. *Burnt clay paving units.* 1.3 edn. Pretoria: Standards South Africa.

SAPA, 2 Aug 2012. *Sexwale slams 'chancers' in construction*. [Online] Available: http://www.fin24.com/Economy/Sexwale-slams-chancers-in-construction-20120802 [Accessed 24 November 2012].

SAVANNA BRICKS. Maxi Brick. [Online] Available: http://www.savannabricks.co.za/products_maxi.html#thumb [Accessed 21 March 2012].

SEN, T. and JAGANNATHA REDDY, H.N., 2011. Various industrial applications of hemp, kinaf, flax and ramie industrial fibres. *International Journal of Innovation, Management and Technology,* 2(3), pp. 192-196.

SEXWALE, T., 2010. Innovators urged to come with alternative building technology [Homepage of Department of Human Settlements]. [Online] Available:http://www.info.gov.za/speech/DynamicAction?pageid=461&sid=13312&tid=20206 [Accessed 2 April 2011].

SIDDIQUE, R. and KHAN, M.I., 2011. *Supplementary Cementing Materials.* 1 edn. Heidelberg: Springer.

SIKA, 2012. *Price of densified silica fume in South Africa*. Personal communication on 26 November 2012 with Cape Town branch (+27 21 555 0755). Cape Town.

SILVA, F., TOLÊDO FILHO, R.D., MELO FILHO, J.A. and FAIRBAIRN, E.M.R., 2010. Physical and mechanical properties of durable sisal fiber-cement composites. *Construction and Building Materials,* 24, pp. 777-785.

SINGH, B.P., ed, 2010. *Industrial Crops and Uses.* 1 edn. Chippenham: CAB International.

SINGH, D.P., 1998. *Ramie.* New Delhi: Indian Council of Agricultural Research.

SINGH, S.M., 1985. Alkali resistance of some vegetable fibres and their adhesion with portland cement. *Research and Industry,* 15, pp. 121-126.

SMITH, R.C., 1973. *Materials of construction.* 2 edn. McGraw-Hill.

STATISTICS SOUTH AFRICA. 2012. *Census 2011 Fact sheet.* Pretoria: Statistics South Africa.

STRUIK, P.C., AMADUCCI, S., BULLARD, M.J., STUTTERHEIM, N.C., VENTURI, G. and CROMACK, H.T.H., 2000. Agronomy of fibre hemp (*Cannabis sativa* L.) in Europe. *Industrial Crops and Products,* 11, pp. 107-118.

TED BLOG, 23 March, 2012-last update, Born to innovate: Fellows Friday with Alex Odira Odundo [Homepage of TED], [Online]. Available: http://blog.ted.com/2012/03/23/born-to-innovate-fellows-friday-with-alex-odira-odundo/ [Accessed 28 November 2012].

TOLÊDO FILHO, R.D., GHAVAMI, K., ENGLAND, G.L. and SCRINEVER, K., 2002. Development of vegetable fibre-mortar composites of improved durability. *Cement & Concrete Composites,* 25, pp. 185-196.

TOLÊDO FILHO, R.D., JOSEPH, K., GHAVAMI, K. and ENGLAND, G.L., 1999. The use of sisal fibre as reinforcement in cement based composites. *Revista Brasileira de Engenharia Agricola e Ambiental,* 3(2), pp. 245-256.

TOLÊDO FILHO, R.D., SCRIVENER, K., ENGLAND, G.L. and GHAVAMI, K., 2000. Durability of alkali-sensitive sisal and coconut fibres in cement mortar composites. *Cement and Concrete Composites,* 22(2), pp. 127-143.

TOLÊDO FILHO, R.D., SILVA, F.A., FAIRBAIRN, E.M.R. and MELO FILHO, J.A., 2009. Durability of compression molded sisal fiber reinforced mortar laminates. *Construction and Building Materials,* 23(6), pp. 2409-2420.

TURNER, D.Z., 2012. *Calculating the volume of a brick using tetrahedrons.* Message from D.Z. Turner (dzturner@sun.ac.za). Sent Monday 26 November 2012.Stellenbosch.

UNITED NATIONS*. 2007.* The Millennium Development Goals Report*.* New York: United Nations.

VAN DAM, J.E.G., 2002. *Coir Processing Technologies - Improvement of Drying, Softening, Bleaching and Dyeing Coir Fibre/Yarn and Printing Coir Floor Coverings.* Rome: Food and Agriculture Organization.

VAN WYK, L., 2010. The Role of Innovative Technology in Sustainable Human Settlements. *Human Settlements Review.* 1 edn. Pretoria: Department of Human Settlements, pp. 175-195.

VITORINO, F.C., 2012. *The chemical composition and particle size distribution of Silmix silica fumes.* Message from F.C. Vitorino (fabriciosktboard@hotmail.com). Sent Wednesday 18 April 2012. Rio de Janeiro: COPPE/UFRJ.

WORLD BUSINESS COUNCIL FOR SUSTAINABLE DEVELOPMENT. 2005. *The Cement Sustainability Initiative: Progress Report.* Conches-Geneva: World Business Council for Sustainable Development.

YARENKO, C., 2012. *Durability of flax fiber reinforced concrete*. M.Sc. University of Saskatchewan.

Appendix A – Thermal analysis

The 7 and 14 day TGA results are presented here. Samples HCP1 and HCP6 was omitted from the 7 day TGA due to human error.

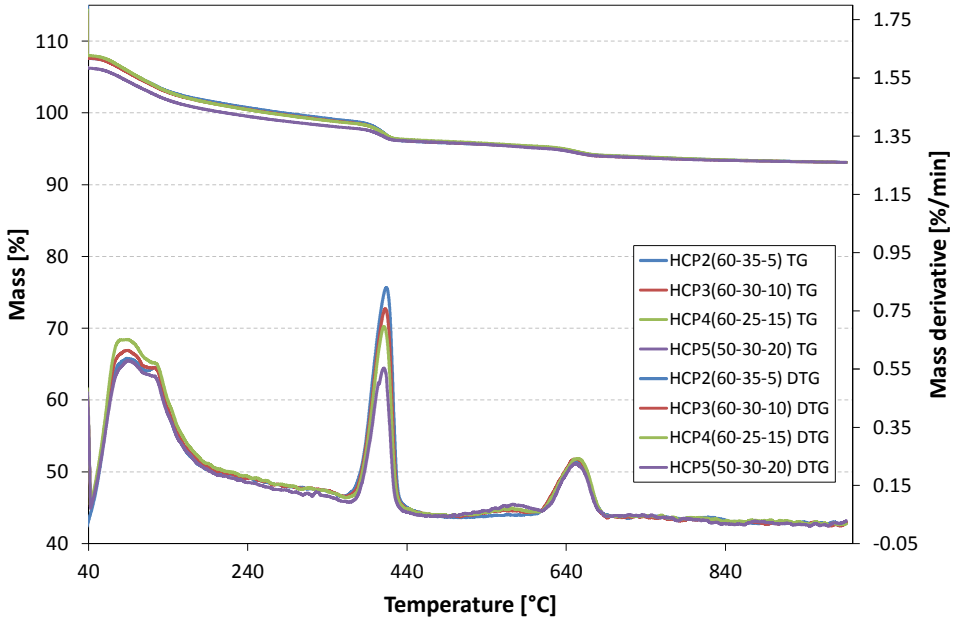

Figure A.1: *TG and DTG curves of pastes at 7 days*

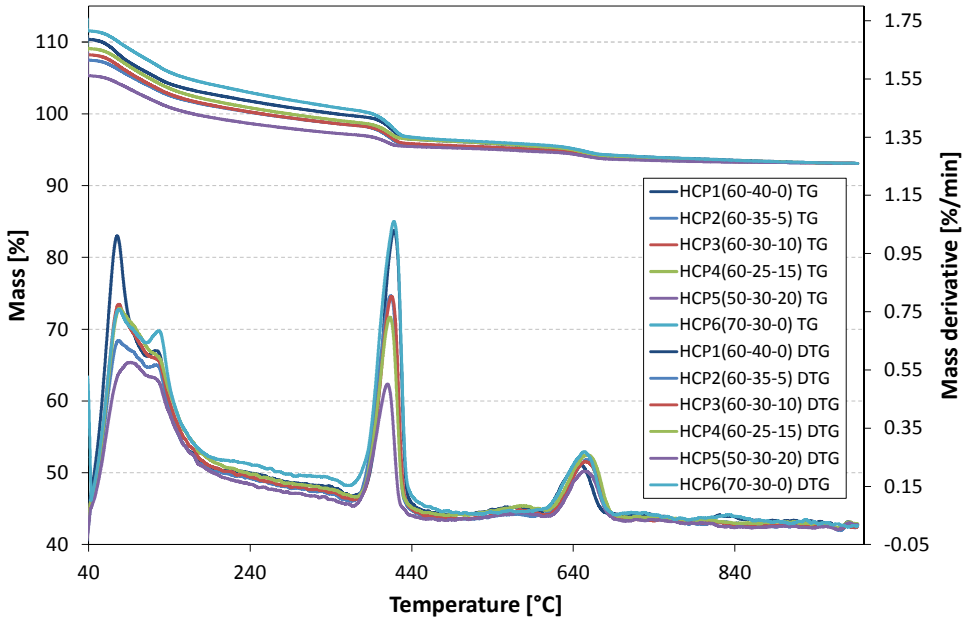

Figure A.2: *TG and DTG curves of pastes at 14 days*

Appendix B – Shrinkage results

The shrinkage test results are presented here using a linear time scale.

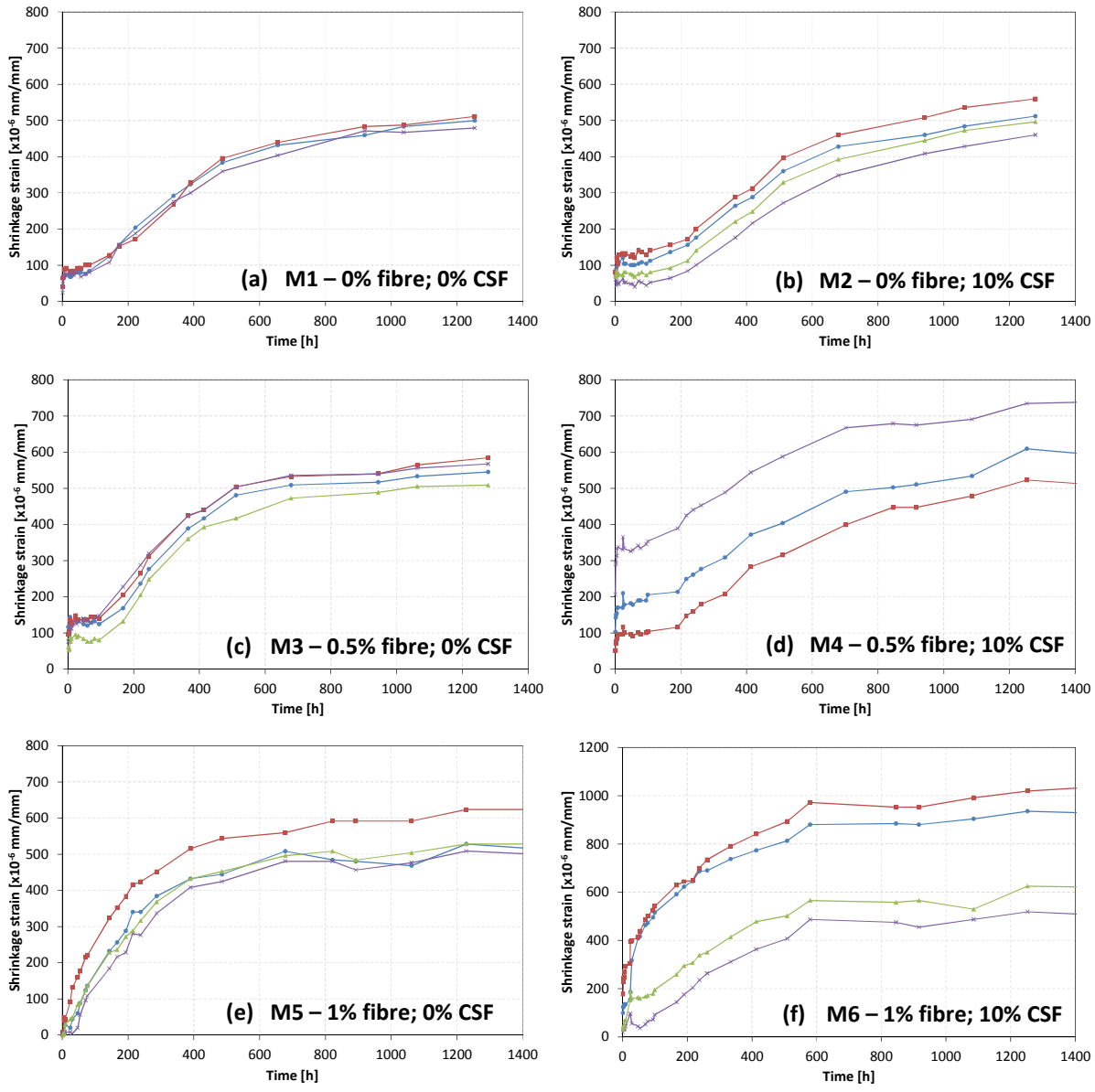

Figure B.1: *Drying shrinkage of solid block mixes (linear time scale)*

The results for mass loss during shrinkage are presented here using a natural logarithmic time scale.

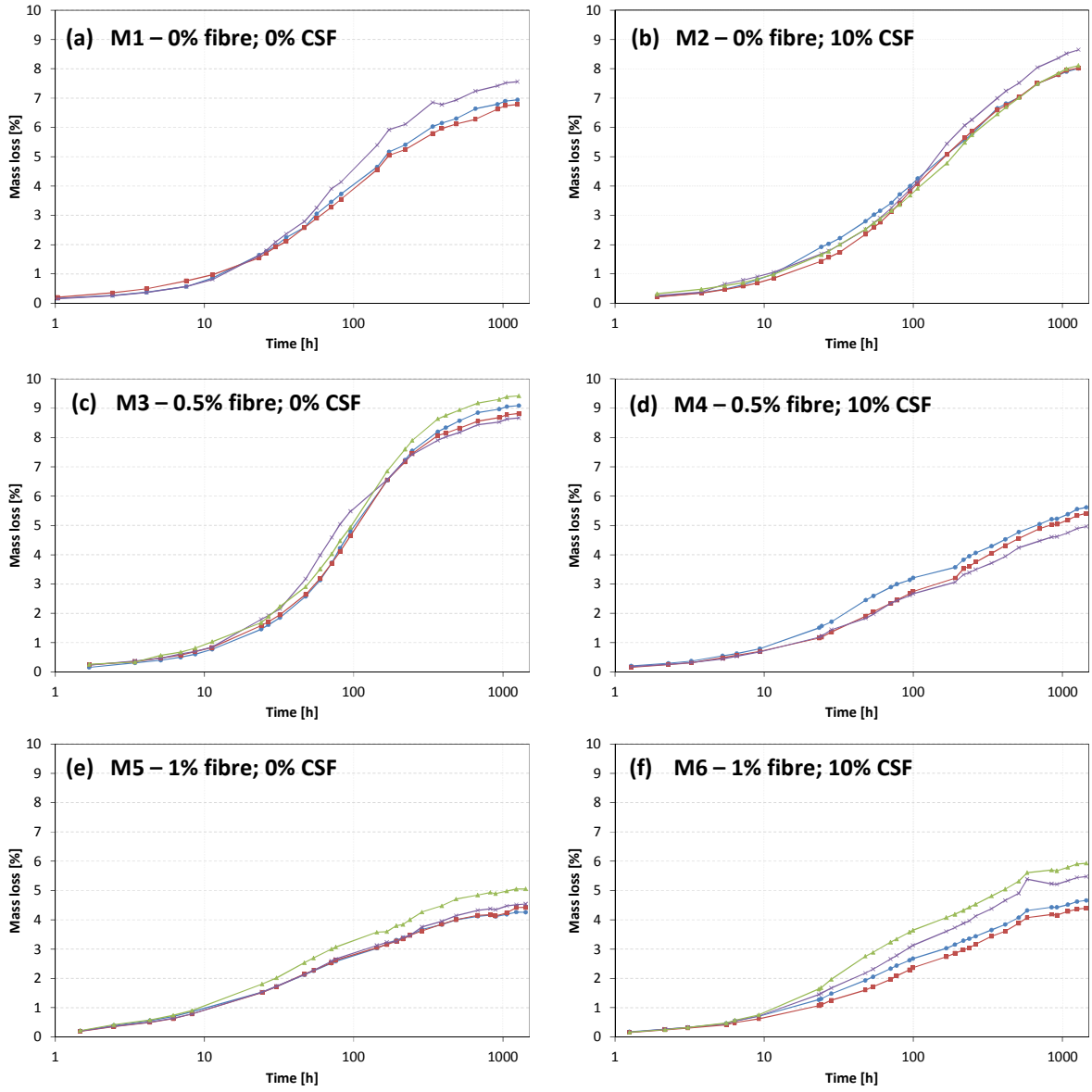

Figure B.2: *Mass loss of solid block mixes (linear time scale)*